Mechanisms regulating CXCR4 intracellular traffic and polarization in human hepatocellular carcinoma cells: cross-talk with the TGF-β pathway

Edgar B. Cepeda

Mechanisms regulating CXCR4 intracellular traffic and polarization in human hepatocellular carcinoma cells: cross-talk with the TGF-β pathway

Report presented by

Edgar B. Cepeda

to obtain the title of Doctor of Philoshophy (PhD)

Supervised by:

Isabel Fabregat Romero, PhD

Senior researcher at Institut d'Investigació biomèdica de Bellvitge (IDIBELL)

Associate professor at Universitat de Barcelona (UB)

Estanislao Navarro Gómez, PhD

Researcher at Institut d'Investigació biomèdica de Bellvitge (IDIBELL)

Biological clues of the invasive and metastasic phenotype group
Institut d'investigació biomèdica de Bellvitge (IDIBELL)

PhD program in Biomedicine (Universitat de Barcelona)

COME UP TO MEET YOU
TELL YOU I'M SORRY
YOU DON'T KNOW HOW LOVELY YOU ARE.
I HAD TO FIND YOU
TELL YOU I NEED YOU
TELL YOU I SET YOU APART.

TELL ME YOUR SECRETS
AND ASK ME YOUR QUESTIONS,
LET'S GO BACK TO THE START.
RUNNING IN CIRCLES,
COMING UP TAILS
HEADS ON A SCIENCE APART.

NOBODY SAID IT WAS EASY,
IT'S SUCH A SHAME FOR US TO PART.
NOBODY SAID IT WAS EASY,
NO ONE EVER SAID IT WOULD BE
THIS HARD.
OH! TAKE ME BACK TO THE START.

This work has been developed at the Laboratori d'Oncologia Molecular (LOM) at IDIBELL (L'Hospitalet de Llobregat, Barcelona).

The author enjoyed the following financial support:

- "FPI predoctoral fellowship" from Ministerio de Educación y Ciencia (MEC), Gobierno de España (November 2010 – November 2014).
- Contract granted by the BFU2012-35538 grant (MINECO, Spain, cited below)

Finantial support from grants of the following companies and institutions:

- Gobierno de España: 1) Ministerio de Ciencia e Innovación (MICINN) (2010-2012). BFU2009-07129. Título del proyecto: Análisis de las vías de transducción de señal inducidas por TGF-beta en células hepáticas humanas como estrategia para el desarrollo de nuevas terapias en patologías del hígado; 2) Ministerio de Economía y Competitividad (MINECO) (2013-2015). BFU2012-35538. Título del proyecto: Papel del tráfico intracelular, el citoesqueleto y las integrinas en la señalización inducida por TGF-beta en células hepáticas. Relevancia en fibrosis y hepatocarcinogénesis; 3) Instituto de Salud Carlos III -Red Temática de Investigación Cooperativa en Cáncer (RTICC): RD06/0020; RD12-0036-0029.

- Generalitat de Catalunya - Agència de Gestió d'Ajuts Universitaris i de Recerca (AGAUR) (2009-2013). 2009SGR-312. Título del proyecto: Mecanismos moleculares y celulares asociados al fenotipo tumoral y metastásico.

- People Programme (Marie Curie Actions) of the FP7-2013, under REA grant agreement #PITN-GA-2012-316549 (IT-LIVER).

ACKNOWLEDGEMENTS

Recuerdo como si fuera ayer el día que decidí embarcarme en esta gran aventura, aunque hayan pasado 5 años desde entonces. Aquel 2 de noviembre no podía imaginar que este camino de éxitos y fracasos, de risas y llantos y de descubrimientos me enseñaría tanto de ciencia como de mí mismo. Y lo más importante, me demostraría lo mucho que tengo que agradecer a quienes están a mi alrededor.

Espero que entendáis que no os pueda dedicar todo el espacio que merecéis y que seguramente olvide nombrar a gente que, de alguna forma, ha sido muy importante durante este tiempo. Ruego que me disculpéis y que no os sintáis excluídos de esta sección. También os pido que entendáis la dificultad que entraña este ejercicio introspectivo, así que intentaré "abrirme en canal" para intentar plasmar en estas líneas lo que espero haberos demostrado estando a vuestro lado.

Como en cualquier larga travesía, la figura del guía parece indispensable. Este personaje estaría encarnado por mis dos directores de tesis. Gracias Isabel por darme esta oportunidad, por trasmitirme la ilusión por la ciencia y por enseñarme el valor del trabajo bien hecho. Y Estaris, de ti me llevo tu predisposición a ayudarme siempre que lo he necesitado y tu sutil sentido del humor.

En esencia, gracias a los dos por enseñarme que, citando a Voltaire, "la ignorancia afirma o niega rotundamente; la ciencia duda".

Esta experiencia no tendría sentido sin mis compañeros de viaje. Judit, gracias por apoyarme en todo momento, por contagiarme tu fuerza cuando la he necesitado, por poner cordura en los momentos más difíciles y por esas risas de quitarle hierro al asunto. Dani, tu llegada fue un soplo de aire fresco. Te agradezco tu predisposición incondicional a ayudarme y tu capacidad de transformar cualquier cosa en "fantasía", que es lo que le da calidad al viaje. De Joaquim me quedo su visión particular del mundo. Gracias por dejarme ver a través de ese filtro en "technicolor" y por inundar mis auriculares con buena música. Andrea, y el "quindi" que llevas dentro, gracias por confiar en mí y por saber valorarme incluso cuando ni siquiera yo mismo sabía hacerlo. Eva y yo hemos compartido muchos años de viaje. Gracias por compartir tu visión de la ciencia conmigo, ¡quizás nuestros caminos se vuelvan a cruzar! Jitka, gracias por tu sinceridad y sencillez, y por esa fina ironía aguda como el Tourmalet. Y Esther, gracias por compartir tu experiencia y ser nuestra brújula en el laboratorio. En definitiva, no me imagino este viaje sin vosotros. Gracias por ser mis compañeros y mis amigos.

con algunos compartí menos tiempo porque acabaron su viaje antes. Jèssica, gracias por tenderme tu mano, por preocuparte por mí y por enseñarme a dar mis primeros pasos en el laboratorio. Joan sería "l'home que treballe fent humor..." Gracias por tu generosidad al enseñarme, tanto en el laboratorio como en el humor. Giulia, gracias por responder siempre con una sonrisa y por ese punto de locura.

Tampoco quiero dejar de agradecer el apoyo que me dieron las que durante varios años fueron mis compañeras de laboratorio en el lejano COM2. Gracias Naiara por ser mi maestra, mi asesora y mi amiga, en el COM2 and beyond. También te agradezco tu dulzura, Anna Roig, y los ánimos que me has dado en las largas tardes de ordenador. Y Ana, ¡cómo agradecerte que me contagiaras tu vitalidad dentro y fuera del laboratorio!

One of the most amazing things of my trip was to meet a lot of people from Poland. First I met Kasia, who I thank a lot for sharing her knowledge, you were really generous. And Magda, Ewa, Gosia, Ann and Dania, thanks for your patience, for your implication, for your support and for your enthusiasm. You cannot imagine how much I have learnt from all of you!

Somos muchos los que hemos pasado por el COM durante estos 5 años. Me llevo un trocito de todos, tanto de los que hemos pasado allí una larga temporada como de los que pasásteis más fugazmente. Con Juan, Silvia, Olga, Miguel y Laura he compartido risas, música y confidencias en la sala de cultivos. ¡Así daba gusto pasar horas allí! David y Santi, sois los post-docs más geniales que he conocido. Raffa y Clara, ¡menudo tándem! Gracias por transmitirme vuestra energía. Helena, Adri, Ana Angulo, Ana Fonseca, Javié, Erika, y en general gentes del COM3, ha sido genial teneros cerca para empapaise de vuestro buen rollo (y ese singular punto de "lomra"...). De Laia Muixí me quedo con nuestras conversaciones desenfadadas. Dani (alias "oloroso cubano"), eres un tío grande en todos los sentidos. Y Antònia, gracias por compartir tu conocimiento y por tu complicidad.

Finalmente, no me olvido del "pasillo de las 7 puertas". Gracias Àngels Fabra por tus consejos, por estar dispuesta a ayudar cuando lo he necesitado y por compartir tu punto de vista conmigo. Rosa, ha sido un placer hablar de ciencia y de la vida contigo con esa complicidad y sentido del humor. Gracias Cristina Muñoz por hacerme sentir respaldado. Òscar, Mariona, Àngels Sierra y Cristina Costa, gracias por hacerme sentir acogido en esta "gran familia".

Al margen del CAM, pero sin salir del IDIBELL, no puedo no acordarme de Rosa, "mi mamá del IDIBELL". Muchas gracias por cuidarme y por preocuparte tanto por mí. Y en general, ha sido un placer compartir una pequeña parte de este tiempo con todos cuantos he conocido.

En esta gran aventura mis amigos han sido un apoyo imprescindible. Carlos y Raquel, esta pista negra ha sido más fácil a vuestro lado. Gracias por escucharme y por convertir muchos días del calendario en recuerdos ¡inborrables. Gemma y Jony, gracias por estar siempre ahí y por vuestra confianza, tengo suerte de contar con gente como vosotros a mi lado. Manich y Berta, gracias por contagiarme con vuestro optimismo. A los del máster, gracias por compartir vuestros "superpoderes". Y a los chic@s del Dir, ¡qué hubiera sido de mí sin esos ratos de desconexión! En definitiva, gracias a todos mis amigos (siento no poder nombraros a todos...) por darme fuerza y estar siempre dispuestos a echar una mano.

Finalmente, para cerrar esta sección, mi familia. A vosotros os lo debo todo, sin vosotros no estaría donde estoy. Mi madre (la más que famosa Pepi) es mi apoyo incondicional, la persona que siempre me ha escuchado, quien me ha impulsado a seguir adelante,

quien más consejos me ha dado, quien más ha sufrido en las horas bajas y quien ha celebrado más vehementemente los éxitos de estos años. Perdóname por haberte hecho sufrir, sé que has vivido este viaje muy intensamente. Nunca podré agradecerte lo suficiente todo lo que has hecho por mí. Hago extensivo este agradecimiento a mi hermano Rubén y a Berna, juntos siempre hemos podido con todo. A Laura tampoco le podré agradecer como se merece todo lo que ha significado durante estos años. Gracias por escucharme, por entenderme, por ser tan honesta, por cuidarme, por hacerme reír y por ser tan generosa conmigo. Gracias por caminar a mi lado. También me quiero acordar de mi yaya Bibi. Gracias por haber creído en mí y por todo tu cariño. Esto también es, en parte, tuyo. Y a toda mi familia, gracias por apoyarme, por estar animándome en esta carrera de fondo. Que no os quepa la menor duda que este logro es tan mío como vuestro.

ABBREVIATIONS

ALK5	Activin receptor-like kinase 5
AP	Adaptator protein
APC	Allophycocyanin
aPKC	atypical protein kinase C
BEC	Bile duct epithelial cell
BFA	Brefeldin A
BIS	Bisindolylmaleimide
BMP	Bone morphogenic protein
BSA	Bovine serum albumin
CAF	Carcinoma-associated fibroblast
CIE	Clathrin-independent endocytosis
CME	Clathrin-mediated endocytosis
COPI	Coat protein-I
DAPI	4',6-diamidino-2-phenylindole
DMA	Dimethylamiloride
EDTA	Ethylenediaminetetraacetic acid
EEA1	Early endosome antigen 1
EGF	Epidermal growth factor
EGFP	Enhanced green fluorescent protein
EGFR	Epidermal growth factor receptor
EMT	Epithelial-to-mesenchymal transition
ERC	Endocytic recycling compartments
ERK	extracellular-signal regulated kinase
EXOC4	Exocyst complex 4
FAK	Focal adhesion kinase
FBS	Fetal bovine serum
FGF	Fibroblast growth factor

fMSC	Fetal mesenchymal stem/stromal cell
GDF	Growth and differentiation factor
GPCR	G-protein coupled receptor
GPI	Glycosylphosphatidylinositol
GSK-3β	Glycogen synthase kinase-3β
HBV	Hepatitis B virus
HCC	Hepatocellular carcinoma
HCV	Hepatitis C virus
HGF	Hepatocyte growth factor
HIF	Hypoxia-inducible factor
HIV	Human immunodeficiency virus
HSC	Hepatic stellate cell
IGF	Insulin-like growth factor
IGF2R	Insulin-like growth factor type 2 receptor
IL-1	Interleukin-1
JNK	c-jun N-terminal kinase
LB	Lysogeny broth
M6PR	Mannose-6-phosphate receptor
MAPK	Mitogen-activated protein kinase
MDCK	Madin-Darby canine kidney
MET	Mesenchymal-to-epithelial transition
MMP	Matrix metalloproteinase
MβC	Methyl-β-cyclodextrin
NADPH	Nicotinamide adenine nucleotide phosphate
NF-κB	Nuclear factor-κB
PAGE	Polyacrilamide gel electrophoresis
PBS	Phosphate-buffered saline

PCP	Planar cell polarity
PDGF	Platelet-derived growth factor
PDZ	post-synaptic density 95; discs large; zonula occludens-1
PFA	Paraformaldehyde
PI	Propidium iodide
PI3K	Phosphatidylinositide 3-kinase
PTEN	Phosphatase and tensin homolog
PVDF	Polyvinylidene fluoride
RIPA	Radioimmunoprecipitation assay
ROS	Reactive oxygen species
sCXCR4	(cell) surface-located CXCR4
SDF-1α	Stromal derived factor-1α
SDS	Sodium dodecyl sulfate
SMA	Smooth muscle actin
STX	Syntaxin
TGF-β	Transforming growth factor-β
TGN	Trans-Golgi network
TβRI	Transforming growth factor-β receptor I
TβRII	Transforming growth factor-β receptor II
TβT-FaO	Transforming growth factor-β-treated FaO cells
VCC-1	VEGF correlated chemokine-1
VEGF	Vascular endothelial growth factor
VEGFR	Vascular endothelial growth factor receptor
VHL	von Hippel-Lindau
ZO-1	Zonula occludens-1

TABLE OF CONTENTS

INTRODUCTION

1. The liver

1.1. Liver physiology

The liver is the largest internal organ and one of the most structurally and functionally heterogeneous in mammals, considered second only to brain in its complexity.

Historically, many models explaining liver architecture have arisen for the last centuries since Weppler first noted the lobular pattern of the liver in 1665. Despite the functional unit of the liver has been hotly debated over the last decades, Matsumoto's primary lobule structure remains the most widely accepted nowadays. This model, emerged in 1979, is based on vessel architecture and on a three-dimensional tortuous and branching shape of the individual lobules. Subsequent models proposed during the last two decades of the 20th century did not have the same acceptance as Matsumoto's.

According to the liver structure, it macroscopically comprises 4 lobes: right, left, quadrate and caudate. Remarkably, at any given moment the liver contains blood equivalent to approximately 25% of cardiac output due to its irrigation by two main supplying vascular systems: the portal vein and the hepatic artery. The portal vein provide about 70% of the blood flow and 40% of the oxygen and the hepatic artery around 30% of the blood flow and 60% of the oxygen (Malarkey et al., 2005; Spear et al., 2006).

Microscopic liver architecture comprises lobules as the repeating structural unit. Strikingly, the same histological appearance is observed no matter the angle that a liver is sectioned. Lobules are defined as hexagonal structures consisting of plates of hepatocytes with a central vein and six portal triads at the edge of each lobule. Each portal triad is formed by an intrahepatic bile duct, a portal vein and a hepatic artery. Assuming this highly organized liver architecture, it would be expectable to think about numerous different cell types to form this organ. Hepatocytes are the predominant cell type, accounting for around 60% of the cells and 80% of the cellular mass. At least other 14 cell types are found in human liver, for instance, cholangiocytes (also named bile duct epithelial cells; BECs), Kupffer cells and hepatic stellate cells (HSC). These cells

represent the 40% of total liver cells and display different localizations and different functions (Fausto and Campbell, 2003; Malarkey et al., 2005; Si-Tayeb et al., 2010; Spear et al., 2006).

In this regard, the lobular organization has a functional consequence. The position of the hepatocytes within the liver lobule was found to determine the compartimentalization of function, which is called zonal heterogeneity or metabolic zonation. This phenomenon permits to the liver to perform opposite metabolic pathways in non-overlapping anatomic regions. In broad outline, it provides a general view of the complexity of liver structure which is determining to understand the functions performed by this organ (Fausto and Campbell, 2003; Malarkey et al., 2005; Spear et al., 2006).

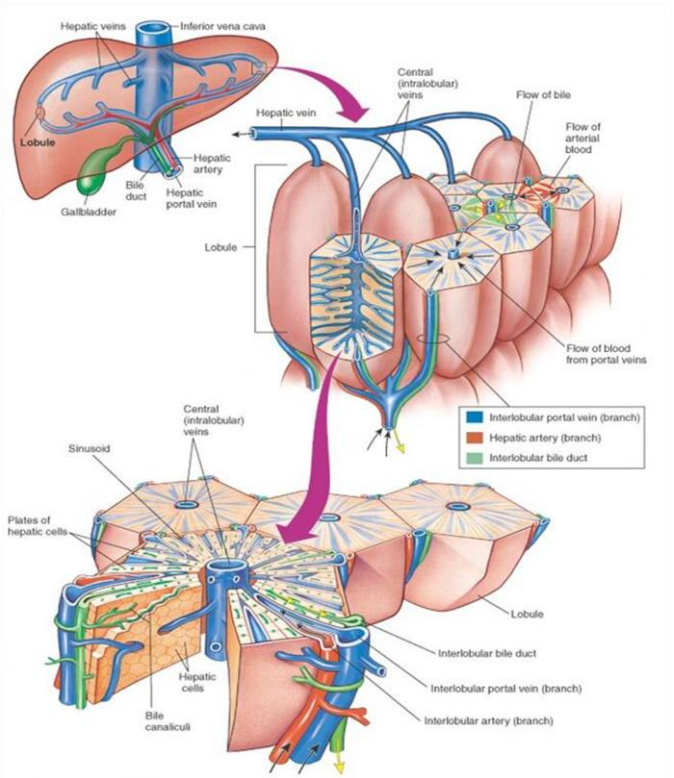

Figure I.1. Schematic view of the liver anatomy (Lynch CJ).

Physiologically, the portal vein entails the main entrance of blood rich in nutrients while hepatic artery implies the entrance of oxygen-rich blood in the liver. Blood moves along plates of hepatocytes through small capillaries called sinusoids to the central veins that converge into hepatic veins, finally leading to the vena cava. The sinusoidal side of hepatocytes interfaces the space of Disse, which forms the barrier between the blood and hepatocytes, while the

apical side (opposite to sinusoidal side) forms the canalicular membrane. Furthermore, the channels between adjacent hepatocytes, called bile canaliculi, take part in the transport of the bile to the bile duct, in opposite direction to blood flow. The canal of Hering forms the transition area between the canaliculi and intrahepatic bile duct and it is lined by hepatocytes and cholangiocytes. Finally, intrahepatic bile ducts converge to join the bile duct and transport bile to the gall bladder (Malarkey et al., 2005).

Assuming this very complex structure of the liver, it is easy to think about a not less complex functionality. The liver accomplishes several important functions for the organism. For brevity's sake, it is responsible for production, removal and breakdown of serum proteins; production and removal of carbohydrates during periods of fasting or eating respectively (it is worth to highlight the unique ability of the liver to carry out gluconeogenesis); processing of fatty acids and triglycerides; maintaining of cholesterol homeostasis through synthesis or catabolism; synthesis and interconversion of non-essential amino acids; decomposition of toxic endogenous compounds; production and secretion of bile; detoxification of xenobiotic agents; and storage of several substances. Furthermore, it is able to regulate blood pressure by modulating the blood volume (Malarkey et al., 2005; Si-Tayeb et al., 2010; Spear et al., 2006).

1.2. Hepatocellular carcinoma

Liver cancer is the fifth most common cancer among men and the ninth among women. In general, the region with the highest incidence is Eastern Asia (adding South-Eastern Asia in the case of men and Western Africa in the case of women) and the region with the lowest one is Northern Europe (European Association For The Study Of The Liver and European Organisation For Research And Treatment Of Cancer, 2012).

As for mortality, liver cancer is among the three most common cause of cancer-related death worldwide (European Association For The Study Of The Liver and European Organisation For Research And Treatment Of Cancer, 2012).

Between the 70-90% of the cases of hepatocellular carcinoma (HCC) are developed from a previously established chronic liver disease. The 80% of

hepatocellular carcinoma arise in Eastern Asia and sub-Saharan Africa, where the main risk factor is chronic infection with hepatitis B virus (HBV) and also the exposure to aflatoxin B1. Contrary, in Europe, North America and Japan infection with hepatitis C virus (HCV) together with alcohol intake are the dominant risk factors. Additionally, infection with HCV could have a synergistic effect with other risk factors, for instance non-alcoholic fatty liver disease, a body-mass index greater than 40 and tobacco, whereas coffee consumption decreases the risk to develop hepatocellular carcinoma (Bruix et al., 2014; Wallace and Friedman, 2014).

As for genetic susceptibility, HCC shows a risk association with rare monogenic syndromes as alpha-1-trypsin deficiency, hemochromatosis, glycogen storage disease type I, some types of porphyria and hereditary tyrosinemia type I and also a risk for polygenic diseases, for instance autoimmune hepatitis, type 2 diabetes, HCC familiar antecedents and hypothyroidism. Nonetheless, in the majority of the cases HCC is a consequence of genetic heterogeinity, so HCC could be explained by several unlinked single gene defects (Dragani, 2010).

1.2.1. HCC molecular pathways

HCC is a complex multi-step process that leads to an accumulation of genetic and epigenetic modifications. Additionally, it is important to emphasize that a high heterogeneity have been found among the different tumors but even between the different nodules within the same malignancy. Although there is a limited availability of models for the study of initiation and progression of HCC, some molecular pathways are known to be involved. Nevertheless, it is still a long way to completely understand all the molecular pathways implicated in HCC due to its characteristic complexity.

To begin with, it has been reported an up-regulation of the epidermal growth factor (EGF) pathway in HCC. This is not surprising since proliferation pathways are one of the most commonly altered paths in several types of cancer. Our group has previously demonstrated that the over-activation of the EGF pathway leads to increased proliferation and apoptosis resistance in HCC (Caja et al., 2011a).

Other pathways affected in HCC are RAS and AKT. The activation of RAS triggers a path leading to the activation of MEK and ERK proteins resulting in a proliferative and anti-apoptotic effect. Despite no mutations have been described in HCC, it is usual to observe over-expression of this protein. Thus, these proteins become downstream executers of the growth factor signals, such as EGF described above (Newell et al., 2009).

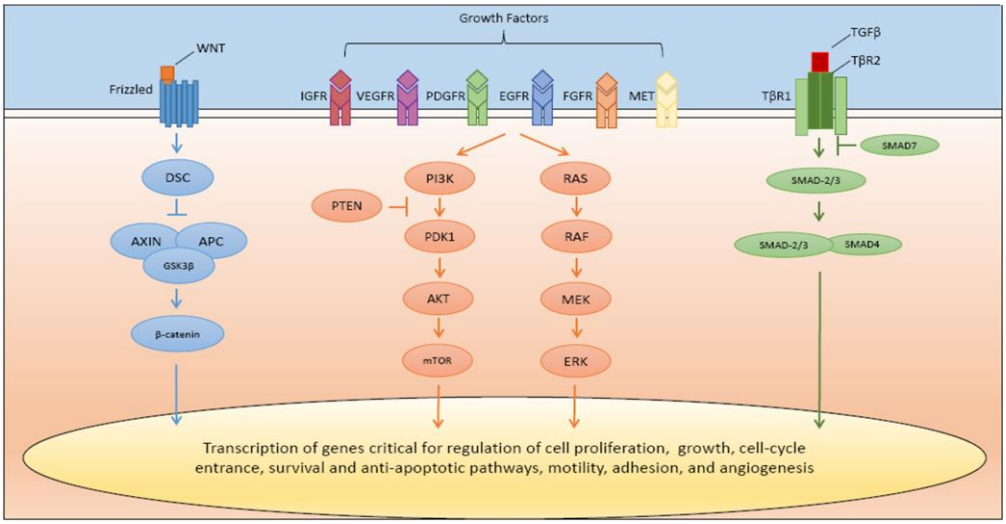

Figure I.2. Diagram of the potential molecular pathways altered in HCC (Harding and Abou-Alfa, 2013).

The insulin-like growth factor (IGF) and the hepatocyte growth factor (HGF) pathways are also disregulated in HCC. Over-expression of IGF2 is commonly found in HCC but also allelic loss of IGF type 2 receptor (IGF2R) (De Souza et al., 1995). By its part, HGF is the unique ligand of MET receptor, which is over-expressed in 20-48% of HCC cases. This receptor over-expression has been correlated with increased hepatic metastases, but its decreased expression has been also reported in liver cancer (Newell et al., 2009).

Besides the modification of proliferation pathways, HCC progression is also favored by the dysregulation of some paths related with development and cell differentiation. Hence, proteins of the wingless-related integration site (WNT)/β-catenin pathway have been found to be dysregulated in HCC, for instance CTNNB1 (catenin) and AXIN1 genes. Hedgehog signaling pathway, with a very

similar cascade to WNT, has been characterized as another modified pathway in human HCC samples (Branda and Wands, 2006; Llovet and Bruix, 2008).

Neovascularization is another characteristic feature of cancer, including HCC in which this capacity is enhanced in hypoxic conditions. Between the different proteins promoting this effect, it has been described that vascular endothelial growth factor receptors (VEGFR) -1 and -2 are usually over-expressed in liver tumors. Moreover, the high levels of VEGF in the serum indicate a poor prognosis after resection (Llovet and Bruix, 2008).

Furthermore, unavoidably the p53 pathway must be described when speaking about modified molecular pathways in cancer as it is mutated in the half part of all human tumors. The role of p53 consists on the induction of apoptosis or cell cycle arrest after DNA damage. Hence, mutation of p53 provokes a loss of function leading to an accumulation of cell DNA mutations with a potential role to facility the progression of malignancies. In HCC, p53 is found to play a role in early stages of hepatocarcinogenesis but also influences on the late stage of the disease formation (Aravalli et al., 2008; Villanueva et al., 2007; Zender et al., 2010).

Last but not least, the transforming growth factor-β (TGF-β) is one of the most important regulator pathways in HCC. This cytokine affects the tumor microenvironment as well as it participates in several tumorigenic processes of HCC such as inflammation and the acquisition of an invasive phenotype. Given the relevance of the TGF-β pathway in this work, this topic will be introduced in a separate section (See *6. TGF-β*).

2. Intracellular trafficking

The plasma membrane is a cell structure that not only has an eminent protective function but it is also serving as a front line of the communications between the cell and its environment. These communications are mediated by different processes involving vesicle structures. On the one hand, vesicles from the cytoplasm fuse with the plasma membrane in a process called exocytosis; on the other hand, endocytosis consists on vesicles budding off the plasma membrane and entering the cytoplasm. Both mechanisms mediate some processes such as nutrient uptake, termination of receptor signaling, cytokinesis and cell migration, among others (Ivanov, 2008).

Vesicular trafficking was first discovered in the late 19th century by Ilya Mechnikov. Since then, an increasing interest on membrane trafficking has been arising due to its impact in the understanding of normal and pathological events in cells. In order to succeed in its function, vesicular trafficking requires intermediate steps involving vesicle fusion with different compartments of the cell. The formation of membrane vesicles is a complex process that depends on the protein coat and the cargo (Ivanov, 2008).

2.1. Exocytosis

Exocytosis is a process by which cargo-filled vesicles fuse with the plasma membrane to incorporate biomolecules into it or to release them into the extracellular space (Heider and Munson, 2012).

Currently, the knowledge about transport and secretion of chemokines is poorly understood. Few reports underline the importance of the secretory pathways, routes, organelles and molecular machinery that regulate time and directional release of cytokines from cells (Huse et al., 2006; Stow et al., 2009). All eukaryotic cells share the same early steps of secretory pathway involving the endoplasmic reticulum as the fate for the newly synthesized protein precursors. Into the endoplasmic reticulum proteins are folded and their integrity is checked. Additionally, proteins obtain the beggining of glycosylation if it proceeds. Then, they are transported into vesicular carriers to the Golgi apparatus, where post-translational processing and glycosylation continue (Farquhar and Palade,

1998; Reynders et al., 2011; Stow et al., 2009). After Golgi apparatus journey, the last localization of proteins and other biomolecules is into the trans-Golgi network (TGN), from where they are directed to the plasma membrane through different routes (Stow et al., 2009).

In the case of the immune cells, at least 3 different exocytic pathways for cytokines have been described. The first one consists on a constitutive secretory pathway implicating small, pleiomorphic vesicles from the TGN to the cell surface or intracellular endosomes. However, the upregulation of some molecules can increase trafficking for a higher release of cytokines in response to cell activation (Lieu et al., 2008). Secondly, some secretory cells, for instance that ones with exocrine or endocrine functions, have an additional granule-mediated secretory pathway in which specialized cargo is redirected to secretory granules and stored until its release is triggered by specific signals. Lastly, some cytokines such as IL-1α and β use a non-classical secretory route characterized by the synthesis of the biomolecule in the cytoplasm and an endoplasmic reticulum and Golgi complex independent exocytosis (Stow et al., 2009).

In general terms, the Golgi apparatus could be considered as the first station in the exocytic trip of biomolecules to the plasma membrane. The Golgi apparatus is an organelle that serves as the hub in the secretory pathway. It is componed by seven cisternal membranes surrounded by transport vesicles (Ladinsky et al., 1999; Xiang and Wang, 2011). These Golgi stacks are connected by tubules forming a peri-nuclear structure. In the middle nineties, it has been described the concept of “Golgi matrix” as a detergent and salt-resistant protein complex (Slusarewicz et al., 1994; Xiang and Wang, 2011). Afterwards, the proteins forming these complexes have been defined as golgins, which are associated with the cytoplasmic face of Golgi membranes. Many of the golgins have multiple Rab binding sites, facilitating the capture of membranes bearing specific Rabs and excluding others. Depending on their localization, golgins are divided into cis-golgins and trans-golgins (Tang and Wang, 2013).

As a case in point, GM-130 is a well known cis-golgin firstly described in 1995 by Nakamura et al. (Nakamura et al., 1995). It mediates the endoplasmic

reticulum-to-Golgi transport and the formation of cis-Golgi cisternae (Tang and Wang, 2013). Trans-golgins include golgin-97, which is localized in the trans-Golgi through the binding to Arl1-GTP protein and is implicated in the TGN-to-plasma membrane anterograde traffic (Lock et al., 2005; Tang and Wang, 2013; Xiang and Wang, 2011). In the case of the mannose-6-phosphate receptors (M6PR), they establish a link between the TGN and the endosomes. An important aspect in M6PR trafficking is the regulatory mechanisms by the clathrin adaptator AP1, increasing the efficiency of cargo sorting (Kametaka and Waguri, 2012). Likewise, β-cop protein consists on a COPI forming protein, which in turn is localized along the whole Golgi apparatus cisternae, being implicated in anterograde transport (Maxfield and McGraw, 2004).

Making a careful study of the exocytic pathway, TGN should be considered as the first step after Golgi apparatus trafficking. AP1, AP3 and AP4 have been identified as adaptor protein complexes in TGN/endosomal membranes. Nevertheless, only AP1 is implicated in the clathrin coat formation. It has been reported that AP1 plays a role in the sorting of proteins to the epithelial basolateral membrane of LLC-PK1 renal epithelial cell line (Ivanov, 2008; Robinson, 2004).

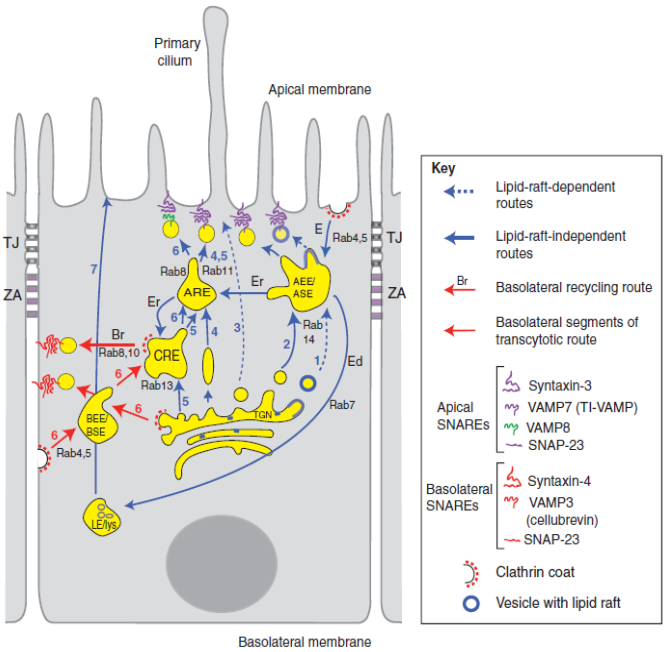

Figure I.3. Diagram of the exocytic pathways in epithelial polarized cells (Weisz and Rodriguez-Boulan, 2009).

Later stages of exocytic route implicate the function of the Rab GTPases and their effectors in the assembly of coats and vesicle formation, budding, tethering and fusion (Ivanov, 2008; Robinson, 2004). Rab GTPases are necessary to the recruitment of membrane-tethering and docking factors that facilitate membrane traffic, but also to the formation of transport vesicles. Interestingly, Rab proteins trigger the scaffold formation and constitute a tag for compartment identity (Pfeffer, 2001).

Finally, prior to cell surface exposition, exocyst complex rises up as the last step of the exocytic route. Exocyst is a highly conserved protein complex formed by 8 subunits: Sec3, Sec5, Sec6, Sec8, Sec10, Sec15, Exo70 and Exo84. Firstly, the several subunits have been discovered in S.cerevisiae and in yeast, but homologues of all of them exist in multicellular eukaryotes (Heider and Munson, 2012). The exocyst is localized in determined areas of the plasma membrane, as expected for a complex involved in the polarized vesicle exocytosis. It has been found that exocyst is concentrated in cell-cell contact sites in polarized epithelial cells and in the leading edge of cell motility processes (Heider and Munson, 2012). Between the exocyst complex functions, it is worth to highlight its ability to enhance the tethering of the exocytic vesicles to the plasma membrane by indirectly facilitating SNARE-docking and fusion in a polarized manner. In this line, exocyst complex is capable to activate specific SNARE proteins, which finally act as effector agents for vesicle fusion to the plasma membrane. Furthermore, other functions are attributed to the exocyst complex. Among them, it has been reported a role for exocyst complex in cancer progression and metastasis, being required for cell migration (Heider and Munson, 2012; Hertzog and Chavrier, 2011). For example, exocyst-mediated exocytosis is required for MMPs secretion in tumor cell invadopodia (Heider and Munson, 2012; Liu et al., 2009; Yamamoto et al., 2013).

Strikingly, it has been recently found that the exocyst complex regulates the localization of the atypical protein kinase C (aPKC) at the leading edge (Rosse et al., 2009) through the formation of a complex. The formation of the complex is necessary for NRK cell migration and for the localized activation of c-Jun N-terminal kinase (JNK) and extracellular-signal-regulated kinase (ERK) at the leading edge of migrating cells (Boeckeler et al., 2010; Rosse et al., 2009).

These data have revealed the cross-talk between the cell polarity regulating mechanisms and the membrane trafficking machinery during cell migration (Liu and Guo, 2012).

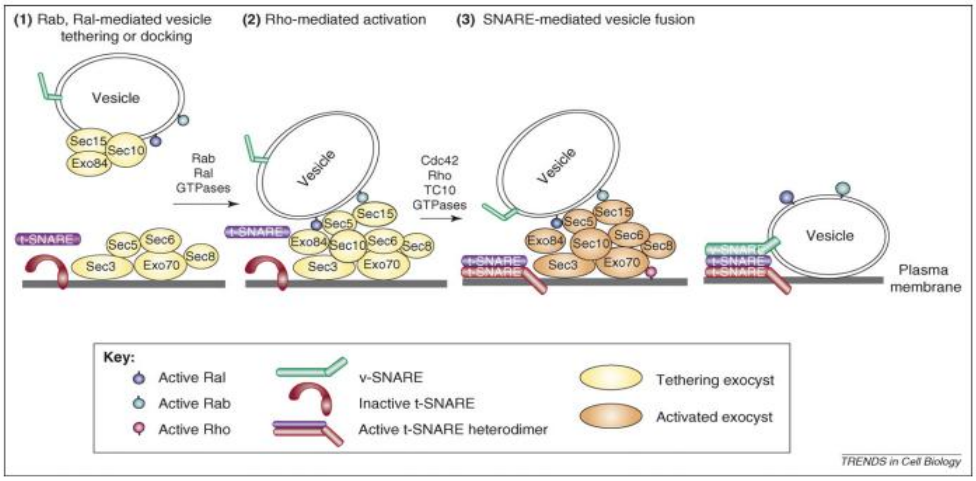

Figure I.4. The exocyst complex (Wu et al., 2008).

2.2. Endocytosis

Chemokines localized at the cell surface basally undergo a slow, tonic internalization process in the absence of ligand. The endocytic trafficking of G-protein coupled receptors (GCPRs) can be greatly enhanced by ligand binding (Neel et al., 2005). The receptors trafficking pathways may depend on many factors such as the presence or the absence of ligand, but in general two different routes are available: the clathrin-mediated (CME) and the caveolae-dependent endocytosis (taking part in the general mechanisms named clathrin-independent endocytosis, CIE). However, many additional internalization routes have been described, although their mechanisms still remain partially unknown. The selection of the endocytic pathway by the receptor depends on several factors, for instance the cell type or the lipid composition of the membrane, although some of them take advantatge of both paths (Neel et al., 2005).

To be more specific, clathrin-mediated endocytosis is a major mechanism by which chemokine receptors undergo ligand-induced internalization. After the activation of the receptor, it can bind to adaptor molecules that eventually link it to a clathrin latticework, facilitating chemokine receptor endocytosis. Finally, the

association of the receptors with the adaptor molecules results in the recruitment of clathrin and the formation of clathrin-coated pits, which "drop off" the plasma membrane by the action of dynamins becoming clathrin-coated vesicles. These clathrin-coated vesicles independent of the plasma membrane are later uncoated and the receptor-ligand complex enters the early endosome bodies. In this point, the chemokine receptor can either enter the perinuclear recycling compartment and trip back to the plasma membrane to be reexposed to ligand, or it can enter the late endosomal compartment to be degradated into the lysosomal compartment (Neel et al., 2005).

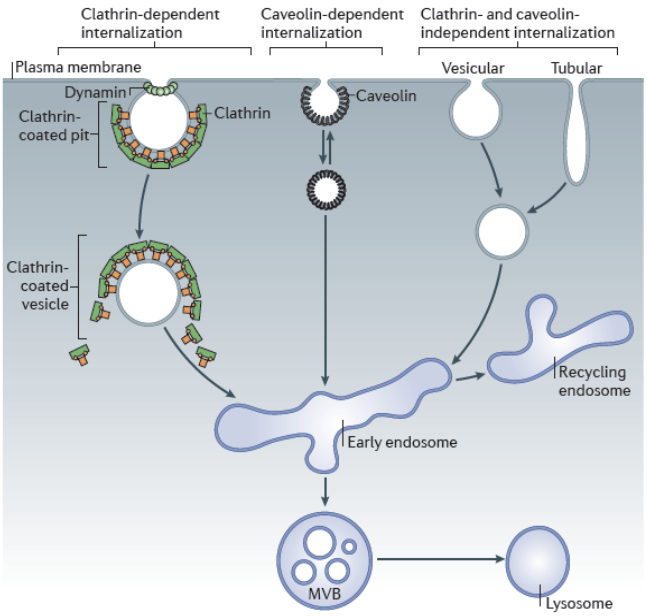

Figure I.5. Schematic view of the different endocytic pathways studied (McMahon and Boucrot, 2011).

Caveolae-dependent pathway is the most intensively characterized clathrin-independent internalization pathway. Caveolae are defined as cholesterol- and sphingolipids-enriched plasma membrane invaginations, also accumulating special cholesterol-binding proteins termed caveolins on the cytoplasmic side of vesicles (Ivanov, 2008). Conversely to clatrin-coated vesicles, caveosomes do not accumulate transferrin and do not contain early endosome antigen 1 (EEA1) or other early endosome markers (Ivanov, 2008). Caveolin-1, -2 and -3 are a set of proteins responsible to define the shape and the organization of caveolae. Caveolins have the ability to self-assemble in a high mass of oligomers to take part in the synthesis of a cytoplasmic coat on plasma

membranes invaginations. Afterwards, once internalized, the caveosome fuses with early endosomes, as clathrin-coated vesicles do, though a mechanism not completely known (Neel et al., 2005). It is thought that caveolin-dependent endocytosis could play a key role in recycling pathway as these compartments are highly enriched in cholesterol and other lipidic components (Gagescu et al., 2000; Neel et al., 2005).

In both clathrin- and caveolin-dependent pathways dynamin becomes a critical regulator. Dynamin is a GTPase with the ability to self-activate through oligomerization. Its main function consists on the fission of plasma membrane vesicles to the cytoplasm. Thus, in general, both internalization pathways can be classified as dynamin-dependent endocytosis (Hinshaw, 2000; Ivanov, 2008).

Despite caveolin-dependent is the most studied clathrin-independent internalization route, cells can use other types of endocytosis even non-related with dynamin. In this issue, macropinocytosis is an internalization pathway first described in the thirties by Warren Lewis when he observed that rat macrophages had the ability to close big vesicles inside the cytoplasm provoked by the movement of the plasma membrane. Macropinocytosis is a signal-dependent process responding to growth factor stimulation, for example EGF or PDGF. However, some cells such as presenting-antigen cells are capable of constitutive macropinocytosis (Lim and Gleeson, 2011). The vesicles internalized through this route, named macropinosomes, are significantly larger than clathrin-coated ones. Other remarkable differences are the absence of coat structures of macropinosomes and the subsequent massive entrance of substances into the cell due to the big size of these vesicles. Once macropinosome is formed, it maturates into the cytoplasm until it drives the internalized biomolecules to different fates, although the exact mechanism by which this transport is guided remains unclear. On the one hand, the cell fate of macropinosomes is to deliver cargo to lysosomes, previously acquiring markers of late endosome such as Rab7. On the other hand, they can be directed back to the plasma membrane for the cargo to be recycled (Lim and Gleeson, 2011).

2.3. Recycling

After internalization, chemokines traffic through endosomal compartments either to lysosomes, following the degradative pathway, or to recycling endosomes back to the plasma membrane. This latter route, termed recycling pathway, is essential for the returning of essential molecules that perform specific functions to the appropiate compartments (Maxfield and McGraw, 2004). The recycling pathway plays a key role in the maintenance of the distinction between apical and basolateral membranes in polarized cells. Actually, hepatocytes target newly synthesized apical membrane proteins to the basolateral membrane for a subsequent deliver to the apical membrane by endocytic routes (Maxfield and McGraw, 2004; Zegers and Hoekstra, 1998).

The proteins to be recycled are first internalized from the plasma membrane to reach early endosomes, which serve as the point to send cargoes to different compartments into the cell. The proteins that are targeted back to the plasma membrane can undergo recycling by two different routes: the direct one traveling from early endosomes to the plasma membrane (named fast recycling pathway) or indirectly through recycling endosomes (termed slow recycling pathway). Alternatively, a third path consist on the retrograde transport delivering the proteins to the Golgi apparatus (Bonifacino and Rojas, 2006; Maxfield and McGraw, 2004; Sönnichsen et al., 2000; Taguchi, 2013). The recycling pathway accomplishes an important function as a regulator of many physiological processes, for instance cytokinesis, polarity in epithelial cells and morphogenesis between others (Taguchi, 2013; Weisz and Rodriguez-Boulan, 2009). Within these several roles of the recycling routes, it is worth to highlight the influence that this transport exert in cell signaling and in cell adhesion and migration by controlling the plasma membrane exposure of GPCRs, cadherins and integrins, respectively (Jones et al., 2006; Taguchi, 2013).

Some Rab GTPases control the recycling mechanisms and discern between the specific routes followed by the biomolecules directed back to the plasma membrane. Therefore, Rab5 is one of the best characterized Rabs that is involved in the formation and function the sorting endosomes. Rab5 collaborates with the EEA1 to regulate the fusion between primary endocytic

vesicles and sorting endosomes. So, Rab5 becomes a protein marker of the fast-recycled endosomes formed directly from the early endosomes (Maxfield and McGraw, 2004). Rab4 modulates the following fast recycling pathway, being a marker of vesicles proceeding directly from the early endosomes after scission of the vesicles in the latter stage before the fusion to the plasma membrane (Jones et al., 2006). Alternatively, Rab11 has been described as a resident protein of the endocytic recycling compartments (ERC), which take part in slow recycling pathway. It has been reported that the perturbation of Rab11 function lead to a concentration of transferrin in the ERCs and a blockade of its following trafficking. Consequently, Rab11 regulates transport from the ERCs, despite the mechanism is still unknown (Maxfield and McGraw, 2004). Strikingly, Rab11 is also localized at the TGN, so it cannot be discarded a role of Rab11 in the exocytic pathway (Maxfield and McGraw, 2004). In fact, Rab11 was first localized at the TGN and TGN-derived membranes, and afterwards at other several intra-cellular post-Golgi vesicles including ERCs and recycling endosomes of polarized cells (Lock and Stow, 2005).

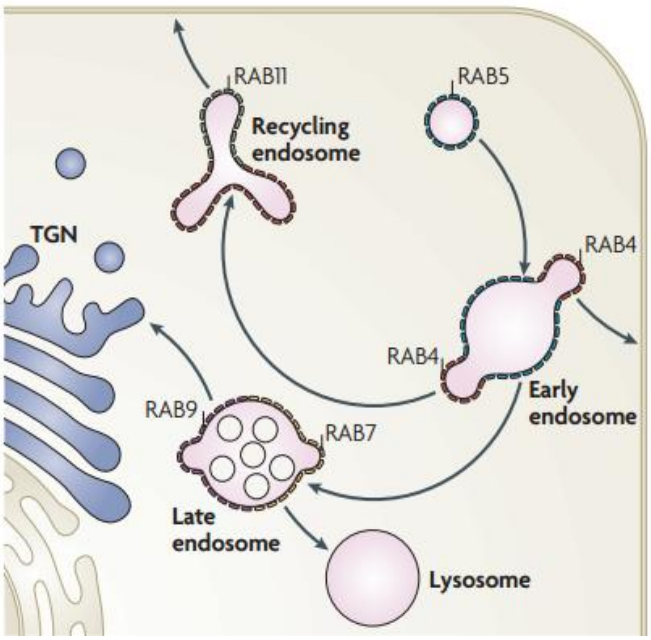

Figure I.6. Diagram of the distinct recycling pathways (Stenmark, 2009).

3. Cell polarity

Physiologically, cells belonging to the different organs display an asymmetric distribution of their proteins along their membranes and into the intracellular spaces. This ability of cells to asymmetrically distribute their biomolecules into the cell is the basis of the cell polarity and is a mechanism evolutionarily conserved. Polarity is a fundamental requirement for a wide range of cellular functions such as directional cell migration, being a key event during embryonic morphogenesis, tissue repair, regeneration and carcinogenic processes. Several types of cell polarity have been described to differently regulate the localization of the proteins within the cell (Khursheed and Bashyam, 2014; Muthuswamy and Xue, 2012).

Apical-basal polarity consists on the asymmetry of the plasma membrane showed by columnar epithelial cells. These epithelial cells can form organized structures such as tubes, alveoli and stratified sheets which function as permeability barriers and protect against mechanical forces due to the ability to maintain robust cell-cell and cell-matrix adhesions. Cells maintaining epithelial phenotype have two main differentiated regions of the plasma membrane, as follows: in the one hand, the apical basal membrane which is in contact with the luminal space and plays a role in secretion, absortion and excretion. On the other hand, basolateral membrane allows the formation of the cell-cell unions such as tight and adherens junctions, and scaffolds the epithelial tissue to the underlying connective tissue. Noticeably, the maintenance of the epithelial polarity is essential for the normal physiological functions as well as for the tissue integrity (Halaoui and McCaffrey, 2015; Muthuswamy and Xue, 2012).

In this connection, epithelial cells can switch into a mesenchymal phenotype under determined conditions through a process commonly termed epithelial to mesenchymal transition, which will be defined below (*see 5. Epithelial to mesenchymal transition*). The acquisition of mesenchymal features provide migratory abilities to the cells which are due to the alignment of intracellular compartments and proteins to control the direction of cell migration, a process known as **front-rear polarization** (Muthuswamy and Xue, 2012).

Additionally to apical-basal polarity, cells usually are polarized within the plane of the tissue in a two dimension plane. This type of cell polarity, termed **planar cell polarity**, allows to maintain the tissue order and to achieve larger scale morphogenesis. Although planar cell polarity is mostly studied in *Drosophila* models, it has been reported to be responsible for the right orientation of the epidermis of vertebrates, for instance the scales of fish and hair of mammals. However, deepening into cells, planar polarity also exists at the subcellular level, for example in the common orientation of cilia on a multiciliated cell, as well as in the whole tissues such as in mouse limb hairs (Adler, 2002; Goodrich and Strutt, 2011; Muthuswamy and Xue, 2012).

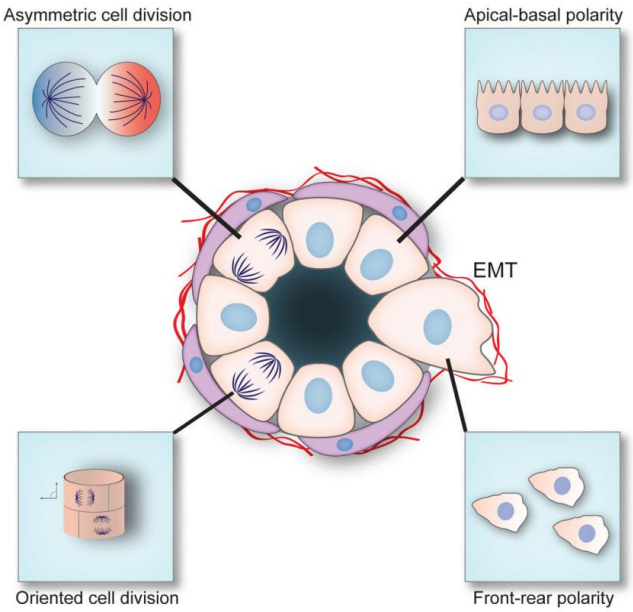

Figure I.7. Types of cell polarity (Adapted from Muthuswamy and Xue, 2012).

Last but not least, dividing epithelial cells regulate the plane of cell division for an efficient disposal of the daughter cells into the tissue through the spindle orientation into a mechanism known as **spindle polarity**. This type of cell polarity not only affects adult dividing cells into the tissues but also embryo cells in which leads to precise space relationships between them (Muthuswamy and Xue, 2012; Walston and Hardin, 2006).

3.1. Apical-basal polarity complexes

The apical-basal cell polarity establishment and maintenance are highly conserved processes from bacteria to humans. Although the genes implicated in the regulation of cell polarity have been iniatially reported in Caenorhabditis elegans and Drosophila melanogaster, further studies focused in mammalian epithelial cells in physiological but also in pathological conditions (Muthuswamy and Xue, 2012).

The different proteins regulating apical-basal polarity can be classified in complexes depending on their subcellular localization: the Par, the Scribbled and the Crumbs complexes (Muthuswamy and Xue, 2012).

3.1.1. Par complex

The first genes involved in cell polarization were identified in 1988 by Kemphues et al. in a *C.elegans* zygote model (Kemphues et al., 1988). They have reported that the different proteins of the Par complex were responsible for the asymmetric divisions of *C. elegans* embryo and identified six genes called *par* (for partitioning defective). The products of *par* genes have diverse biological functions, as follows. Par1 [also known as MARK2 or microtubule-affinity-regulating kinase (Drewes et al., 1997); and EMK1 for ELKL-motif kinase (Espinosa and Navarro, 1998)] and Par4 (also termed LKB1 in human) are serine/threonine protein kinases. Par3 and Par6 (which accounts with the isoforms *PARD6A*, *PARD6B* and *PARD6G*) are scaffold proteins that contain PDZ (post synaptic density 95; discs large; zonula occludens-1) domains. Par2 is a RING finger protein that may function as an E3-ubiquitin ligase but no human homolog is known. Finally, Par5 is a 14-3-3 protein (Muthuswamy and Xue, 2012).

Regarding cell polarization in mammal epithelia, the apical-lateral border is structurally defined by the tight junctions, a specialized intercellular adhesion complex (Aranda et al., 2008a; Tsukita et al., 2008). Par complex is properly composed by Par3, Par6 and the atypical protein kinase C (aPKC). This complex localizes at tight junctions defining the limit between the apical border and the basolateral one and contributes to its formation (Hirose et al., 2002).

Par3 promotes junction assembly by the regulation of actin dynamics (Chen and Macara, 2006) and provides an anchorage to bind Par6 and recruit Par6-associated proteins to the apical-basolateral border (Aranda et al., 2008a). Par6 physically interacts with aPKC through its PB1 domains and acts as an inhibitor of aPKC kinase activity and also recruit Par3, a well-known substrate of aPKC (Hirano et al., 2005). Cdc42-GTP, a small GTPase of the Rho family, has the ability to bind to Par6/aPKC complex (Joberty et al., 2000) and enhances the phosphorylation of Par3 through aPKC activity (Izumi et al., 1998; Nagai-Tamai et al., 2002). Furthermore, Par3 interacts with Tiam1, a Rac guanine nucleotide-exchange factor, becoming an important step for tight junction formation and epithelial morphogenesis (Aranda et al., 2008a; Mertens et al., 2005).

By its part, the aPKC was found to account with several different substrates, being many of them polarity regulators. Phosphorylation of other polarity regulators outside the Par complex establishes the cross talk necessary to maintain plasma membrane asymmetric domains. So, Crumbs protein is restricted to the apical domain thanks to aPKC-mediated phosphorylation and, concomitantly, it upregulates aPKC activity for the efficient inhibition of the activity of basolateral regulators such as the Scribble complex at the apical space (Aranda et al., 2008a; Sotillos et al., 2004). In this sense, aPKC controls the establishment of the basolateral domain by phosphorylating Lgl to exclude it from the apical membrane and restricting its activity to the basolateral border (Aranda et al., 2008a; Yamanaka and Ohno, 2008). Consequently, it has been demonstrated that aPKC regulates the maintenance of the apical-basal polarity by taking part in distinct complexes, for instance by interacting with both Lgl and Par3 in a mutually exclusive manner (Aranda et al., 2008a; Hutterer et al., 2004).

3.1.2. Crumbs complex

Very briefly, the Crumbs complex localizes in the apical border and comprises three proteins: the transmembrane Crumbs protein, Pals1 and PATJ (Pals1-associated TJ protein). Crumbs complex defines apical identity by recruiting actin cytoskeleton regulators Moesin and β H-spectrin (Médina et al., 2002; Muthuswamy and Xue, 2012). Moreover, PATJ seems to play a key role in Par complex-dependent directional migration of MDCK cells (Khursheed and Bashyam, 2014; Shin et al., 2007).

3.1.3. Scribble complex

The Scribble complex comprises three proteins: Scribble, Discs large (Dlg) and Lethal giant larvae (Lgl). All three proteins are thought to act as scaffold proteins with the ability to regulate protein-protein interactions. The Scribble complex localizes at the lateral membrane and functions restricting the apical domain by antagonizing the Par complex (Humbert et al., 2006; Muthuswamy and Xue, 2012). Additionally, it has been reported a role for the Scribble complex in the regulation of the planar cell polarity by physical interaction with core components of the PCP machinery (Humbert et al., 2006; Montcouquiol et al., 2006). Although a direct physical interaction between Scribble and Lgl2 in polarized mammalian epithelial cells has been reported, the interactions between Scribble, Lgl and Dlg are still poorly understood (Humbert et al., 2006; Kallay et al., 2006). However, Scribble has been shown to interact with ather several proteins that potentially could mediate its effects on cell polarity such as components of Wnt signaling pathway, the Rho-GTPase regulatory βPIX-GIT1 complex and G-protein coupled receptors. Regarding the other Scribble complex components, Dgl has been described to bind Wnt signaling components and Lgl has been shown to bind myosin II, vesicle trafficking SNARE components and the Par polarity complex (Wirtz-Peitz and Knoblich, 2006). Thus, even the mechanisms coordinating these processes remain obscure, it has been suggested a role for the Scribble complex in the regulation of signal transduction, cytoskeletal remodeling and vesicle trafficking (Humbert et al., 2006).

At this point, we will focus on the Par complex as it is responsible for the establishment of differentiated plasma membrane domains, so contributing to the maintenance of the epithelial phenotype and an apical-basal polarity. Furthermore, as it will be explained below, the Par complex has been reported as the unique polarity complex sharing a transduction pathway with TGF-β.

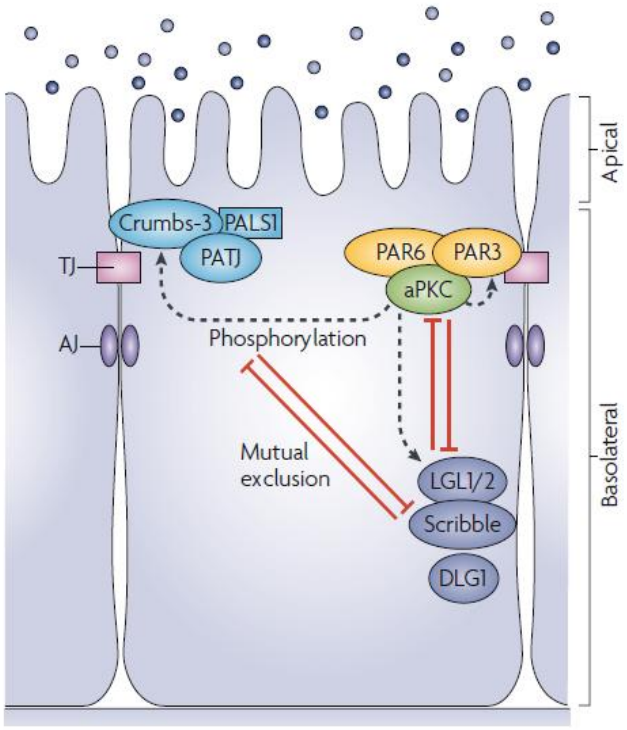

Figure I.8. Protein complexes responsible for apical-basal cell polarity and their interactions (Iden and Collard, 2008).

3.2. Par polarity complex related pathways

The ability of Par3 and Par6 to bind different adaptor and signal through the aPKC-dependent phosphorylation of distinct substrates and downstream effectors confers the Par polarity complex the capability to modulate the outcome of extracellular inputs by dinamically changing its composition (Aranda et al., 2008a; Bose and Wrana, 2006). In this connection, it has previously reported that the Par complex plays a role interacting with other signaling systems such as small GTPases or phosphoinositide signaling (Etienne-Manneville and Hall, 2002; Martin-Belmonte and Mostov, 2007). Although very little is still known, modulators of aPKC such as Dap60/intersectin may unravel

new connections between the Par complex and other signaling pathways, for instance the link with Ras signaling (Aranda et al., 2008a; Wang et al., 2005).

Another protein linked to the Par complex is the glycogen synthase kinase-3β (GSK-3β). The aPKC-mediated phosphorylation of GSK-3β determines the direction of migration of astrocytes and fibroblasts while in 3D organized kidney epithelial cells inhibits apoptosis (Aranda et al., 2008b; Etienne-Manneville et al., 2005; Farooqui et al., 2006). Alternatively, insulin signaling is negatively regulated by Par6-aPKC in myoblasts. The suggested mechanism consists on Par6-aPKC-dependent inhibition of Akt and insulin receptor substrate 1 induced by insulin (Aranda et al., 2008a; Weyrich et al., 2004, 2007).

Furthermore, although more studies are necessary to completely understand this issue, it is worth to underline that the members of the Par complex may have different cell-type specific functions. So, aPKC has been described to participate in c-Jun and NF-κB pathway although the precise function of aPKC in these systems remains unknown (Aranda et al., 2008a; Moscat et al., 2006).

Nevertheless, probably the Par6-TGF-β pathway is one of the better studied connections between the Par complex and other systems. Par6 binds to TGF-β receptor I (TβRI) in tight junctions and is recruited by TGF-β receptor II (TβRII), which phosphorylates Par6 on serine 345 and maintains it bound to the receptor complex. The prevention of serine 345 phosphorylation of Par6 blocks TGF-β-dependent loss of tight junctions (Bose and Wrana, 2006; Ozdamar et al., 2005). This process is independent on transcriptional regulation of gene expression by the Smad complex. By contrary, it has been suggested that the Par6 polarity complex directly regulates Smad functions, since it has been reported that Smad3 may interact with Par3 (Bose and Wrana, 2006; Warner et al., 2003).

After forming the complex Par6-TGF-β receptors and following phosphorylation of Par6 on serine 345, this last is able to recruit the E3 ubiquitin ligase Smurf1 to tight junctions. Smurf1 targets RhoA ubiquitinating and degradating it within a process that finally lead to the dissolution of the tight junctions. Moreover, the TβRII also phosphorylates and activates the TβRI. For its part, the TβRI trigger the Smad transcriptional pathway ending up, together with the tight junction

dissolution effect, to the promotion of TGF-β-dependent EMT (Bose and Wrana, 2006; Ozdamar et al., 2005).

Furthermore, it has been also reported a cross-talk between the TGF-β pathway and Cdc42. The TGF-β-dependent activation of Cdc42 has been shown to modulate cell movement in motile cells coordinated with the TGF-β-induced EMT (Bose and Wrana, 2006; Edlund et al., 2004).

Finally, Par3 has been reported to be down-regulated by TGF-β during the EMT process in rat proximal epithelial cells. Additionally, the Par complex is disrupted after TGF-β treatment, being Par6-aPKC complex mislocalized into the cytosol. Hence, a protective role for Par3 in TGF-β-induced EMT has been established (Wang et al., 2008b). Nonetheless, more studies are necessary to extend in the mechanisms regulating the Par complex.

3.3. Par complex in cancer

As previously reported, cell polarity consists on a huge protein network and pathways capable of maintaining a plasma membrane asymmetry to physiologically uphold the tissue functionality. For this reason, the loss of the normal physiological polarity or the switch from an apical-basal to a front-rear one is required for other biological processes such as cancer. In this sense, cell polarity has been reported to be implicated in stem cell division and in cell migration (Aranda et al., 2008a; Lee and Vasioukhin, 2008) suggesting to have a role during carcinogenic processes (Aranda et al., 2008a). Actually, some cellular mechanisms, such as stem cell regulation and epithelial-to-mesenchymal transition, which require spatial asymmetry and polarized signaling, highlighted the potential relevance of cell polarity as a regulator of multiple aspects of oncogenesis (Aranda et al., 2008a; Moreno-Bueno et al., 2008).

Par complex has been observed to participate in polarized cell migration due to its capability to spatially control actomyosin fiber activity and GTPase activity. In astrocytes and fibroblasts, integrins are ligated at the leding edge, recruiting Cdc42 and activating aPKC bound to Par6 (Aranda et al., 2008a; Etienne-Manneville and Hall, 2002). The aPKC remains restricted at the leading edge

and phosphorylates GSK-3β at an inhibitory serine, dettaching it from its substrate and making it free to bind to the plus end of microtubules, anchoring them at the plasma membrane through binding to Dlg1 (Etienne-Manneville, 2013). This anchorage will promote the formation of a polarized cytoskeleton and redistributes the microtubule organization center in the direction of migration (Aranda et al., 2008a; Gomes et al., 2005). Cdc42 contributes to polarized migration by regulating Par6 and aPKC (Anderson et al., 2008; Aranda et al., 2008a) but also regulates actin polymerization and microtubule organization center orientation through Par-independent mechanisms (Aranda et al., 2008a; Cau and Hall, 2005). Furthermore, Par3 and Par6 have complementary functions to achieve spatio-temporal control of GTPase signaling during polarized migration. Par6-aPKC complex recruits the E3 ubiquitin ligase Smurf1 at the leading edge and leads to the RhoA degradation. Alternatively, Par3 binds to Tiam1 to restrict Rac activity (Nakayama et al., 2008; Zhang and Macara, 2006).

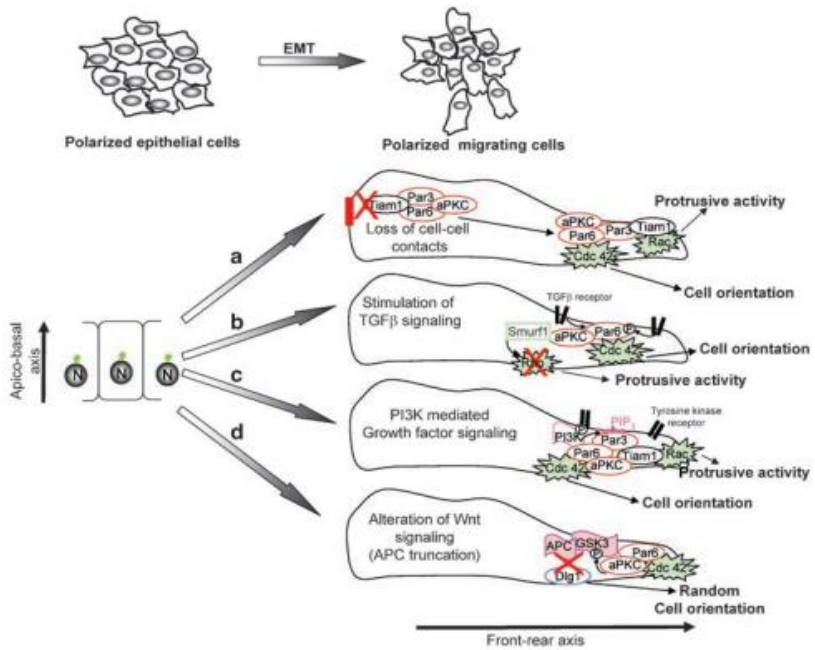

Figure I.9. Implication of the Par complex in cancer progression (Etienne-Manneville, 2008).

In addition to the role of the Par complex in polarized cell migration, it has been also reported a role for the Par complex in the regulation of oncogenic and tumor supressor pathways. In breast tumors, it has been published that Par6 is genetically amplified and promotes activation of mitogen-activated protein kinase (MAPK) signaling and growth factor-independent proliferation through a Cdc42- and aPKC-dependent interaction (Aranda et al., 2008a; Nolan et al., 2008). Moreover, the hyperactivation or mislocalization of the aPKC have been reported to affects tumor growth, motility and proliferation (Cohen et al., 2006; Kuribayashi et al., 2007; Sun et al., 2005). Another interesting tumor supressor pathway that may be regulated by the Par complex is the von Hippel-Lindau (VHL) factor, which modulates proliferation through the levels of hypoxia-induced factors and has been shown to physically bind and induce degradation of aPKC (Aranda et al., 2008a; Kuehn et al., 2007).

ErbB2, a tyrosine kinase receptor playing a relevant oncogenic function in breast cancer and amplified in 25-30% of the cases (Yarden and Sliwkowski, 2001), regulates Par complex and consequently cell polarity, which becomes a checkpoint in breast tumor transformation. The interaction between ErbB2 and the Par6-aPKC complex is able to transform organized epithelial cell by recruting both proteins away from Par3 and the apical-basal border, thus disrupting the Par3-Par6-aPKC complex (Aranda et al., 2006).

4. Intracellular trafficking and cell polarity

Exocytic intracellular trafficking hubs are able to specifically target proteins or other biomolecules to precise regions of the plasma membrane of polarized cells. In this issue, membrane proteins account with a cytoplasmic domain to facilitate their assembly in vesicles and to sort them to apical or basolateral membranes. Glycosylphosphatidylinositol (GPI)-anchor, N- or O-linked glycosylation are apical sorting signals as specialized transmembrane domains or cytoplasmic determinants while basolateral sorting signals include tyrosine-based cytoplasmic domains, dileucine and monoleucin motifs, pleomorphic sequences and yuxtamembrane sequences (Mellman and Nelson, 2008; Muthuswamy and Xue, 2012). It is worth to underline that, in general, basolateral signals are more frequent than apical ones.

Although very little is known about the cross-talk between the intracellular traffic mechanisms and cell polarity (especially in human models), it has been reported by Peng and collaborators that mutated AP-1 and AP-2-interacting protein Nak and mutation of the AP-2α subunit induced mislocalization of Dlg from the basolateral membrane in the *Drosophila* salivary gland (Muthuswamy and Xue, 2012; Peng et al., 2009).

SNARE proteins are implicated in the docking and fusion of the vesicles containing cell membrane proteins. Syntaxins (STX) are members of the SNARE family that provide vesicles a target to specifically localize membrane proteins in the differentiated domains. Despite the inespecificity of STX2, STX3 particularly target vesicles to the apical domain whereas STX4 targets to basolateral membrane (Low et al., 1996). Scribble and Dlg proteins (*Below, see 5.1.3 Scribble complex*) interact with STX4 in mammalian cells (Massimi et al., 2008; Muthuswamy and Xue, 2012).

Another regulator protein family important for intracellular traffic is the Rab GTPases, being involved in all steps of trafficking. Rab11 is essential for the junctional maintenance of E-cadherin and Crumbs (Muthuswamy and Xue, 2012; Roeth et al., 2009). Furthermore, Rab8 and Rab11 target Par3 to the apical membrane in MDCK cells through the interaction with the exocyst complex (Bryant et al., 2010).

Despite these initial evidences demonstrate the existence of a relationship between cell polarity proteins and intracellular traffic machinery, they importantly highlight the gap in our knowledge about how cell polarity and vesicle trafficking interact to generate intracellular asymmetry (Muthuswamy and Xue, 2012).

5. Epithelial-to-mesenchymal transition

Prior to precisely define the epithelial-to-mesenchymal transition (EMT), it is worth to underline some characteristics defining the epithelial and the mesenchymal cell phenotype. Epithelial cells associate among them by using cell-cell contact structures at the lateral membrane (Lamouille et al., 2014). One of the most important one is tight junctions, which are membrane fusions at the border between lateral and apical domains. Occludins and claudins are important components of the intercellular tight junctions strands while the cytoplasmic components Zonula Occludens (ZO)-1, -2 and -3 are the responsible for the actin fibers attachment contributing to the strength and integrity of tight junctions (Tsukita et al., 2001). On the other hand, adherens junctions are located at the lateral membrane below the tight junctions (Niessen and Gottardi, 2008). The transmembrane adhesion receptor E-cadherin binds to β-catenin, which in turn binds to α-catenin, and anchors to the cytoskeleton (Wheelock and Johnson, 2003).

EMT consists on a transient and reversible switch from an epithelial, polarized, to a mesenchymal or fibroblastoid cellular phenotype occurring during physiological conditions such as embryogenesis but also during pathological processes, for instance fibrosis and cancer (Hollier et al., 2009; Thiery and Sleeman, 2006). The inverse process, the mesenchymal-to-epithelial transition (MET), can be carried out after migration and homing into new sites during embryogenesis or tumor progression (Heldin et al., 2009). EMT requires disassemble of adherens junctions and reorganization of the actin cytoskeleton driving to the formation of stress fibers anchored to focal adhesions to take place. The loss of E-cadherin is considered as a hallmark event of EMT initiating a series of signaling events, but it should not be taken as the sole pivotal event in EMT. Cells undergoing EMT acquire a mesenchymal phenotype providing them motile or invasive features (Thiery, 2003). Furthermore, mesenchymal cells express some specific cytoskeletal proteins, such as vimentin, and increase the production of extracellular matrix proteins, for instance fibronectin and collagens. This extracellular matrix components induce

the formation of focal adhesion complexes, then facilitating cell migration (Imamichi and Menke, 2007; Thiery and Sleeman, 2006).

Several different signaling molecules are capable of trigger EMT, for example the epidermal growth factor (EGF), fibroblast growth factor (FGF), hepatocyte growth factor (HGF) and transforming growth factor-β (TGF-β), among others. These stimuli up-regulate the expression of some families of transcription factors including Snail and Zeb families which contribute to the control of EMT by leading changes in gene expression patterns to promote a decrease of the epithelial-related genes and a gain of the mesenchymal-related ones (Barrallo-Gimeno and Nieto, 2005; Moreno-Bueno et al., 2008). Commonly used molecular markers for EMT include, additionally to the previously mentioned ones, the reduced expression of cytokeratins, increased expression of N-cadherin and the nuclear localization of β-catenin (Lee et al., 2006).

Regarding the role of EMT in cancer, the epithelial cells undergoing EMT acquire a more invasive phenotype which allows them to enter the circulatory system through intravasation. This process results in the dissemination of cancer cells away from the primary tumor, establishing new cancer cells location. The colonization of these secondary sites is completed through the MET process, which allows cancer cells to establish new tumor foci (Hugo et al., 2007).

In general, EMT leads to a loss of apical-basal polarity and it allows cells to switch to a front-rear polarity that facilitates their ability to migrate in a directional fashion. The increased expression of extracellular proteases such as matrix metalloproteinases, allow cells to degrade extracellular matrix proteins enhancing their migratory capabilities to acquire an invasive behavior (Moustakas and Heldin, 2007).

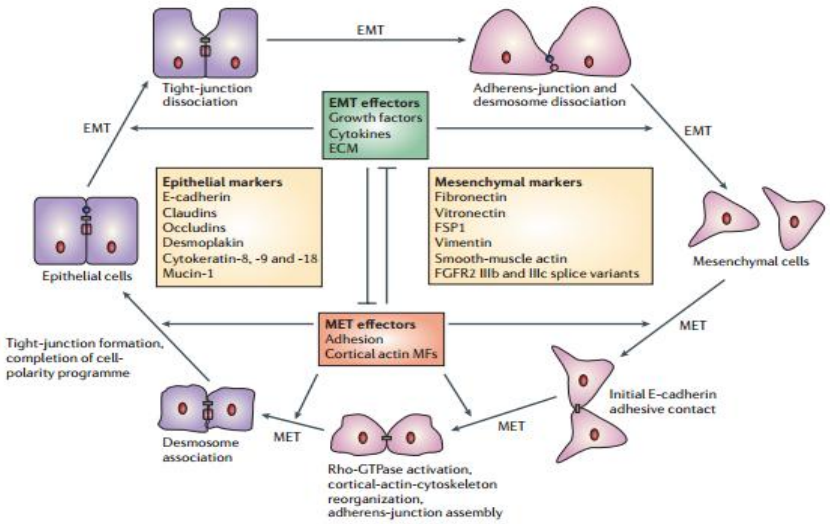

Figure I.10. The cycle of epithelial cell plasticity (Thiery and Sleeman, 2006).

6. Transforming growth factor-beta (TGF-β)

The transforming growth factor-beta (TGF-β) is a cytokine secreted by several cell types implicated in some physiological processes, but interestingly it is taking part in many human diseases such as bronchial asthma, heart disease, immune disorders, Marfan syndrome, diabetes, fibrosis, and also several types of cancer. Our group has been faithfully focused on the study of the role of the TGF-β in the healthy liver as well as in liver pathologies, including liver cancer. Precisely, our previous studies encompass the role of TGF-β pathway in cell death, differentiation, migration, invasion and proliferation in liver fibrosis and, of course, in hepatocarcinogenesis. Consequently, in this section it will be specifically dissected the implication of TGF-β in liver and in liver cancer.

6.1. TGF-β in cancer

As previously mentioned, the over-activity of the TGF-β family membrers has been correlated with many diseases, including cancer. It has been reported that cancer cells but also tumor stroma, blood platelets and tumor-infiltrating cells release high amounts of TGF-β after tissue injury (Massagué, 2008). To understand the role of TGF-β in human cancer malignancies, it is important to highlight the dual role that it exerts. On the one hand, TGF-β acts as a tumor suppressor during early stages of tumorigenesis. On the other hand, it promotes invasiveness and metastasis in late stages when cells acquire resistance to TGF-β-tumor suppressive effects. Cancer cells commonly accumulate inactivating mutations in Smad proteins, which are the canonical signal effectors of TGF-β, as described in pancreatic, colorectal and ovarian tumors, between others. However, the mutations and deletions of TGF-β signaling-related genes are infrequent in HCC (Fabregat et al., 2014; Zhang, 2009).

Although TGF-β promotes HCC acting as an autocrine or paracrine growth factor of tumor cells (termed intrinsic activity), it also acts on the surrounding cells, termed stroma (termed extrinsic activity), where it can also promote tumor cell survival, angiogenesis, invasiveness and metastasis. Furthermore, cancer cells over-produce TGF-β in advanced cancer stages, inducing the expression of some mitogenic factors, for instance HGF or PDGF, and interacting with the

tumor stromal environment by targeting fibroblasts, myofibroblasts, vascular cells and immune cells. It is worth to underline that the intrinsic effects are mainly observed in highly invasive tumor conditions in which TGF-β promotes tumor proliferation and survival but also an increased metastatic potential, given by the fact that cells surviving to TGF-β supressor effects undergo EMT (Fabregat et al., 2014; Heldin et al., 2009; Pardali and Moustakas, 2007).

In the concrete case of hepatocarcinogenesis, TGF-β specific gene expression signature has been useful to classify and to predict the prognosis of HCC patients. A comparative functional genomics approach demonstrated that a temporal TGF-beta gene expression signature established in mouse primary hepatocytes successfully discriminated distinct subgroups of HCC. This TGF-β gene expression signature demonstrated to have a predictive value for patients with HCC (Coulouarn et al., 2008). TGF-β exhibits tumor stage dependent properties: suppresive effects, (consisting in growth inhibition) or oncogenic effects (that is, invasiveness). The early TGF-β signature is associated to supressor genes and a longer survival of patients. However, late TGF-β signature is associated to EMT, migration and invasion, coinciding with a shortened mean survival time for patients. Furthermore, the late TGF-β-responsive genes lead to the acquisition of an invasive phenotype, an increased tumor recurrence and a potential liver metastasis. So, this study discriminated HCC cell lines by degree of invasiveness (Coulouarn et al., 2008).

6.2. TGF-β signaling pathway

The TGF-β superfamily consists of several members in humans, including growth factors such as bone morphogenic proteins (BMPs), growth and diferentiation factors (GDFs), activins and inhibins, nodal and anti-Müllerian hormone and TGF-βs. They play important roles during developments and in physiological processes but also in some diseases controlling cell proliferation and differentiation, apoptosis, extracellular matrix production and migration. The disruption of TGF-β signaling has been reported to contribute to the progression of several diseases, for instance, fibrosis, autoimmune diseases and cancer. (Heldin et al., 2012; Pardali and Moustakas, 2007; Ross and Hill, 2008).

Three different isoforms of TGF-β are known: TGF-β_1, TGF-β_2 and TGF-β_3. All of them are synthesized by the cell as a pro-peptide precursor that is cleaved to be mature. TGF-β signaling requires the formation of a tetrameric complex of type I and type II serine/threonine kinase receptors. Although different type I and II receptors are described, TGF-β preferentially signals through the activin receptor-like kinase 5 (ALK5) type I receptor and the TGF-β type II receptor (TβRII). The constitutively active type II receptor phosphorylates and activates the type I receptor, which then phosphorylates downstream effectors of the Smad family through the **canonical TGF-β signaling**. In humans, Smad family consists of eight members that can be divided in three subgroups: receptor-associated Smads (R-Smads), a co-operating Smad (Co-Smads) named Smad4 and two inhibitory Smads (I-Smads) termed Smad6 and Smad7. As for R-Smads, vertebrates have 5 different ones called Smad1, 2, 3, 5 and 8. Only Smad2 and 3 mediate the TGF-β signaling, while Smad1, 5 and 8 is utilized exclusively by the BMP branch. Upon TGF-β stimulation, Smad2 and Smad3 are phosphorylated and they bind to Smad4 forming a complex that is translocated to the nucleus and acts as a transcription factor regulating the expression of different genes by the binding to its promoters (Drabsch and ten Dijke, 2012; Heldin et al., 2009; Morrison et al., 2013; Padua and Massagué, 2009; Ross and Hill, 2008).

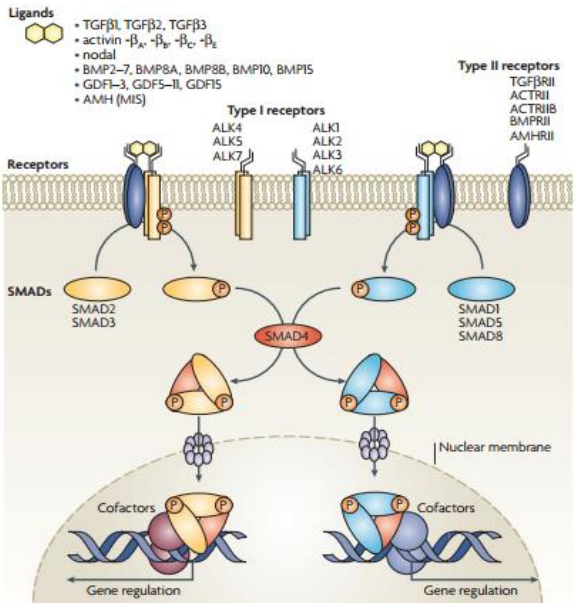

Figure I.11. Canonical TGF-β pathway (Schmierer and Hill, 2007)

Additionally to the canonical Smad-dependent pathway, TGF-β also activates non-Smad pathways such as non-receptor protein kinases Src and FAK, PI3K/AKT, MAPK and Rho-GTPases Ras, Rho and Rac1 to mediate some other biological responses. Moreover, these non-canonical pathways can also regulate the Smad-dependent pathway (Drabsch and ten Dijke, 2012; Heldin et al., 2009; Morrison et al., 2013; Murillo et al., 2005; Pardali and Moustakas, 2007; Yu et al., 2008).

In addition, the reported cross-talk between TGF-β and EGF signals in hepatocytes strengthen the evidence of the resistance to TGF-β supressor effects through the increase of the EGFR ligands. It has been described that TGF-β activates EGFR, which is required for Akt activation. In fact, TGF-β activates ADAM17, which promotes the shedding of EGFR-like ligands and leads to c-Src activation. The activation of EGFR plays a role impairing apoptosis but it is not essential for the EMT process (Del Castillo et al., 2006; Moreno-Càceres et al., 2014; Murillo et al., 2005; Wang et al., 2008a).

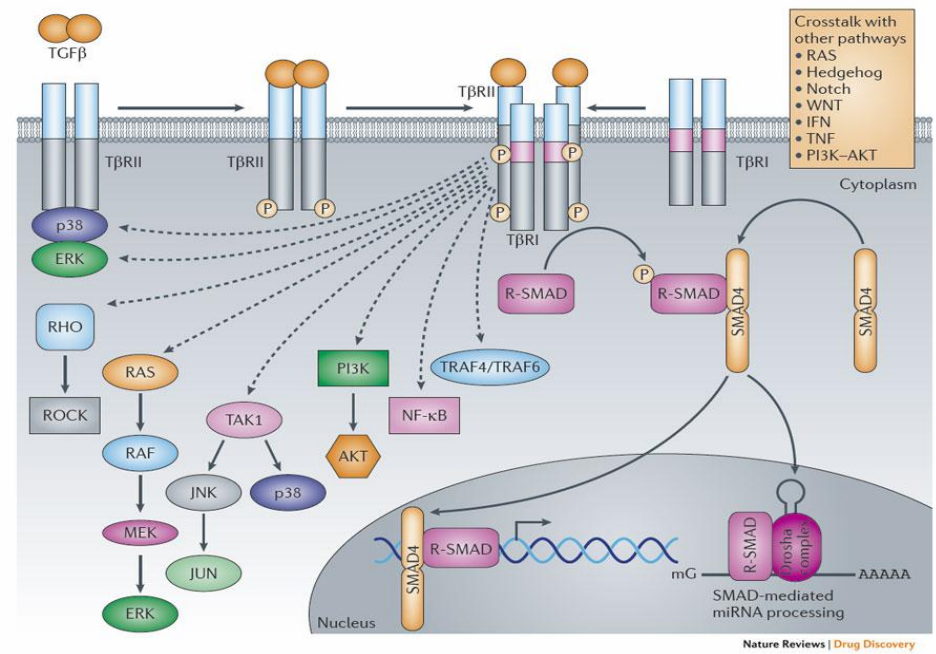

Figure I.12. Non-canonical TGF-β pathway (Akhurst and Hata, 2012)

6.3. TGF-β and EMT

As previously described, EMT is a complex cellular mechanism involved in both physiological and pathological processes. Among all the possible EMT inducers, TGF-β is one of the most studied.

TGF-β has the ability to induce EMT and to consequently down-regulate epithelial markers such as E-cadherin, some specific cytokeratins and ZO-1 and up-regulate mesenchymal markers such as vimentin, fibronectin and α-smooth muscle actin (SMA). Fitting with the previous introduction, TGF-β also provokes a rearrangement of actin cytoskeleton from a cortical organized to a stress fibers network connected to focal adhesions (Pardali and Moustakas, 2007).

Focusing in the liver, both normal and tumoral hepatocytes surviving to TGF-β-induced apoptosis undergo EMT (Caja et al., 2007; Rossmanith and Schulte-Hermann, 2001). TGF-β mediates EMT through Smad dependent and independent pathways through the regulation of the expression of EMT effector genes. It has also been reported that TGF-β cooperates with Ras and Wnt pathways to induce EMT (Massagué, 2008). It is known that TGF-β up-regulate some transcription factors, for instance Snail and Slug, as EMT inducers (Miyoshi et al., 2005; Sugimachi et al., 2003). Snail1 has been reported to confer resistance to TGF-β-induced cell death, being sufficient to induce EMT in adult hepatocytes. Furthermore, Snail1 silencing prevents EMT and restores TGF-β-mediated cell death (Franco et al., 2010). In this situation, hepatocytes are induced to start a dedifferentiation process and to lose epithelial markers and increase mesenchymal ones (Cicchini et al., 2006; Valdés et al., 2002).

Finally, even though EMT process depends on the ability of the cells to overcome TGF-β-induced apoptosis, this process later induces survival signals to prevent from further cell death (Valdés et al., 2002). In this issue, Snail has been shown to become a key player in the protection against apoptosis (Franco et al., 2010).

6.4. TGF-β biological roles

As previously mentioned, TGF-β regulates various cellular processes such as cell proliferation, migration, extracellular matrix production, cytokine secretion and apoptosis. Focusing in the liver tissue, TGF-β induces **cell cycle arrest** in hepatocytes at low doses (Sánchez et al., 1996), an effect counterbalanced by the EGF or insulin proliferative signals (Carr et al., 1986; Sánchez et al., 1998). Moreover, the role of TGF-β as an antiproliferative effector has been reported in partial hepatectomy rat and mouse models with the function of preventing uncontrolled hepatocyte proliferation (Braun et al., 1988; Mead and Fausto, 1989).

Additionally, TGF-β also acts as an **inducer of apoptosis** through the Smad-dependent pathway (Pardali and Moustakas, 2007). However, other Smad-independent mechanisms are described in a variety of cell lines to promote apoptosis by TGF-β stimulation. Nevertheless, this signal ends up with the activation of pro-apoptotic caspases and changes in the expression, localization and activation of pro- and anti-apoptotic members of the BCL2 family. It is worth to foreground that the apoptotic signaling induced by TGF-β consists in a complex network of apoptosis-related events that might occur differently dependent on cell type but also on the cell context and the extracellular environment (Padua and Massagué, 2009).

In epithelial cells, for instance fetal rat hepatocytes, TGF-β-induced apoptosis is coincident with reactive oxygen species (ROS) production (Sánchez et al., 1996, 1997) through two different mechanisms: on the one hand, the induction of a nicotinamide adenine dinucleotide phosphate (NADPH) oxidase system that increases extramitochondrial ROS (Herrera et al., 2004); on the other hand, the depletion of antioxidant proteins that increase mitochondrial ROS (Coyle et al., 2003; Franklin et al., 2003; Herrera et al., 2004).

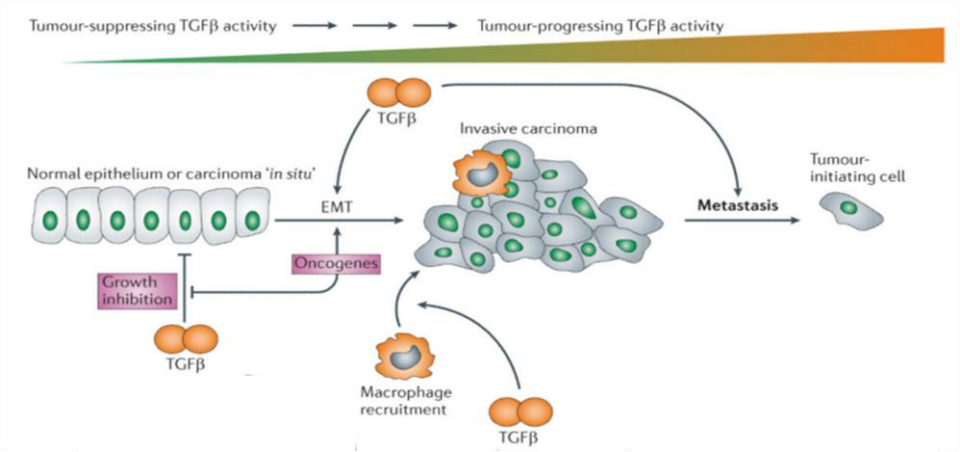

Figure I.13. Biological roles of TGF-β in cancer progression (Adapted from Akhurst and Hata, 2012)

However, TGF-β can also activate **survival pathways** by the promotion of a pro-apoptotic effect through the activation of AKT signaling and the subsequent increase of anti-apoptotic proteins (Song et al., 2006; Valdés et al., 2004; Wilkes et al., 2005). Nonetheless, AKT activation is transient and might be related to the capability of TGF-β to transactivate c-Src and EGFR pathways (Murillo et al., 2005; Park et al., 2004). TGF-β would then mediate the autocrine production of EGFR ligands, confering resistance to apoptosis in hepatocytes (Del Castillo et al., 2006; Murillo et al., 2007) and HCC cells (Caja et al., 2011b), and the inhibition of the EGFR pathway enhances TGF-β-induced apoptosis (Sancho et al., 2009). Interestingly, this capacity of hepatocytes to survive to TGF-β is dependent on their differentiation status (Sánchez et al., 1999). Similarly, the diverse features of different HCC cells, for instance the EGFR or MEK/ERK pathways activation, may be responsible of different outcomes after TGF-β stimulation (Caja et al., 2009, 2011b).

7. Chemokines: classification and function

Chemokines are small molecules governing aspects of host defense and inflammation such as cell trafficking of several types of leukocytes through the interaction with seven-transmembrane, G protein-coupled receptors (GPCR), originally reported to mediate different pro- and anti-inflammatory responses. Chemokines are sub-divided into four families depending on the position of the cysteine residues in the N-terminal region: CXC, CC, C and CX3C families (Ghanem et al., 2014; Zlotnik and Yoshie, 2000).

Numerous cell types of leukocytes are described to secrete chemokines which were originally described as mediators in leukocyte migration to inflammatory sites and to secondary lymphoid organs. Chemokines exert their functional effect through the binding to GPCRs, which are named differently coinciding with subclassification for chemokines, as follows: CXCR, CCR, CR and CX3CR. These proteins play important physiological roles, as previously cited, in immune response but also in the maintenance of the homeostasis in lymphoid tissues. However, additionally to the physiological functions, they can also take part in pathological processes due to their ability to induce cytoskeletal rearrangement, firm adhesion to endothelial cells and directional migration (Baggiolini, 1998; Campbell and Butcher, 2000; Ghanem et al., 2014).

Precisely, chemokine were reported to play an essential role in cancer. To be brief, chemokines facilitate tumor progression through increasing cell growth, inducing angiogenesis and mediating tumor cell evasion of immune system. Moreover, some studies sustain an active role for some chemokines in initiation, promotion and tumor progression, taking part in cellular migration, invasion, angiogenesis, tumor growth and metastasis (Vandercappellen et al., 2008; Zhu et al., 2012).

Chemokines are active players in the pathogenesis of HCC, regardless of his etiology. Generally, prior to HCC transformation, an inflammation and lymphocytic infiltration followed by the development of cirrhosis are mediated by chemokines. Furthermore, the role of chemokines in HCC pathogenesis is

supported by the fact that HCV patients who respond to interferon have a 20% lower risk of developing HCC (Castello et al., 2010; Ghanem et al., 2014).

Prior to HCC, liver inflammation by HCV infection is a process which is regulated by chemokines, for instance CXCL9, CXCL10, CXCL11, CCL3, CCL4 and CCL5 driving migration and activation of T-lymphocytes in patients expressing CXCR3 or CCR5. When these chemokines attract non-specific T-lymphocytes, a perpetuate inflammation is produced (Kang and Shin, 2011; Larrubia et al., 2008; Roberts, 2005).

Regarding the implication of chemokines in HCC, some receptors and ligands (altogether named axes) are described to participate actively in its development. Currently, it is an increased interest in CCL20/CCR6 axis as it may take part in growth and progression of HCC through phosphorylation of MAPK. Reports indicate that this axis plays a role in Huh7 growth promotion and that CCR6 expression levels are related with the degree of differentiation (Fujii et al., 2004; Huang and Geng, 2010). Moreover, it is considered as a poor prognostic factor after resection, being associated with a higher incidence of intrahepatic metastasis (Ding et al., 2012; Uchida et al., 2006). Other axes implicated in HCC are the CCL5/CCR1, which can promote metastasis and invasion of Huh7 cell line, the CCL3/CCR1, which contributes to the growth and progression of HCC, and serum CCL20, which is a potential marker of HCC in HCV-infected patients (Huang and Geng, 2010; Soliman et al., 2012). VCC-1 (VEGF correlated chemokine-1), also known as CXCL17, is a recently discovered chemokine suggested to play a role in invasion and tumor growth, indicating a potential role in HCC progression although its role in migration remains unclear, as well as VCC-1 interacting receptor (Huang and Geng, 2010; Mu et al., 2009; Zhou et al., 2012). Interestingly, chemokine axes are not restricted to contribute only to induce pro-tumorigenic effects but also take part in anti-tumorigenic processes. In this regard, CX3CL1/CX3CR1 axis regulates HCC cell cycle and enhances the anti-tumor effect of the immune system, inhibiting tumor growth. Anyway, studies have demonstrated that CX3CR1 is not a risk factor for HCC and further studies are needed to unravel its concrete mechanism.

Currently, there is an increasing interest in the study of the CXCR4/stromal derived factor-1 alpha (SDF-1α) axis as there have been reported some many evidences of its implication in HCC progression.

7.1. CXCR4/SDF-1α axis

CXCR4 chemokine receptor and its ligand, SDF-1α (also named CXCL12), are two important molecules that highlight the crosstalking between cancer cells and the microenvironment, which has a relevant role in driving the cancer cell biology and consequently becoming promising targets for cancer therapy.

SDF-1α was first characterized as a growth-stimulating factor for a B cell precursor clone, being isolated from murine stromal cell lines (Nagasawa, 2014). SDF-1α is a pleiotropic chemokine widely expressed in different organs including the brain, colon, lung, heart, kidney and liver. Its main function consists in chemoattract immature and mature hematopoietic cells, consequently playing a role in inflammation and immune surveillance of tissues. Moreover, SDF-1α functions as an emergent salvage signal for initiating tissue regeneration and repair. Despite SDF-1α mainly binds to CXCR4 to trigger the cellular response, interaction with another chemokine receptor, CXCR7, has been reported, which can heterodimerize with CXCR4 and activate G proteins in vitro. However, the relevance of the interaction between SDF-1α and CXCR7 in vivo remains unclear in mammals. Otherwise, the role of CXCR4/SDF-1α axis is better known. (Balabanian et al., 2005; Cojoc et al., 2013; Levoye et al., 2009; Ma et al., 1998; Nagasawa, 2014; Odemis et al., 2012).

Physiologically, CXCR4 is expressed in several different types of leukocytes, concretely in neutrophyls, eosinophyls, basophyls, monocytes and T-lymphocytes, allowing the response to SDF-1α gradients in terms of cell migration to inflammatory foci (Cojoc et al., 2013; Ma et al., 1998; Nagasawa, 2014). When SDF-1α is bound to CXCR4, heterotrimeric G protein is dissociated in operational subunits, triggering a cellular response through its downstream pathways. The downstream protein kinase B (AKT)/MAPK signaling pathway is activated, leading to alterations of gene expression, actin polimerization, cell skeleton rearrangement and cell migration. As described above for chemokines, CXCR4 also plays a role in physiological processes

such as maintenance of immunity homeostasis (for instance, allowing the migration of progenitor cells in embryonic development and the following differentiation into organs and tissues), hematopoiesis, brain development and physiological angiogenesis. Otherwise, some pathological functions related with tumor progression, for instance metastasis, survival and tumor-related angiogenesis are mediated by the CXCR4/SDF-1α axis. At the same time, CXCR4 was discovered to function as a co-entry receptor for human immunodeficiency virus HIV-1 in $CD4^+$ T-cells (Feng et al., 1996).

Although CXCR4 function was initially thought to be restricted to the immune system, afterwards some reports demonstrated an increased expression of CXCR4 in cancer cells. More than a decade ago, Muller et al. reported the CXCR4 overexpression in human breast cancer cell lines and primary and metastatic tumors when compared to normal breast tissue (Müller et al., 2001). At this time, more than 20 different human tumor types are shown to overexpress CXCR4, including prostate, oesophageal and liver cancer (Bertran et al., 2013; Kukreja et al., 2005; Wu et al., 2014). Furthermore, overexpression of CXCR4 has been also detected in tumor progenitor/cancer stem cells in different tumors, consequently increasing the interest in the study of CXCR4/SDF-1α axis.

7.1.1. CXCR4/SDF-1α axis in tumor progression

The CXCR4/SDF-1α axis was first described as a regulator of trafficking of B cells from patients with chronic lymphocytic leukemia. Few years later, CXCR4 was identified as a regulator of the trafficking and invasion of breast cancer cells to the metastasis sites. Currently, it is know that CXCR4 is highly expressed in more than 23 different types of tumors and that SDF-1α expression is higher in organs that commonly become sites of metastasis, for instance the liver, bone marrow and lungs. Taking this in consideration, tumor cells may use the chemokine-mediated trafficking patterns that in normal physiological conditions are used during organogenesis, vascularization and tissue regeneration (Cojoc et al., 2013).

Cancer cells expressing CXCR4 can migrate through a SDF-1α gradient to target tissues via chemotaxis, strengthening a role in the development of

metastases. Nevertheless, chemotaxis induced by CXCR4/SDF-1α axis is not only implicated in pathological processes but also in physiological ones, as indicated above. Chemotaxis has been observed to participate in physiological processes such us embryogenesis and hepatic regeneration after liver injury. In some cancer models, for instance melanoma, prostate, colon and hepatocellular carcinoma, it is known that CXCR4 directes metastasis through a SDF-1α gradient (Müller et al., 2001; Phillips et al., 2003; Zeelenberg et al., 2003). In fact, it has been recently established that in more than 75% of all cancers CXCR4 is playing a central role in tumor cell dissemination and metastasis (Cojoc et al., 2013).

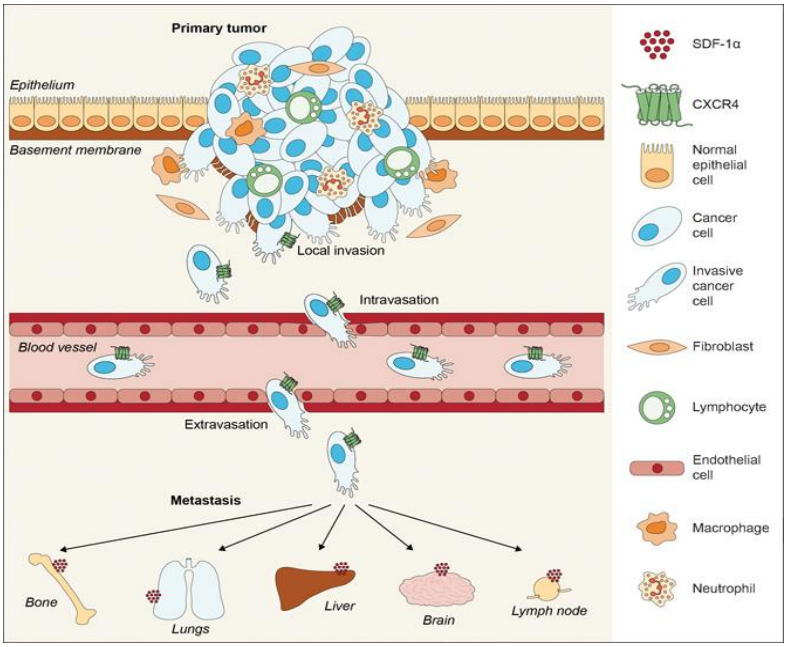

Figure I.14. Schematic view of the implication of CXCR4 in SDF-1α gradient-dependent cell migration during cancer progression (George et al., 2014).

On the one hand, the CXCR4/SDF-1α axis is directly mediating migration through the activation of PI3 kinase by $G_{\beta\gamma}$ and G_{α} subunits of G protein, which in turn is activated after the binding of SDF-1α to CXCR4. PI3K activation results in the phosphorylation of several focal adhesion components such as focal adhesion kinase (FAK) and paxilin, and consequent downstream Cdc42 and Rac activation. In addition, G_{α} subunit is able to signal through Erk 1/2, activating the Ras signaling pathway and promoting chemotaxis (Teicher and Fricker, 2010). On the other hand, the tumor microenvironment is involved in

the acquisition of chemotactic properties by the tumor cells, indirectly promoting cell invasion and migration. It has been reported that the carcinoma-associated fibroblasts (CAFs), which constitute the major cellular component of the tumor microenvironment, highly secrete SDF-1α and metalloproteinase-1 (MMP-1). The SDF-1α produced by CAFs directly stimulates the invasiveness of breast cancer cells (Orimo et al., 2005). Likewise, MMP-1 is a key enzyme to degrade the extracellular matrix, then facilitating the cancer cell invasion by elimination of the main physical barrier for cells (Cojoc et al., 2013; Shuman Moss et al., 2012).

Multiple reports about the participation of CXCR4 in oncogenic metastatic processes have arisen during the last decades. Besides the described role in leukocyte mobility, other cancer cell models demonstrated the implication of CXCR4 in migration. In multiple myeloma cells, it was observed that motility and pseudopodia formation were increased after SDF-1α stimulation. As we previously described, AMD3100, a CXCR4 inhibitor, has been noticed to inhibit migration (Bertran et al., 2009, 2013). Similar results were described by using an anti-CXCR4 blocking antibody (Alsayed et al., 2007). Breast cancer cells were shown to directionally migrate and invade following a SDF-1α gradient and this effect was impaired after the treatment with a blocking anti-CXCR4 antibody, which indicates that SDF-1α is one of the main chemotactic factors for breast cancer cells (Müller et al., 2001). Also in gastric cancer cells CXCR4 contributes to the ability to migrate to lymph nodes in response to SDF-1α gradient (Zhao et al., 2011). The CXCR4 knock-down has been also shown to be effective reducing the invasiveness in breast cancer 4TO7 cells (Krohn et al., 2009).

Furthermore, the CXCR4/SDF-1α-mediated invasion of tumor cells in the stromal layers permits cells to directly attach to stromal cells through the activation of adhesion molecules such as $\alpha_v\beta_3$ integrins, what has been described for prostate cancer cells. Additionally, integrins activation has shown to provide malignant cells with pro-survival signaling in vitro (Domanska et al., 2013; Zheng et al., 1999). In point of fact, the $CXCR4^+$ cells recruited in the stromal microenvironment are exposed to pro-survival site-specific soluble factors (Burger and Peled, 2009; Domanska et al., 2013). Equally important,

CXCR4/ SDF-1α axis promotes cell survival through the activation of AKT by PI3K, but also through both p38 and Erk 1/2 activation (Bertran et al., 2009; Teicher and Fricker, 2010).

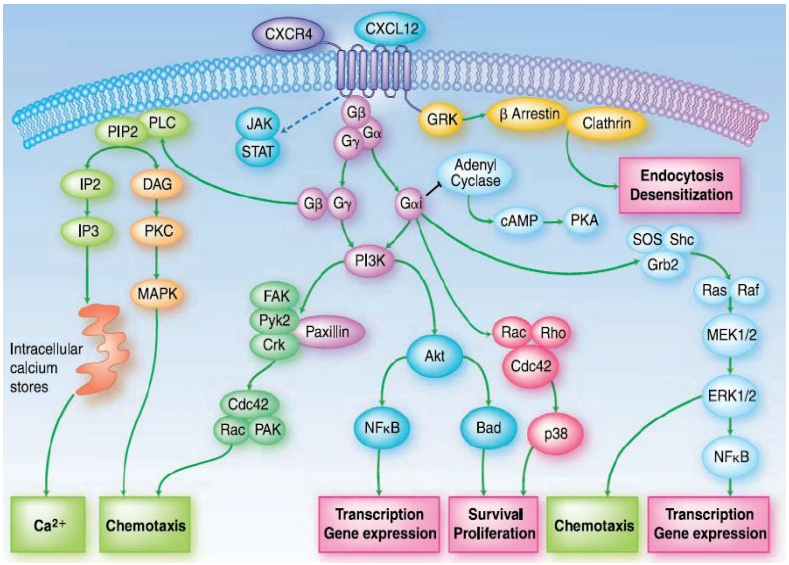

Figure I.15. CXCR4/SDF-1α signaling pathway (Teicher and Fricker, 2010)

Regarding the tumor growth, both a direct and an indirect effect are attributable to the CXCR4/SDF-1α axis. A direct effect in the promotion of tumor growth has been assessed by inhibiting CXCR4 with specific inhibitors in multiple studies *in vivo*. For instance, the treatment with CTCE-9908, an inhibitor of CXCR4, of transgenic breast cancer mouse model resulted in a 56% reduction in primary tumor growth rate. This was concomitant with a 30% reduction in p-AKT/AKT expression (Hassan et al., 2011). Similarly to chemotactic effects, an indirect role through the CAFs enhances the tumor growth. The high levels of SDF-1α found in the tumor, produced by CAFs, attract $CXCR4^{+}$ inflammatory and stromal cells into the tumoral mass, supporting the tumor growth by the secretion of growth factors (Domanska et al., 2013).

Hence, continuing with the link between the tumor mass and the role of the microenvironment in tumor progression related to the CXCR4/SDF-1α axis, CAFs derived SDF-1α also promotes neoangiogenesis by recruiting endothelial progenitor cells into tumor mass (Cojoc et al., 2013). Actually, a positive feedback loop has been described between CXCR4 and VEGF pathways,

suggesting a role of CXCR4 in the promotion of tumor angiogenesis, but also a cross-talk of CXCR4 with Platelet derived growth factor D (PDGF-D) reports the effect of CXCR4 as a neoangiogenesis regulator (Liang et al., 2007; Liu et al., 2011). Studies with orthotopically implanted breast cancer cells in mice have demonstrated that, in the end, the inhibition of CXCR4 by AMD3100 decreases metastasis even when cells overexpress PDGF-D (Liu et al., 2011).

7.1.2. CXCR4/SDF-1α axis in HCC

Regarding the liver, despite the contribution of the CXCR4/SDF-1α axis has been investigated mainly in HCC, it seems relevant to note that it is also participating in previous physiopathological liver stages. It has been confirmed that CXCR4 mRNA is upregulated in the liver after HCV infection (Ghanem et al., 2014; Mitra et al., 1999). Overexpression of CXCR4 has been observed at active inflammatory foci resembling lymphoid structures of cirrhotic livers (Wald et al., 2004). SDF-1α was overexpressed in inflammatory and cirrhotic liver samples of HCV and HBV infected patients compared to normal human liver tissue. Furthermore, SDF-1α showed elevated levels at the plasma of patients with high fibrosis, suggesting a role directing the recruiting of endothelial progenitor cells (Wald et al., 2004). In contrast, data indicating that the CXCR4/SDF-1α signaling contributes to hepatic protection, liver regeneration and prevention of liver fibrosis progression have been published, so further studies are still needed to clarify the role of CXCR4/SDF-1α axis in liver pathogenesis (Tsuchiya et al., 2012). In any case, it has been demonstrated the participation of the CXCR4/SDF-1α axis in hepatic stroma remodeling and the potential therapeutic applications of CXCR4 inhibitors as anti-fibrotic agents (Ghanem et al., 2014).

During the last decade, an increasing number of publications brought up the important role of the CXCR4/SDF-1α axis in hepatocellular carcinoma progression. Some reports have demonstrated the presence of CXCR4 only in HCC tissue but not in normal hepatic tissue (Liu et al., 2008). Although contrasting publications have been published, the majority of the studies have underlined a correlation between high CXCR4 expression and aggressiveness, metastasis development and poor prognosis, becoming an independent risk

factor for reduced patient survival (Bertran et al., 2013; Xiang et al., 2009). Moreover, HCC cells expressing CXCR4 can be attracted by tissues expressing high levels of SDF-1α (Ghanem et al., 2014).

As previously described, the CXCR4/SDF-1α is playing a role as an inducer of cell growth, migration and invasion of HCC cells. Furthermore, a several number of mechanisms are responsible of the overexpression of CXCR4 and its consequent effects. Chemotherapy and loss of the phosphatase and tensin homolog (PTEN) function promoted cell invasiveness by the upregulation of the CXCR4/SDF-1α axis through a ROS-dependent pathway in prostate and pancreatic cancer cells (Arora et al., 2013; Chetram et al., 2011). Thus, a microenvironment rich in ROS and pro-inflammatory molecules occuring during HCC progression may influence the expression and function of CXCR4, which could in turn enhance cancer progression and metastasis (Ghanem et al., 2014).

Furthermore, it has been described that SDF-1α induces the activation of MMP-9 so promoting the cell invasion. Additionally, the CXCR4/SDF-1α axis was also observed to mediate MMP-2 secretion in Hca-H and Hca-F mouse cells, facilitating lymph node metastasis (Chu et al., 2007; Ghanem et al., 2014; Zhang et al., 2011).

Nonetheless, contradictory data has been published about the role of the CXCR4/SDF-1α axis in HCC cells. It has been described that HepG2 cells are unable to respond to CXCR4 due to a defect in the receptor. Otherwise, Kim *et al*. reported that in five HCC cells lines, for instance HepG2, Hep3B and PLC/PRF/5, CXCR4 remained trapped in the cytoplasm so they barely respond to SDF-1α. However, SDF-1α bound to CXCR4 in the small fraction localized in the cell surface inducing the phosphorylation of AKT and ERK1/2, although neither migration nor proliferation were seen (Ghanem et al., 2014; Kim et al., 2008; Mitra et al., 2001).

7.1.3. Regulation of the CXCR4/SDF-1α axis by TGF-β

Currently, some reports highlight a role for TGF-β in the regulation of CXCR4/SDF-1α axis, being implicated in many diseases, including cancer. In these last years, our group contributed to expand the available knowledge on the cross-talk between the CXCR4/SDF-1α axis and the TGF-β, concretely in HCC.

In the beginnings of the 21st century, a role for TGF-β in the regulation of CXCR4 expression in naive T cells has been reported (Franitza et al., 2002). Some evidences have indicated that TGF-β might up-regulate CXCR4 in melanoma cells enhancing the response to SDF-1α to promote invasion and cell dissemination (Bartolomé et al., 2004). A decade later, TGF-β secreted by neuroblastoma cells has been found to play a pivotal role up-regulating CXCR4 in human NK cells (Castriconi et al., 2013). However, very little was known about the role of TGF-β in the regulation of CXCR4 in liver cells.

Our first evidences of the cross-talk between the CXCR4/SDF-1α axis and the TGF-β pathway required the establishment of the TβT-FaO (TGF-β-treated FaO) rat hepatoma cell line, selecting those FaO cells that undergo EMT and survive to the apoptotic effect of TGF-β (Bertran et al., 2009). We have found that TβT-FaO cells, which showed an increased migration capacity, also expressed high levels of CXCR4 as a response to TGF-β, in contrast with the low levels of CXCR4 observed in FaO cells, which do not respond to SDF-1α. Interestingly, CXCR4 has been reported to locate in the presumptive migration front of TβT-FaO and the contribution of CXCR4 has been demonstrated since the treatment of these cells with AMD3100, a CXCR4 antagonist, attenuates their migratory capacity on collagen gels (Bertran et al., 2009). In contrast to FaO cells, extracellular SDF-1α activates the ERK pathway increasing cell scattering and preventing serum deprivation-mediated apoptosis (Bertran et al., 2009).

Regarding the knowledge achieved in human liver cells, our group has reported that TGF-β play an important role in the acquisition of a mesenchymal-like phenotype and increased migratory ability in human HCC cells through the activation of the CXCR4/SDF-1α axis. Moreover, CXCR4 has been found to

localize in the migratory front of tumor tissues coinciding with overactivation of the TGF-β signaling (Bertran et al., 2013). Silencing of the TβRI or its specific inhibition is able to recover the epithelial phenotype and attenuate CXCR4 expression, so leading to the inhibition of cell migratory capacity (Bertran et al., 2013). In hepatocellular carcinoma tumors, high levels of CXCR4 always correlate with activation of the TGF-β pathway, a less differentiated phenotype and a cirrhotic background. Moreover, CXCR4 is found at the tumor border and at perivascular areas, which suggests its potential involvement in tumor cell dissemination. This has been further confirmed by the AMD3100-mediated inhibition of the cell migration in those cells expressing high levels of CXCR4 and showing this protein strongly polarized in the migration front (Bertran et al., 2013).

7.1.4. Intracellular trafficking of CXCR4

Regarding the exocytic trafficking of CXCR4 little is known about how it reaches the plasma membrane and how it is regulated. As CXCR4 is described to be an N-glycosylated protein, it must cross the Golgi apparatus before reaching plasma membrane (Bieberich, 2014; Reynders et al., 2011; Zhou and Tai, 1999). Nonetheless, post-Golgi egress and trafficking remain almost unknown. It has been described that CXCR4 uses some Rab GTPases for the anterograde traffic to the plasma membrane, concretely Rab2, Rab6 and Rab8, in Jurkat cells (Charette et al., 2011). However, no data about exocytic trafficking of CXCR4 has been still reported in HCC cells.

CXCR4 has been reported to be localized in lipid enriched areas of the plasma membrane. Moreover, it is constitutively associated with proteins associated with raft proteins such as CD4 (Mañes et al., 1999; Neel et al., 2005; Xiao et al., 2000). It is also important to underline that the caveolin-dependent endocytosis is dependent on the cell type. For instance, although CXCR4 is internalized only through the clathrin-dependent pathway in HeLa cells, in other cells models such as T cell lines caveolin-dependent route takes part in the chemokine receptor endocytosis (Neel et al., 2005; Nguyen and Taub, 2002; Venkatesan et al., 2003). In any of the cases, it has been previously reported that CXCR4 follows a dynamin-dependent endocytic route in COS-1 and HEK-293 cells

(Orsini et al., 1999) and in human Fetal mesenchymal stem/stromal cells (Pelekanos et al., 2014).

It is still unclear the capability of the cells to internalize CXCR4 through macropinocytosis. However, anecdotal evidence suggests that CXCR4 stimulates macropinocytosis in HeLa cells even in the presence of SDF-1α, in which case internalization of both the receptor and the ligand has been observed (Tanaka et al., 2012).

Finally, the relevance of the recycling route in CXCR4 reexposure at the plasma membrane remains obsure. It is thought that recycling pathway is mediated by many factors, including receptor-ligand binging, Rab proteins participation, cytoskeleton implication and even the lenght of ligand stimulation. In this context, a recent publication has described that CXCR4 is present within $Rab5^+$ and $Rab11^+$ endosomes, consequently using fast and slow recycling pathways to trip back to the plasma membrane in fetal mesenchymal stem/stromal cells (fMSC) (Pelekanos et al., 2014).

7.1.5. CXCR4/SDF-1α axis and cell polarity

Despite the implication of the CXCR4/SDF-1α axis in cell migration has been widely described there is still a lack of knowledge of the role that it is playing as a cell polarity regulator. However, the fact that the activation of the CXCR4/SDF-1α axis leads to a reorganization of the subcellular structures upon a migratory stimulus suggests a necessary change of cell polarity. In this regard, few reports have recently shed light on this matter focusing mainly in hematopoietic cells.

In the beginning of this decade, Shen et al. hypothesized that in endothelial progenitor cells Rac GTPase protein acts as a pivotal signal integrator involving CXCR4/SDF-1α axis and its downstream effectors. So, the activation of this chemokine receptor could be able to change the cell polarity depending on the upstream signals (such as HIF-1) to maintain migrating cells' motion status and to guide them to adhere to the target region. This theoretical scheme is based on their preliminary *in vitro* study in which they have observed that SDF-1α increased levels correlate with the up-regulation of Rac expression and this

phenomenon is concomitant with a polarity change and migration regulation (Shen et al., 2011).

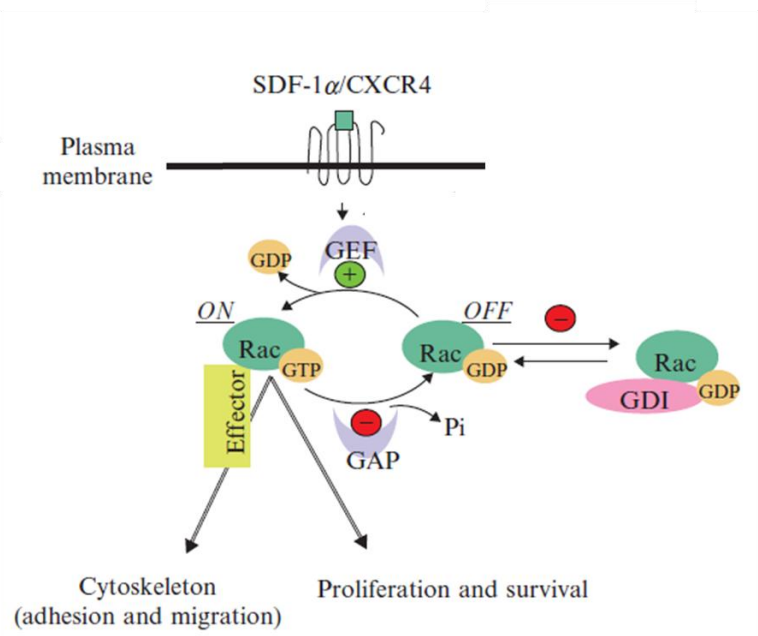

Figure I.16. The SDF-1-RAC pathway (Adapted from Williams et al., 2008).

Previously, it has been described that hematopoietic stem/progenitor cells lacking Rac show a profoundly decreased migration in response to SDF-1α as compared to wild-type cells. Moreover, it has been also observed that Rac proteins are activated by SDF-1α (Williams et al., 2008).

Hence, it has been established a correlation between Rac and the CXCR4/SDF-1α axis highlighting the need of polarity proteins for the cell response to SDF-1α in terms of migration, which could be named as SDF-1α-RAC pathway. However, no information is still available about the possible cross-talk between the CXCR4/SDF-1α axis and the Par3/Par6/aPKC polarity complex as it has not been reported any study establishing a correlation between these two systems.

HYPOTHESIS AND OBJECTIVES

HYPOTHESIS

We hypothesize that CXCR4 exposure in the cell surface of HCC cells could be regulated by intracellular trafficking hubs as well as mechanisms controlling cell polarity. Due to the fact that CXCR4 is differentially localized in HCC cells depending on their TGF-β autocrine production, these mechanisms could be regulated by TGF-β.

OBJECTIVES

The **general aim** of this project is to analyze the mechanisms regulating the asymmetric export of CXCR4 to the plasma membrane of HCC cells and their possible correlation with the mechanisms that control cell polarity. This main objective is divided into **specific objectives**, as follows:

1. To study the CXCR4 intracellular distribution in HCC cells and the role of TGF-β in its regulation.

2. To investigate the role of the exocytic and endocytic routes in the polarized export of CXCR4 to the plasma membrane.

3. To explore the role of TGF-β in the regulation of the localization and expression of PAR3 in HCC cells.

4. To study the role of PAR3 in the asymmetrical distribution of CXCR4 to the plasma membrane.

MATERIAL AND METHODS

1. Cell culture

1.1. Liver tumor cell lines

PLC/PRF/5 and Hep3B cell lines were obtained from the European Collection of Cell Cultures (ECACC), the Snu449 cell line from the American Type Culture Collection (ATCC) and the HLE cell line from the Japanese Collection of Research Bioresources Cell Bank (JCRB Cell Bank). PLC/PRF/5 cells were maintained in DMEM medium, Hep3B cells were maintained in MEM medium whereas Snu449 and HLE cells were maintained in RPMI medium. All media were supplemented with 10% fetal bovine serum (FBS) (v/v). Cells were maintained in a humidified atmosphere at 37ºC, 5% CO_2. Sub-confluent cultures (70-80%) were split by trypsinization. The phenotype of the human liver cancer cells used is shown in **Table I**.

Cell line	Tumor type	Morphology	p53 status	Other characteristics
PLC/PRF/5	Human liver hepatoma cells	Epithelial	Mutated pR249S	-----
Hep3B	Human negroid hepatocyte carcinoma	Epithelial	Deleted	Deficient in functional pRB; mutations within hFas gene
Snu449	Human asian hepatocellular carcinoma	Epithelial; diffusely spreading cells	Mutated K139R A161T	Aneuploid. mutations in CDKN2A
HLE	Human hepatoma (non-differentiated)	Diffusely spreading cells	Mutated G244A R249S V272M	-----

Table I. Molecular characteristics of the human liver cancer cells used

Other two cell lines were used: shTBRI PLC/PRF/5 and shTBRI Hep3B. Both cell lines were previously obtained in our laboratory following the stable silencing gene expression as described (Bertran et al., 2013).

1.2. Treatments used in cell culture

For the serum-deprivation experiments, cells at 70% confluence were serum-starved during 8 to 12 hours before treatments.

Stromal Derived Factor-1α (SDF-1α) (Sigma-Aldrich, St Louis, MO, USA) was added at 100 ng/mL to the cell culture after 8-12 hours of serum deprivation. TGF-β (Calbiochem, La Jolla, CA, USA) at 2 ng/mL was added to cell culture in the same conditions described for SDF-1α treatment. In the case of the Snu449 cell line, given their high sensitivity to serum deprivation, TGF-β was added to 2% FBS in complete medium 8-12 hours prior treatment.

When pharmacological inhibitors and other compounds were used prior to SDF-1α, these were added to the cell culture 30 minutes before SDF-1α, in FBS-deprived cells for the previous 8-12 hours, and at the following concentrations (**Table II**).

Compound/Inhibitor	Company	Dose
AMD3100	Sigma-Aldrich	1 µg/mL
Bisindolylmaleimide II (BIS)	Sigma-Aldrich	10 µM
Methyl-β-cyclodextrin (MβC)	Sigma-Aldrich	2,5 µM
Water soluble cholesterol	Sigma-Aldrich	1 mM
Dynasore	Calbiochem	80 µM
Dimethylamiloride (DMA)	Sigma-Aldrich	100 µM
Brefeldin A (BFA)	Sigma-Aldrich	10 µg/mL
LY364947 (LY)	Calbiochem	3 µM

Table II. Inhibitors and compounds added to cell culture prior SDF-1α or TGF-β treatments.

1.3. Transient transfections of plasmids

1.3.1. Transformation of the vector into E. coli

EGFP-CXCR4 vector DNA was a kind gift of Dr. Peter van Hordjik (Sanquin Blood Supply, Amsterdam, The Netherlands) while wild type rat EXOC4 and dominant negative EXOC4^{S32A} were from GE Lienhard (Dept. of Biochemistry, Dartmouth Med. Sch., Hanover, NH, USA). For transformation, 50 µl competent

JM109 cells, 1µl of EGFP-CXCR4 vector DNA were added into a sterile tube, which was then incubated on ice for 40 minutes, followed by a heat shock at 42 ºC for 45 seconds and further incubation on ice for 20 minutes. Then 0,9 mL of Lysogeny broth (LB) medium was added and the mixture was incubated at 37 ºC with 200 rpm for 1 h. The bacterial solution was then poured on the LB-agar medium with antibiotics (kanamycin 50 mg/L) for selection of transformed cells at 37ºC until single colonies appeared. Randomly chosen colonies were then cultured on LB-agar medium and stored at 4ºC for later use.

1.3.2. Plasmid Mini- and Maxi-Preps

Small- and large-scale DNA plasmid extractions were performed using the Sigma-Aldrich (St Louis, MO, USA) Plasmid Mini and Maxi kits according to the protocol of the manufacturer. Briefly, the procedure consists of alkaline lysis of the bacterial cell wall, removing the cell debris while keeping the supernatant containing the nucleic acids, degradation of RNA by RNase, binding of plasmid DNA to a silica-gel matrix and washing with high-salt solution (to remove the chromosomal DNA and proteins) and elution of plasmid DNA.

1.3.3. Transient transfection of HCC cells

For the transient transfections of plasmids we used the method of magnetofection (magnetic-assisted) devised by IBA GmbH (Goettingen, Germany). Plasmid (at 2 µg/mL), complexed with the the MAtra-A reagent (at 1:600 in complete medium) in a final volume of 500 µL was added to cell cultures at 70% confluence and kept for 15 minutes on the magnet plate. Transfected cells were maintained in a humidified atmosphere at 37ºC, 5% CO_2, and after 8 hours of culture, medium was replaced with fresh complete medium.

1.4. Transient gene-silencing with specific siRNAs

siRNAs (50 or 100 nM) complexed with the TransIT-Quest reagent (Mirus, Madison, WI, USA) at 1:300 in complete medium were added to cell cultures at 70% confluence. Transfected cells were maintained in a humidified atmosphere at 37ºC, 5% CO_2. After 8 hours in the transfection solution, cells were washed

and fresh medium, containing 10% FBS, was added. Cells were cultured for a minimum of 16 hours before starting experiments.

siRNA oligonucleotides were obtained from Genosys (Sigma-Aldrich, St Louis, Mo, USA). siRNAs used are shown in **Table III**. Sequences were designed using the Dharmacon siDESIGN Center website (http://dharmacon.gelifesciences.com/design-center/), targeting the ORF region for siRNA design.

siRNA	Sequence (5' – 3')	Final concentration
EXOC4	ACUCUGUGGUCCUGGGAUA	100 nM
CHC	GGGAAGAAUUGGUGAAGUA	50 nM
PAR3	UUGCCCACUAAAUCUACUC	50 nM
Scrambled	GUAAGACACGACUUAUCC	50 or 100 nM

Table III. Sequences of the siRNAs used in this study

2. Determination of cell viability

2.1. Crystal violet staining

Crystal violet staining allows the quantification of cells which survive a toxic process and remain attached to the culture plate (Drysdale et al., 1983).

Cells were seeded and grown in 24-well plates and submitted to different treatments. After treatment, medium was removed and cells were washed twice with PBS and incubated with a solution of 0.2% crystal-violet in 2% ethanol for 1 hour, at room temperature and with agitation. Staining solution was removed, cells were washed several times with PBS or distilled water, until the excess of dye was eliminated, and plates were air-dryed. Incorporated dye was extracted by incubating with 200µL of a 10% SDS solution for 15 minutes at room temperature and with agitation. The amount of dye was then determined

spectrophotometricaly at 595 nm (maximum of absorbance for crystal violet). Results were represented as the percentage of viable cells relative to control cells (untreated cells).

2.2. Propidium iodide incorporation

Propidium iodide (PI) is both a DNA intercalating agent and a fluorescent molecule with an utmost excitation at 535 nm that returns an emission spectrum that peaks at 617 nm. Without cell fixation, PI is unable to penetrate the cell membrane, unless it becomes permeable as a consequence of a death process.

After incubation in p60 or p100 plates with different stimuli or inhibitors, cell media was recovered, so detached cells were taken, and the remaining cells on the plate were washed twice with PBS. Then, cells were detached using Trypsin-EDTA (0.05 %) and added to the recovered media for centrifugation (5 minutes at 1500 rpm). Afterwards, supernatant was discarded and the pellet was washed with PBS and re-centrifuged. Last step consisted in resuspending the washed pellet in a solution of PI-PBS (0.25 µg/mL) and analyzing the cells by flow cytometry (Gallios cytometer from Beckman-Coulter) within the following 15 minutes. Unlike living cells, dead cells did emit fluorescence due to PI incorporation.

For these studies, flow cytometry data analyses were performed with Kaluza version 1.1 software developed by Beckman Coulter.

3. Gene expression analysis

3.1. RNA isolation and reverse transcription

For the isolation of total RNA we used the “RNeasy Mini Kit (Qiagen, Valencia, CA, USA). Following manufacturer’s instructions for adherent cells. Reverse transcription was performed with random primers on 1 µg of total RNA and using the “High Capacity RNA to cDNA Master Mix Kit” (Applied Biosystems, Foster City, CA, USA) following the manufacturer’s instructions.

3.2. Quantitative PCR

For the quantitative measures of gene expression we used the LightCycler® 480 Real Time PCR system (Roche Applied Science, Mannheim, Germany), with 384-well plates. The PCR reaction was prepared by duplicate with 10 µL of LightCycler® 480 SYBR Green I Master Mix (Roche Applied Science, Mannheim, Germany), 2 µL specific primers (5 µM) (see **Table IV** for a list of the primers used in this work) and 40 ng of cDNA for a final volume of 20 µL.

The levels of mRNA for each gene were determined following manufacturer's protocols considering the 2^ΔCt and normalized with the housekeeping gene ribosomal protein L32 (*RPL32*) (Moreno-Càceres et al., 2014).

Gene (human)	Forward (5' – 3')	Reverse (5' – 3')
PARD3	TATCCACAGCCAGTGATCAGCCTT	ACCCGTTTTCTCAATCTTGTCATC
CDH1	CCCAATACATCTCCCTTCACAG	CCACCTCTAAGGCCATCTTTG
VIM	GGAAGCCTAACTACAGCGAG	CAGAGTCCCAGATGAGCATTG
SNAI1	GCTGCAGGACTCTAATCCAGAGTT	GACAGAGTCCCAGATGAGCATTG
ZEB1	ACCCTTGAAAGTGATCCAGC	CATTCCATTTTCTGTCTTCCGC
L32	AACGTCAAGGAGCTGGAGG	GGGTTGGTGACTCTGATGG

Table IV. Primer sequences used in this work

4. Determination of protein expression by Western Blot

4.1. Cell lysis

Cells were placed on ice, culture medium was removed and dishes were washed twice with cold PBS. 1 mL of cold PBS was added to each dish and cells were scrapped and collected. An additional 1 mL of cold PBS was added to the dish, the remaining cells were scrapped and collected, and then added to the tube. Cells were then pelleted at 1200xg for 10 minutes at 4ºC. The pellet was resuspended with 100µL RIPA lysis buffer (**Table V**) and transferred to an Eppendorf tube. After 1 hour incubation at 4ºC with agitation, lysates were

centrifuged at 13800xg for 10 minutes at 4ºC, and the supernatants were collected and stored at -80ºC until processed.

Component	Concentration
Sodium deoxycholate	5 mM
TRIS-HCl pH 7.4	20 mM
SDS	0.1%
Triton-X-100	0.5%
NaCl	150 mM
EDTA	2 mM
PMSF	1 mM
Leupeptin	5 µg/mL
Na3VO4	0.1 mM
DTT	0.5 mM
B-glycerolphosphate	20 mM

Table V. RIPA lysis buffer

4.2. Protein quantification

4.2.1. BCA commercial kit

The use of BCA commercial kit is recommended in the case of having SDS as a component of the lysis buffer. For each measurement, a standard curve of protein concentration was prepared with BSA in a range from 0 to 2 mg/mL. The reaction was prepared by mixing Solution A and B in a 50:1 ratio and 200 µL of this mix was added to 10 µL of 1:10 diluted sample into a 96-well plate. After 30 minutes of incubation at 37ºC, absorbance was measured by spectrophotometry at a 595 nm wavelength.

4.2.2. Bio-Rad commercial kit

Bio-Rad commercial kit imply an advantage with respect to BCA commercial kit as it is not necessary to wait for 30 minutes incubation prior to spectrophotometer data acquisition. For each measurement, a standard curve of protein concentration was prepared with BSA in a range from 0 to 0.4 mg/mL. The reaction was prepared by mixing Bio-Rad reagent and water in a 1:5 ratio and 200 µL of this mix was added to 10 µL of 1:20 diluted sample into a 96-well plate. Absorbance was measured by spectrophotometry at a 595 nm wavelength.

4.3. Protein immunodetection by Western blot

Protein separation according to their molecular weight was done by denaturing SDS polyacrilamide gel electrophoresis (SDS-PAGE) (Laemmli, 1970). Protein samples were prepared by mixing 30 to 100 µg of protein with Laemmli buffer, heated at 95ºC for 5 minutes to denature, spun down and stored a 4ºC.

Poly-acrylamide gels consisted of two different parts: the stacking and the resolving fraction. The first one was always prepared at the same acrylamide concentration, as it functions to gather proteins. In contrast, the resolving one was prepared at different concentrations depending on the molecular weight of the proteins to be studied, functioning as a sorter for these proteins by their size (after denaturalization). For instance, when proteins to study had a molecular weight was up to 100 kDa, a 12% acrylamide gel was prepared for the resolving part. If proteins had a molecular weight higher than 100 kDa, gel acrylamide concentration was a 10%. Once the gel was ready it was assembled into the gel holder and immersed into the tank, which was filled with electrophoresis buffer (25 mM TRIS-HCl; 0.1% SDS; 0.2 M Glycine; pH 8.3). Then, the samples were carefully loaded into the gel, together with a molecular weight standard in order to know the molecular weight of the studied proteins. After that, protein samples were submitted to electrophoresis following the method described by M. Sambrook in 1989, at a constant voltage (100V, 2 hours).

Once electrophoresis was finished, proteins were transferred to a PVDF membrane using electrical current in semi-dry transfer equipment. The PVDF

membrane was immersed in methanol for 1 minute previous to the protein transfer, following the manufacturer's instructions. Then, together with the membrane, Wattman paper was soaked in transfer buffer (48 nM TRIS-HCl; 0.04% SDS; 39 nM Glycine; 20% Methanol; pH 8.3) for 5 minutes, and the equipment was assembled as follows (from the bottom to the top): 3 Wattman papers – PVDF membrane – acrylamide gel – 3 Wattman papers. A 0.3 amperes electrical current was then applied during 1 hour. Later, the membrane was stained with a 0.5% red Punceau in 1% acetic acid solution to confirm that proteins had uniformly been transferred into the membrane. Then, the membrane was washed several times in 0.05% Tween in PBS solution (PBS-T).

For the antibody detection, the membrane was incubated in 5% non-fat dry milk in PBS-T for 1 hour at room temperature, was incubated with the primary antibody (at 1:500 to 1:5000 in 0.5% non-fat dry milk in PBS-T), washed with PBS-T, and subsequently incubated with the secondary peroxidase-conjugated antibody (at 1:5000 in 0.5% non-fat dry milk in PBS-T) for 1 hour at room temperature. The membrane was washed several times in PBS-T. To visualize the bound antibody, the membrane was incubated with a chemiluminiscent solution, ECL (GE Healthcare, Little Chalfont, UK) and exposed to an Amersham Hyperfilm^{TM} ECL. As secondary antibodies we used: peroxidase-conjugated anti-mouse (NA931V) or anti-rabbit (NA934V) both from GE-Healthcare (Little Chalfont, UK).

Bound antibodies were removed by soaking the membrane in stripping solution (62.5 nM TRIS-HCl pH 6.8; 0.05% SDS; 20% β-mercaptoethanol) for 30 minutes at 50ºC with agitation.

In the densitometric analysis, the ImageJ software was used for pixel intensity quantification.

5. Immunocytochemical detection of antigens

5.1. Immunofluorescence of 2D cultured cells

Cells were seeded on glass coverslips coated with a 2% bovine gelatin in PBS solution and grown upon the desired confluence. Cells were then washed with PBS and fixed with 4% paraformaldehyde (PFA) in PBS for 15 minutes at room temperature, washed 3 times with PBS, permeabilized with 1% Triton X-100 in PBS for 20 minutes at room temperature, washed with PBS once and blocked with 1% BSA; 0.2% Triton X-100 in PBS for 30 minutes. To detect E-cadherin, cells were fixed with cold methanol for 2 minutes and washed 3 times with PBS.

Primary antibodies were diluted in 1% BSA in PBS and incubated for 1 to 4 hours at room temperature or overnight at 4ºC. After 3 washes with PBS, cells were incubated with fluorescently-conjugated secondary antibodies (anti-mouse Alexa 488; anti-mouse Alexa 555; anti-rabbit Alexa 488; anti-rabbit Alexa 555, all from GE Healthcare, Little Chalfont, UK) at 1:1000 in 1% PBS-BSA for 1 hour at room temperature. Finally, cells were washed 3 times with PBS, and coverslides were mounted with ProLong Gold Antifade containing DAPI (Molecular Probes-Life Technologies, Eugene, OR, USA). For F-actin staining, we used a phalloidin Alexa 568-conjugated at 1:500.

Cells were visualized using a Nikon Eclipse 80i epifluorescence microscope provided with a Pan Fluor 40x objective. Representative images were taken with a Nikon DS-Ri1 digital camera using the NIS-Elements BR 3.2 software. For confocal imaging, we used a Leica TSC SL spectral confocal microscope with argon (488 nm) and HeNe (543 nm) lasers, and a HCX PL Apo 63x1.40 oil objective. Adobe Photoshop was used for image edition and ImageJ to perform quantification from TIFF images.

5.2. Immunofluorescence in drop assays

After detaching cells from the dish and following centrifugation, pellets were resuspended in 100 µL of appropriate culture medium with 10% FBS. Cells were then seeded in the center of a circular glass coverslip coated with 2% bovine gelatin in PBS in a 24-wellplate to which 500 µL of medium with 10%

FBS were slowly added by the lateral side of the well. In this way, a radial gradation of cell density is achieved which allows to study the effect of different treatments on cell density. Upon completion of treatments, the different proteins of interest were imaged as described in section *5.1. Immunofluorescence of 2D cultured cells*.

5.3. Transferrin endocytosis assay

Cells attached on glass coverslips coated with 2% bovine gelatin in PBS were serum starved for 30 minutes at 4ºC to inhibit endocytosis. Then, a solution with 20 µg/mL rhodamine-conjugated transferrin in medium was added to the culture and cells were maintained with the fluorescent transferrin for 20 min at 4ºC. At zero time, culture plates were placed at 37ºC for 5, 15 or 30 minutes after which these were fixed and prepared for microscopy analysis as previously described in the section *5.1. Immunofluorescence of 2D cultured cells*.

6. Flow cytometry

6.1. Flow cytometry on live cells

Analysis of live cells by flow cytometry allows the detection of cell surface antigens. Cells were detached from culture dishes and centrifuged at 300xg for 5 min at 4ºC cell-pellets were resuspended in a solution containing 1% BSA in PBS and the tubes were placed on ice during 10 minutes. Cells in suspension were transferred to a 96 V-shaped well plate and the primary, fluorochrome-conjugated, antibody was added in 1% PBS-BSA, incubated for 30 min at 4ºC protected from light and with agitation. Negative controls were prepared similarly except that no primary antibody was added. Cells were then washed with 120 µL of PBS and centrifuged at 300xg for 5 min. Finally, each pellet was resuspended in 100 µL of PBS and transferred into flow cytometry tube with 350 µL of PBS, for a total volume of 450 µL. Flow cytometry was performed in a Gallios cytometer (Beckman-Coulter, Miami Lakes, FL, USA) within the same day. Data obtained was analyzed with the Kaluza v1.1 software (Beckman-Coulter, Miami Lakes, FL, USA).

6.2. Flow cytometry on fixed cells

Fixed cells can be used to analyze the presence of a determined protein in intracellular compartments by flow cytometry. Cells were detached from culture dishes and centrifuged at 300xg for 5 min at 4ºC. Cell pellets were resuspended and fixed in 100µL of 4% PFA in PBS for 15 minutes at 4ºC. 100 µL of PBS were then added, cells were spun down at 300g for 5 min. Cell pellets were then resuspended and permeabilized in 100µL 1% Triton X-100 in PBS for 3 min. Cells were then washed with PBS, blocked with 1% BSA in PBS for 10 minutes and prepared for flow cytometry analysis as described in section *6.1. Flow cytometry on live cells*.

7. Real time migration assay

The xCELLigence System (Roche, Mannheim, Germany) was used for the real time monitoring of cell migration. This apparatus uses designed, proprietary, CIM plates, which have upper and lower chambers separated by a microporous polyethylene terephthalate (PET) membrane with a median pore size of 8 µm. The xCELLigence apparatus measures electrical impedance across micro-electrodes integrated on the underside of the membrane, providing quantitative information about cell migration.

CIM plates were placed onto the Real-Time Cell Analyzer (RTCA) station of the xCELLigence System, both sides of the membrane were coated for 30 minutes with 25.5 µg/cm^2 of a collagen IV solution (Sigma-Aldrich, St Louis, MO, USA). Then, cells were trypsinized and counted and 100 µL of a suspension containing 4x10^5 cells/mL were added to the upper chamber of a CIM plate, while 140µL of conditioned media from NIH-3T3 cells were added to the lower chamber as a chemoattractant. Cell migration was continuously monitored throughout the experiments by measuring changes in the electrical impedance at the electrode/cell interface, as a population of cells migrated from the upper to the bottom chamber. Continuous values were represented as Cell Index (CI), a dimensionless parameter which reflects the relative change in the measured electrical impedance, and quantified as a slope (hours^{-1}) of the first 4 hours.

8. Statistical analyses

Statistical analyses were performed as an estimation of the associated probability to a student's t-test (95% confidence interval) or as a one-way ANOVA with Tukey's multiple comparison test, depending on the involved conditions. Experiments were carried out at least 3 independent times with 2-3 technical replicates. Data were represented as a mean +/- standard deviation (SD). In all cases statistical calculation was developed using GraphPad Prism software (GraphPad, San Diego, USA).

1ary Antibody	2ary Antibody	Company	Ref number	Techniques	Dilution
β-actin	anti-mouse	Sigma-Aldrich	A5441	WB	1:5000
AP1	anti-mouse	Sigma-Aldrich	A4200	IF	1:200
β-catenin	anti-mouse	Pharmingen-BD	610154	IF	1:100
$CD3^{APC}$	-	Pharmingen-BD	555335	FC	fmi
β-cop	anti-mouse	Sigma-Aldrich	G6160	IF	1:400
CXCR4	anti-rabbit	Abcam	ab2074	IF	1:50
$CXCR4^{APC}$	-	Pharmingen-BD	555976	FC	fmi
E-CADHERIN	anti-mouse	Pharmingen-BD	BD-610182	IF	1:100
$EGFR^{PE}$	-	Santa Cruz	sc-120PE	FC	fmi
EXOC4	anti-rabbit	Pharmingen-BD	HPA031443	IF	1:100
				WB	1:1000
GM130	anti-mouse	Pharmingen-BD	610823	IF	1:400
Golgin97	anti-mouse	ThermoFisher	A-21270	IF	1:400
M6PR	anti-mouse	Abcam	ab32815	IF	1:400
PAR3	anti-rabbit	Sigma-Aldrich	HPA030443	IF	1:100
				WB	1:1000
Rab11	anti-mouse	Pharmingen-BD	610656	IF	1:100
Rab4A	anti-mouse	Sigma-Aldrich	WH0005867M1	IF	1:100
TβRI	anti-rabbit	Santa Cruz	sc-399	WB	1:1000
ZO-1	anti-rabbit	ThermoFisher	61-7300	IF	1:100

FC: Flow cytometry; **IF**: Immunofluorescence; **WB**: Western blotting

Table VI. Antibodies used in this work and sorted alphabetically. The "techniques" column indicates the actual use of these antibodies during the development of this work, and not the use suggested by the manufacturer. fmi: following manufacturer's instructions.

RESULTS

1. CXCR4 protein is found at the cell surface as well as in intracellular compartments in PLC/PRF/5 and Hep3B cells

Our group has described that chemokine receptor CXCR4 showed an asymmetric subcellular distribution in mesenchymal-like HCC cells, which also showed increased levels of CXCR4 expression subsequent to TGF-β activation (Bertran et al., 2013). Thus, we decided to undergo the characterization of the mechanisms promoting the asymmetric export of CXCR4 to the plasma membrane of HCC cells.

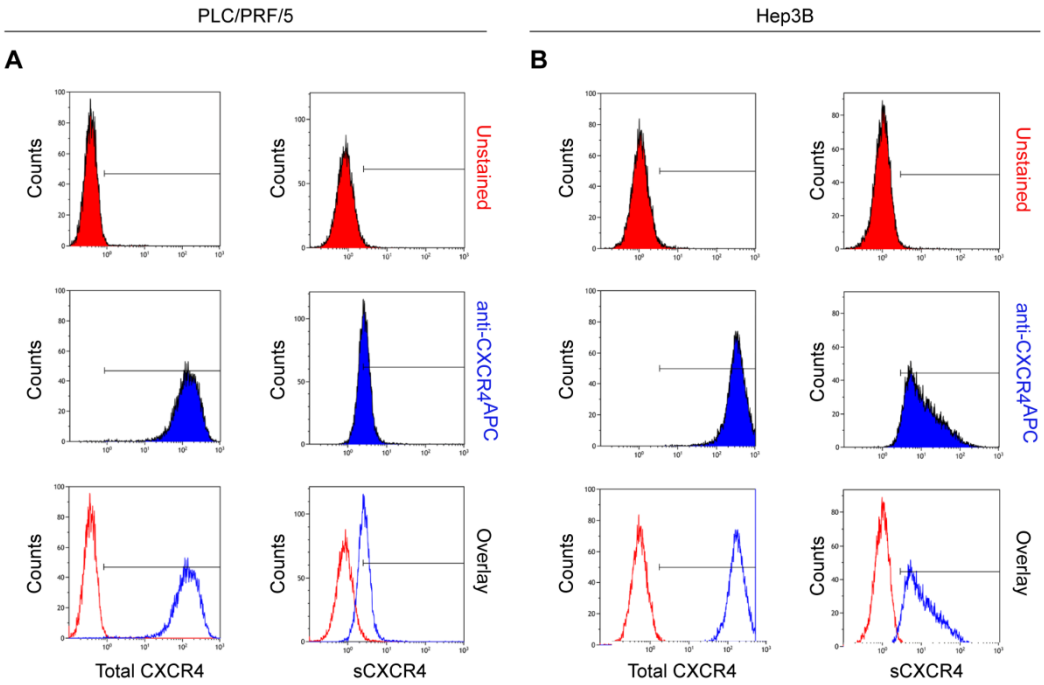

Figure 1. Analysis of the localization of CXCR4 in the HCC cell lines PLC/PRF/5 and Hep3B. A: Flow cytometric analysis of cellular CXCR4 content in permeabilized PLC/PRF/5 cells (total CXCR4, left plots) and cell surface CXCR4 (sCXCR4) in live PLC/PRF/5 (right plots). Upper plots show the pattern displayed by unlabeled cells as control, central plots display cells labelled with an anti-CXCR4^{APC} antibody, and the lower plots show the merge of the two signals. **B:** As in A except that Hep3B cells were used in the analysis.

We studied the mechanisms that regulate intracellular trafficking of CXCR4 in two different human HCC cells: PLC/PRF/5 and Hep3B. PLC/PRF/5 cells show an epithelial-like phenotype with low expression of TGF-β and moderate protein levels of CXCR4, while Hep3B cells show a mixed epithelial/mesenchymal-like phenotype with high autocrine production of TGF-β and increased protein levels of CXCR4, which furthermore are asymmetrically distributed in cells (Bertran et al., 2013).

We first analyzed the expression of CXCR4 by flow cytometry, in live or in fixed and permeabilized PLC/PRF/5 and Hep3B cells, using an APC-labeled, anti-CXCR4-specific antibody. **Figure 1A** shows that CXCR4 was mostly found in internal compartments in PLC/PRF/5 cells. Only a fraction of the cells (over 60%) was positive for CXCR4 at the cell surface (sCXCR4, **Figure 1A**, central right panel), and levels were much lower than those found in permeabilized cells (**Figure 1A**, **central left panel**, and compare fluorescence intensities of the overlay plots of **Figure 1A**, **lower panels**). Conversely, Hep3B cells were strongly positive for sCXCR4 (**Figure 1B**, **central right panel**), although levels were also lower than those found in the permeabilized cells, indicating that CXCR4 is located in intracellular compartments too (**Figure 1B**, **central left panel**, and compare fluorescence intensities of the overlay plots of **Figure 1B**, **lower panels**). The fluorescence plot of Hep3B cells for sCXCR4 showed a wide peak, which indicates high variability in the sCXCR4 levels/cell (**Figure 1B**, **central right panel**).

The low levels of CXCR4 in the plasma membrane of PLC/PRF/5 cells were not due to a possible inability of the APC-conjugated anti-CXCR4 antibody to recognize membrane CXCR4 since it was able to detect the membrane localization of this receptor in Jurkat human T-leukemia cells that we used as positive control (**Figure 2E**). Furthermore, we also performed an isotypic control with an unrelated (anti-$CD3^{APC}$) antibody of the same IgG2a,κ isotype as the anti-CXCR4, to discard unspecific binding.

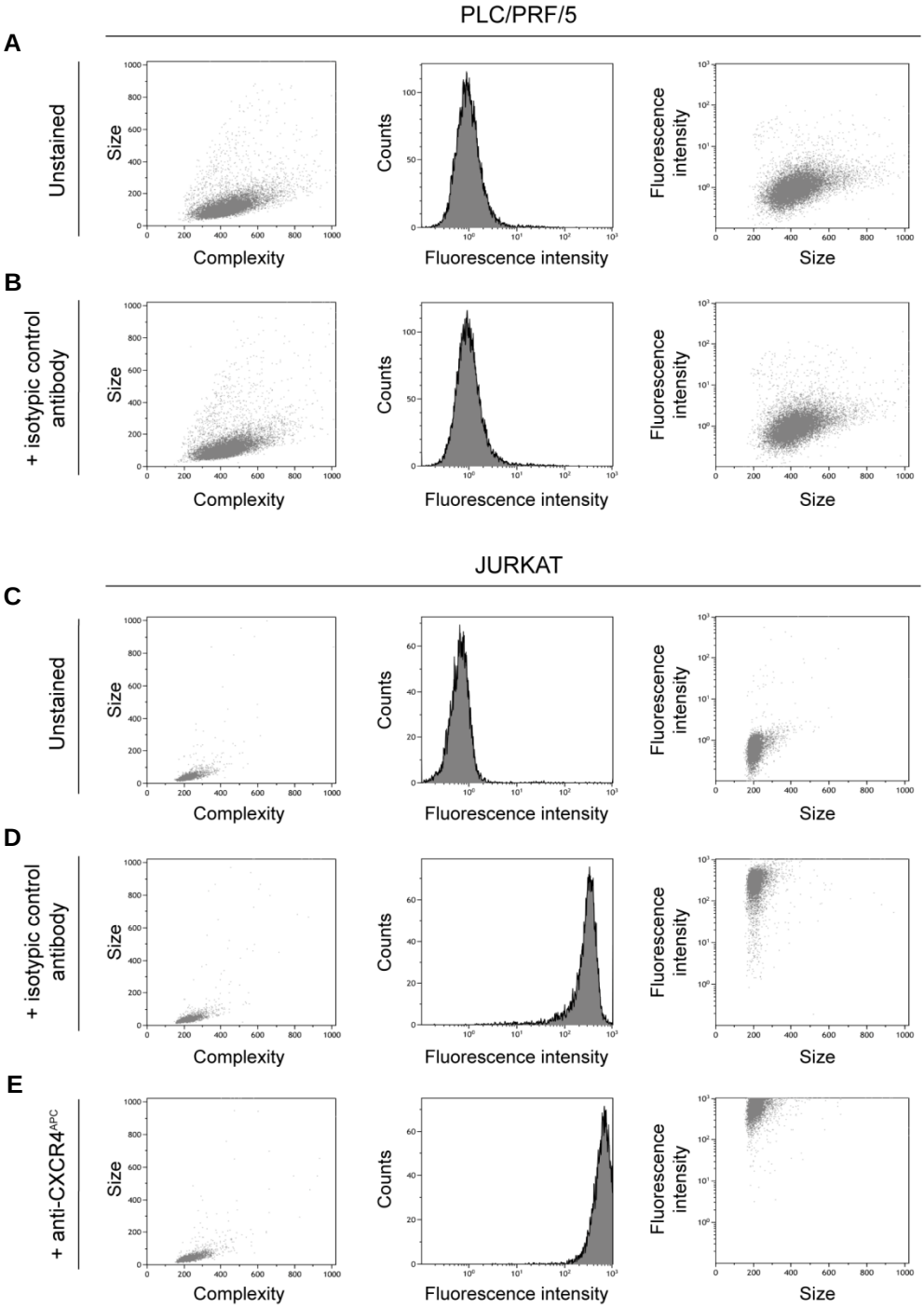

Figure 2. Specificity of the anti-CXCR4^{APC} antibody used for the flow cytometry determination of surface CXCR4 (sCXCR4) in human PLC/PRF/5 cells. Shown are the plots for cell complexity vs. cell size (left panels), fluorescence intensity in counts (central panels) and cell size vs. fluorescence intensity (right panels). **A:** PLC/PRF/5 cells in the absence of antibody. **B:** PLC/PRF/5 cells incubated with the isotypic control anti-CD3^{APC} antibody which have the same isotype (mouse IgG2a,κ) than the anti-CXCR4^{APC} **C:** Jurkat T-leukemia cells in the absence of antibody. **D:** Jurkat T-leukemia cells incubated with the isotypic control anti-CD3^{APC} to confirm its activity. **E:** Jurkat cells incubated with the anti-CXCR4^{APC} antibody to confirm the ability of this antibody to detect CXCR4.

As can be seen in **Figure 2B**, the isotypic control did not show any specific binding to the surface of the PLC/PRF/5 cells, although it was able to bind to the CD3 antigen in the surface of the Jurkat cells **Figure 2D**, thus confirming the specificity of the anti-CXCR4^{APC} antibody.

The subcellular distribution of endogenous CXCR4 in PLC/PRF/5 and Hep3B cells showed the presence of CXCR4 at the cell surface, particularly in the intercellular junctions, as well as in intracellular compartments (**Figure 3**, **left panels**, arrows and arrowheads, respectively). After transfection of both PLC/PRF/5 and Hep3B cells with a CXCR4–EGFP construction, EGFP fluorescence was also located in the intercellular junctions as well as in perinuclear vesicles (**Figure 3**, **right panels**, arrows and arrowheads, respectively).

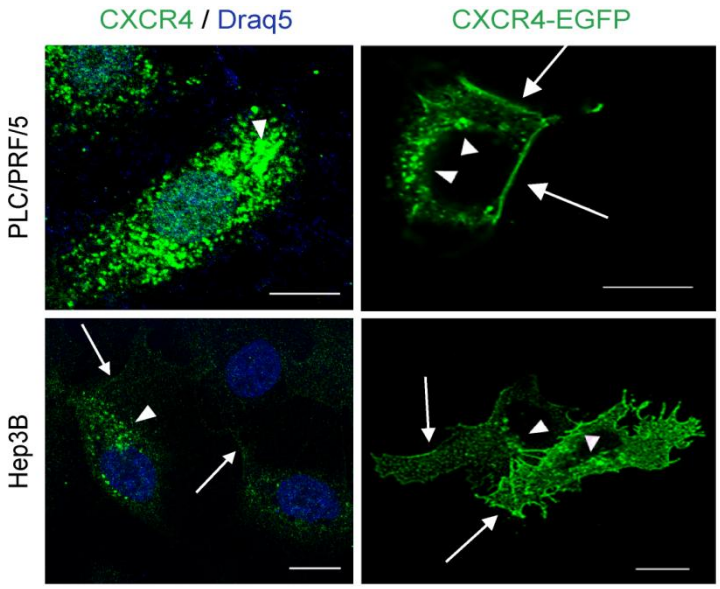

Figure 3. Analysis of the localization of CXCR4 in the HCC cell lines PLC/PRF/5 and Hep3B. Left: Confocal microscopy analysis of PLC/PRF/5 and Hep3B cells labelled with anti-CXCR4^{APC} antibody. A max. projection of two consecutive confocal sections is shown. **Right:** Confocal microscopy analysis of PLC/PRF/5 and Hep3B cells expressing a CXCR4-EGFP construct. A single confocal section at a medium focal plane is shown in PLC/PRF/5 cells. A max. projection of two consecutive confocal sections at the medium focal plane is shown in Hep3B cells. Scale bars are 20 μm. Arrows indicate cell surface CXCR4, and arrowheads internal CXCR4 deposits.

In order to explore if endogenous intracellular CXCR4 was reaching cell surface as a consequence of an autocrine SDF-1α production, we treated PLC/PRF/5 and Hep3B cells with 1μM AMD3100, a specific CXCR4 antagonist. No effect in cell surface CXCR4 levels was observed in none of the cell lines tested, indicating that CXCR4 was maintained in intracellular compartments in these HCC cells by mechanisms that may be independent of its ligand-mediated intracellular trafficking (**Figure 4A** and **B**). Furthermore, we also tested if heterologous regulation of the receptor by PKC could be responsible of its intracellular trafficking modulation. After treating PLC/PRF/5 and Hep3B cells with the PKC inhibitor bisindolylmaleimide II no changes in cell surface CXCR4 could be detected, when compared to the untreated controls (**Figure 4C** and **D**), indicating that the heterologous regulation of PKC did not have a significant effect on the trafficking of CXCR4 to the cell surface. Thus, these HCC cells maintain part of the CXCR4 in intracellular compartments by mechanisms that may be independent of its ligand-mediated intracellular trafficking.

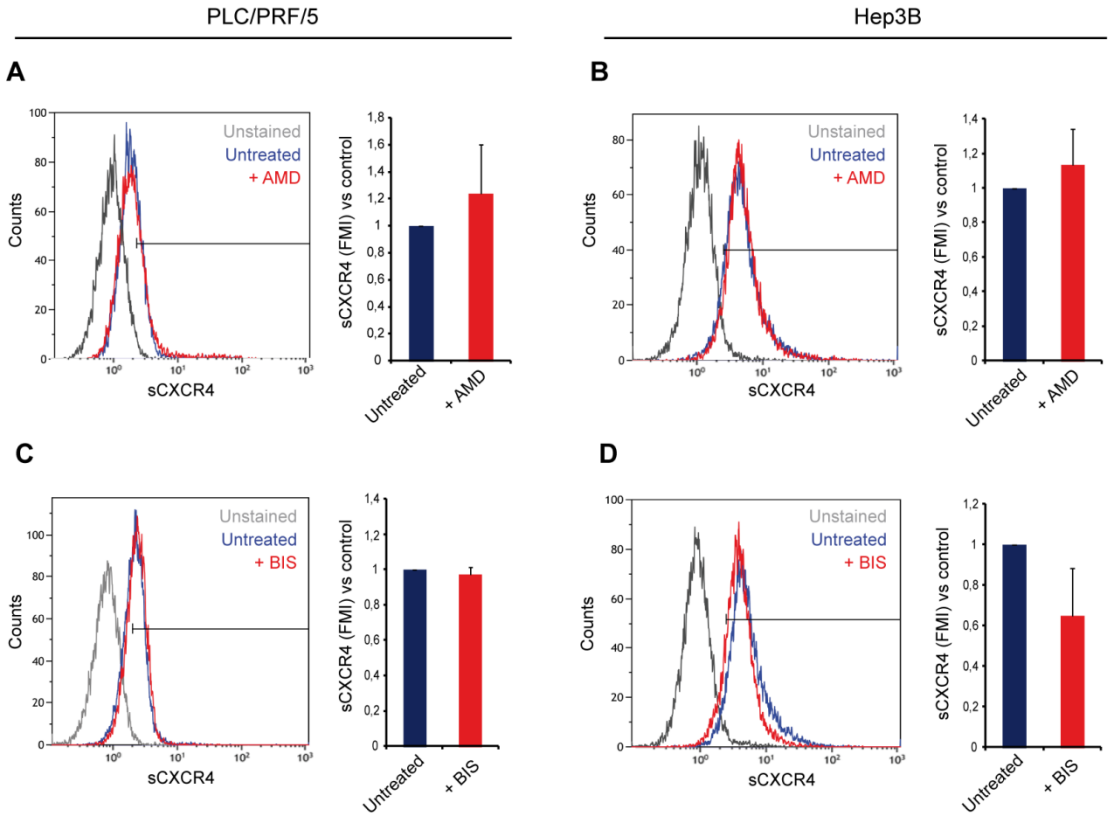

Figure 4. Intracellular deposit of CXCR4 does not correlate with dynamics of autocrine ligand-dependent CXCR4 trafficking. Flow cytometry analysis of sCXCR4 in PLC/PRF/5 or Hep3B alive cells treated with 1 µg/mL AMD3100 (**A** and **B**, respectively) or with 10 µM bisindolylmaleimide II (PKC inhibitor) (**C** and **D**, respectively) during 8 hours. Plots for cell count vs. fluorescence intensity (left representation in each panel). Data, collected from 3 independent experiments, were expressed as sCXCR4 FMI vs. control and shown as the mean±SD (right graphs in each panel).

2. TGF-β controls CXCR4 cell surface localization in PLC/PRF/5 and Hep3B cells

Previous work from our group described a direct correlation between TGF-β production and CXCR4 expression in HCC cells as well as in human tumors. Furthermore, those tumors that produced high amounts of TGF-β also showed an increased expression of CXCR4 located into cells in the migratory front or in areas of vascular invasion (Bertran et al., 2013).

These results prompted the subsequent study of the effect of TGF-β on the CXCR4 cell surface exposition in HCC cells. **Figure 5** shows that the targeted knock-down of the TGF-β receptor I (TβRI) in the epithelial-like PLC/PRF/5 cells produced a slight (non-significant) reduction of sCXCR4 (**Figure 5A** and **C**) correlating with their modest autocrine production of TGF-β (Bertran et al, 2013). In contrast, in the mixed epithelial-mesenchymal-like Hep3B cells, which produce TGF-β in an autocrine way (Bertran et al, 2013), the targeted knock-down of the TβRI produced a decrease in the percentage of cells with high sCXCR4 levels (60% decrease in the sCXCR4 levels in the silenced TβRI cells versus control cells, $p< 0.05$; **Figure 5B** and **D**).

Furthermore, when PLC/PRF/5 cells were treated with TGF-β for a short time they showed a significant increase in sCXCR4, while no changes were observed in Hep3B cells, in concordance with the lower autocrine production of TGF-β by PLC/PRF/5 cells when compared to Hep3B cells (**Figure 6A** and **B**). The use of these two different cell lines in the study of CXCR4 trafficking is interesting because they represent two different epithelial-mesenchymal HCC models.

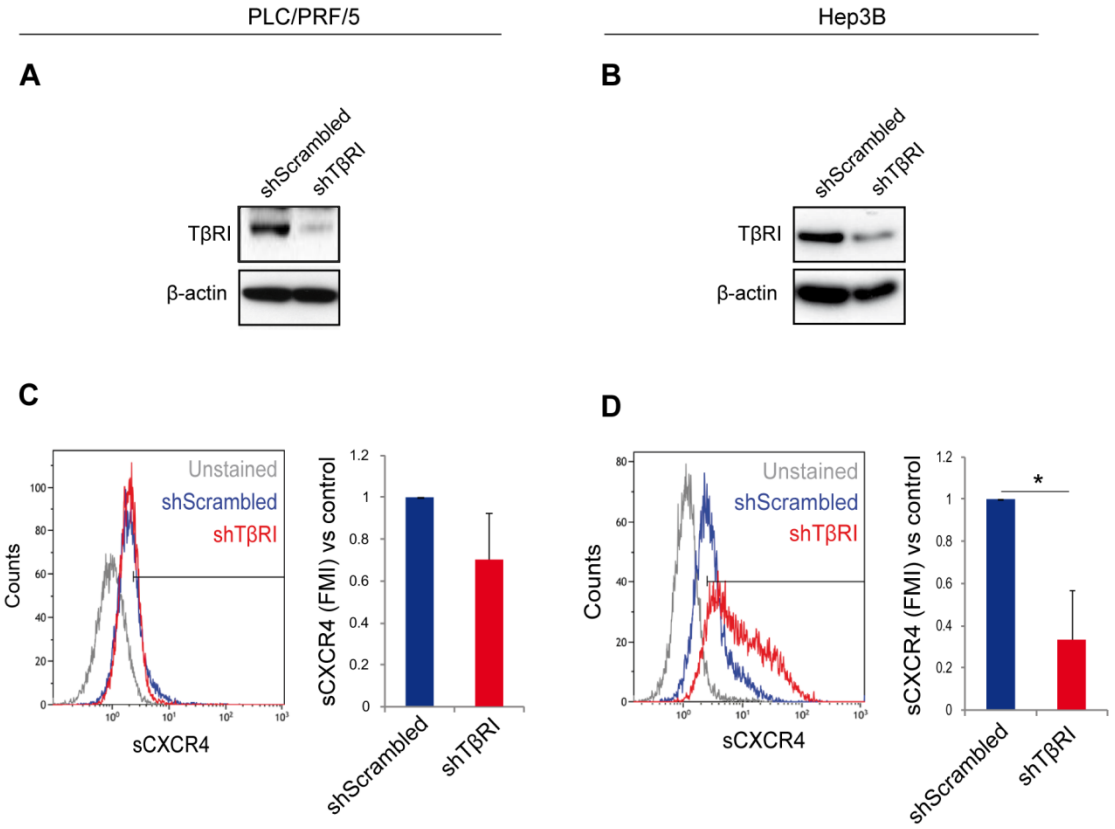

Figure 5. CXCR4 localization is dependent on the autocrine production of TGF-β in Hep3B cells. A and **B:** Western blotting analysis of TβRI expression in PLC/PRF/5 cells (**A**) and Hep3B cells (**B**) after transfection (and selection of the stable clones) with a specific TβRI shRNA (shTβRI) or with a control shRNA (shScrambled). β-actin is shown as a loading control. **C** and **D:** Flow cytometric analysis of sCXCR4 content in TβRI knock-down (shTβRI) vs. control (shScrambled) in PLC/PRF/5 and Hep3B cells (**C** and **D**, respectively, left representations). Data, collected from 3 independent experiments, were expressed as sCXCR4 FMI vs. control and shown as the mean±SD (right graphs in each panel; *: p< 0.05, Student's T test).

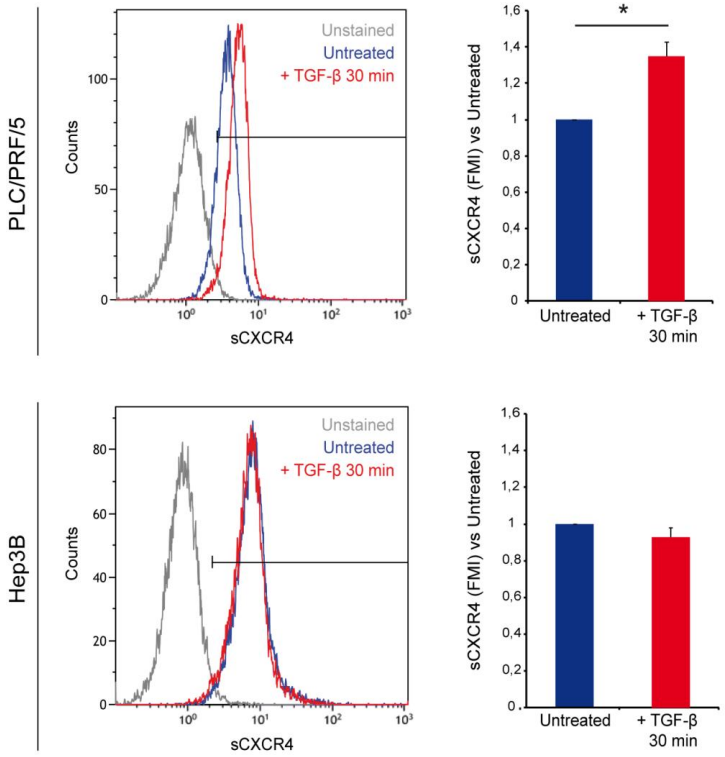

Figure 6. Surface CXCR4 export depends on the autocrine production of TGF-β. Left panels show representative flow cytometric analysis of sCXCR4 content in TGF-β-treated or untreated (control) PLC/PRF/5 and Hep3B cells. Right panels show the statistic analysis of the data collected from 3 independent experiments and expressed as the mean±SD of the sCXCR4 FMI vs. control (*: p< 0.05, Student's T test).

3. Intracellular CXCR4 transport to the plasma membrane follows the Golgi-exocyst axis

We studied the intracellular traffic of CXCR4 by transiently transfecting PLC/PRF/5 and Hep3B cells with a plasmid encoding a chimeric CXCR4-EGFP protein, and then performing co-localization studies with markers of the secretory and endocytic pathways. In this way, the CXCR4-EGFP chimera was shown to fully co-localize with golgin-97, a protein marker of the trans-Golgi network, in PLC/PRF/5 and Hep3B cells, (**Figure 7**; **left panels**, arrows). This conspicuous accumulation of CXCR4-EGFP in the Golgi apparatus was in agreement with the results of the previous flow cytometric assays, which showed high levels of endogenous CXCR4 at intracellular compartments (**Figure 1**). Furthermore, and as previously stated, CXCR4 was also localized at the cell-cell junctions in PLC/PRF/5 and Hep3B cells (**Figure 7**; arrowheads).

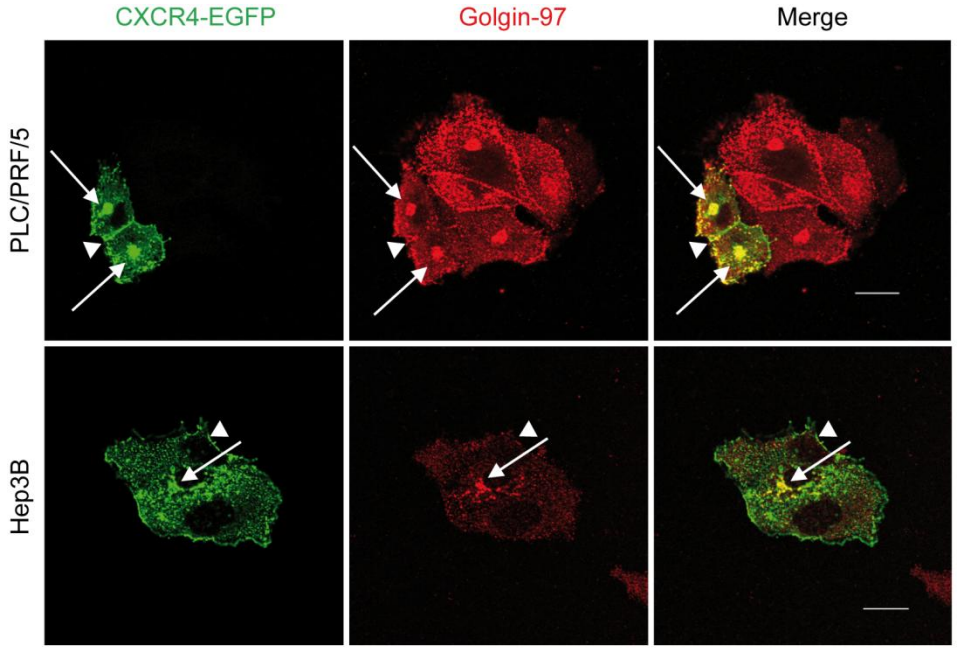

Figure 7. CXCR4 accumulates at the Golgi apparatus in both PLC/PRF/5 and Hep3B cells. Representative confocal images of HCC cells expressing the CXCR4–EGFP chimera (left panels), their staining with an anti-golgin-97 antibody (central panels) and the co-localization of both signals (yellow pixels at the right panels). Arrows point to the colocalization of EGFP–CXCR4 with the Golgi marker. Arrowhead points to EGFP–CXCR4 at cell-cell junctions. In the central and right panels several untransfected cells are also shown. A max. projection of 20 consecutive confocal sections is shown for golgin-97 in PLC/PRF/5 cells. Three consecutive confocal sections at the medium focal plan are shown in Hep3B cells. Scale bar is 16 μm.

To further confirm the CXCR4-EGFP localization in the Golgi apparatus, additional co-localization studies were carried out using additional Golgi markers. PLC/PRF/5 and Hep3B cells transiently transfected with the CXCR4-EGFP construct were stained for the manose-6-phosphate receptor (M6PR), a marker of the trans-Golgi network and of endosomal bodies trafficking to and from late endosomes, for β-cop (coatomer COPI complex), a pan-Golgi marker, and for GM130, a cis-Golgi marker. In all the cases we found a full co-localization of the CXCR4-EGFP chimera with the different Golgi markers in PLC/PRF/5 and Hep3B cells (**Figure 8**, arrowheads in right panels).

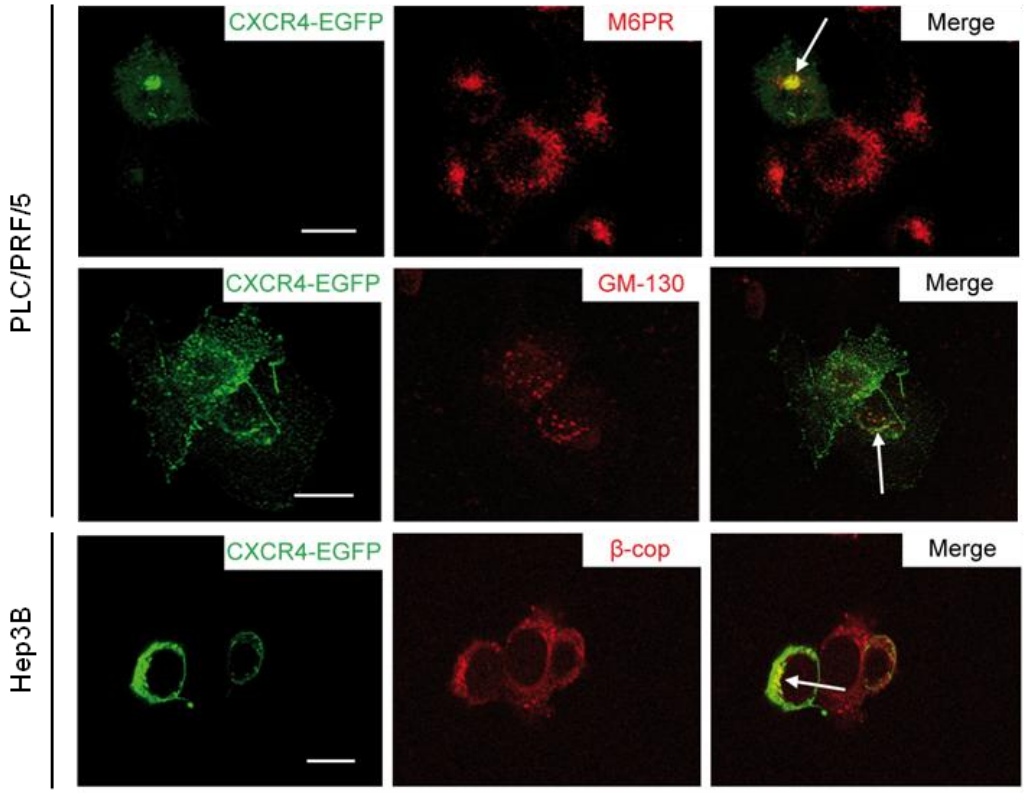

Figure 8. CXCR4 traffics to the plasma membrane through the Golgi apparatus. Representative confocal images of PLC/PRF/5 cells (top and central panels) and Hep3B cells (lower panels) expressing the EGFP-CXCR4 chimera (left panels), their staining with the following anti-Golgi antibodies: anti-M6PR, anti-GM-130 and anti-β-COP (see text for details), at the central panels, and the co-localization of both signals (yellow pixels at the right panels). Arrows point to the co-localization of EGFP-CXCR4 with the markers of the Golgi apparatus. In the central and right panels several untransfected cells are also shown. (Shown are individual confocal sections at a medium focal plane). Scale bars are 20 μm.

We next studied the implication of the secretory pathway in the intracellular traffic of CXCR4 to the plasma membrane by transiently transfecting PLC/PRF/5 and Hep3B cells with the CXCR4-EGFP plasmid and staining cells for the AP-1 adaptin complex, a marker of the secretory route. **Figure 9** documents the clear co-localization of CXCR4-EGFP and AP-1 in both cell types (arrows), indicating that CXCR4 follows the classical secretory route in its journey from the Golgi to the plasma membrane. CXCR4-EGFP labeling could be also detected in cell-cell junctions in the Hep3B cultures (**Figure 9**; arrowhead).

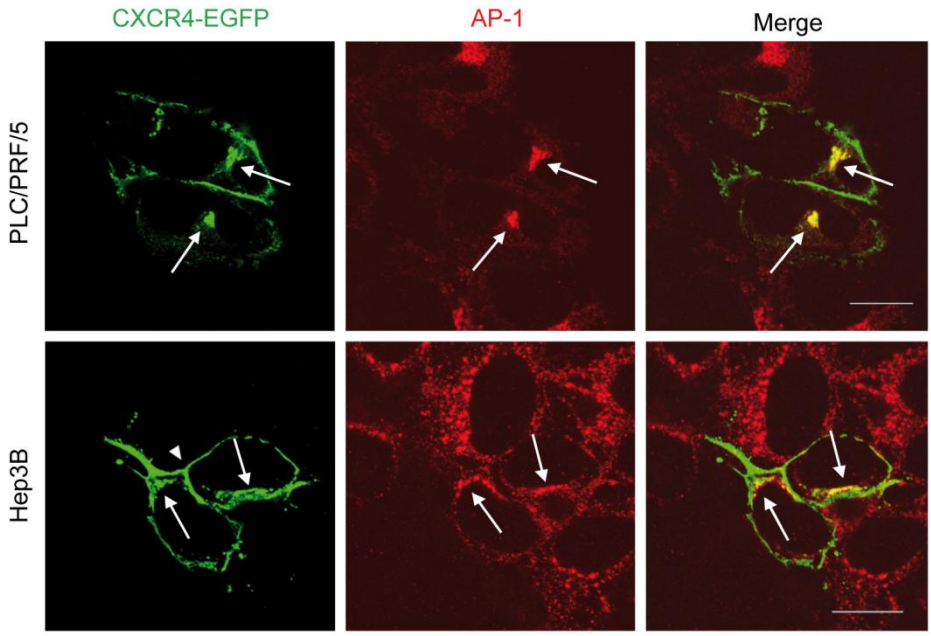

Figure 9. CXCR4 traffics to the plasma membrane following the secretory route. Representative confocal images of PLC/PRF/5 cells expressing the CXCR4-EGFP chimera (left panels), their staining with an anti-AP-1 antibody (central panels), and the co-localization of both signals (yellow pixels at the right panels). Arrows point to the colocalization of EGFP-CXCR4 with the AP-1-adaptin complex. Arrowhead points to EGFP-CXCR4 at cell-cell junction. In the central and right panels several untransfected cells are also shown. A single confocal section at the medium focal plane is shown for AP-1 in PLC/PRF/5. Three consecutive confocal sections at the medium focal plan are shown in Hep3B cells for AP-1. Scale bar is 20 μm.

4. CXCR4 transport to the plasma membrane requires a functional exocyst complex

The exocyst complex is involved in the fusion of the exocytic vesicles with the plasma membrane, as well as in the maintenance of cell polarity so that it is worth studying its potential role in the polarized export of CXCR4 to the plasma membrane.

We first analyzed the subcellular distribution of exocyst complex component 4 (EXOC4) in PLC/PRF/5 and Hep3B cells. By using a specific anti-EXOC4 antibody, this was found at the plasma membrane, at areas where adjacent cells were in contact (**Figure 10**; lower left panel). PLC/PRF/5 cells transiently transfected with the CXCR4-EGFP chimera (**Figure 10**; lower left panel) and stained for EXOC4 showed the co-localization of both signals at the lateral membrane at cell-cell junctions, (see the upper right panel and the three orthogonal sections at **Figure 10**).

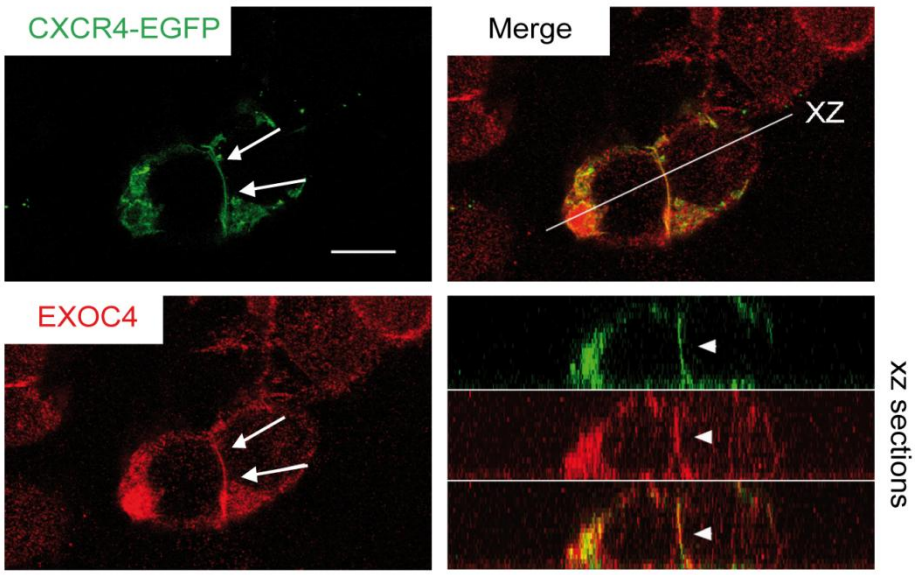

Figure 10. CXCR4 reaches plasma membrane through the exocyst complex. Representative confocal images of PLC/PRF/5 cells expressing the CXCR4-EGFP chimera (upper left panel), their staining with anti-EXOC4 (lower left panel), and the colocalization of both signals (yellow pixels at the upper right panel). Arrows point to the presence of CXCR4-EGFP and EXOC4 at the cell-cell junction of the EGFP-CXCR4 expressing cells. The three small lower right panels are orthogonal XZ sections for the red, green and merge channels of the two cells expressing EGFP-CXCR4, extracted at the level of the white bar of the upper right panel. The main panels show single confocal images at a medium focal plane. Scale bar is 20 μm.

To unravel the potential functional link between CXCR4 and the exocyst complex, we next silenced *EXOC4* expression in PLC/PRF/5 cells by using specific siRNAs. **Figure 11A** documents the specific reduction in EXOC4 levels in the siRNA-transfected PLC/PRF/5 cells when compared to cells transfected with the scrambled control siRNA. Furthermore, by flow cytometry we detected lower levels of surface CXCR4 in the EXOC4^{low} PLC/PRF/5 cells when compared to control cells, suggesting a functional dependence of CXCR4 on EXOC4 to reach the plasma membrane (**Figure 11B**).

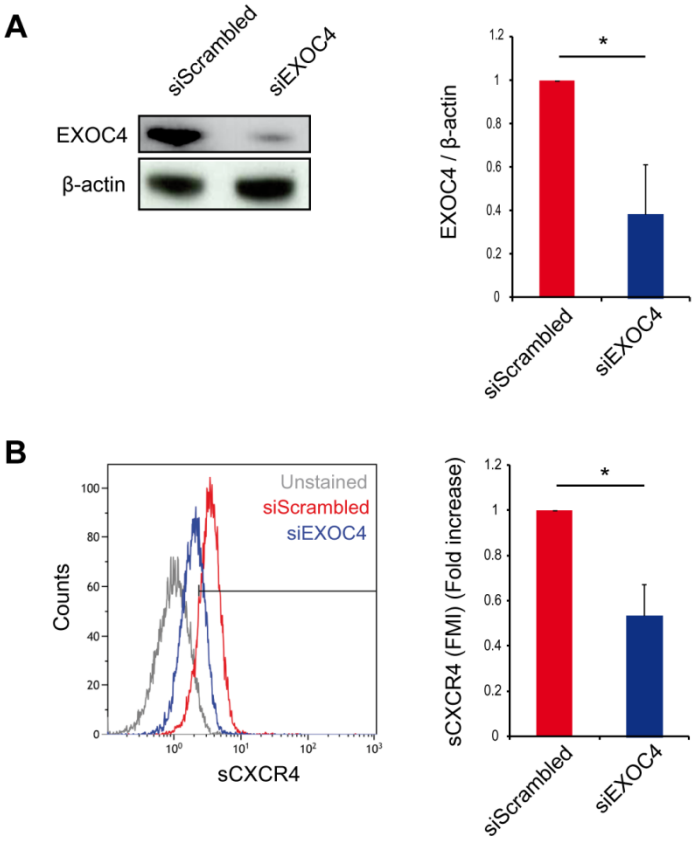

Figure 11. CXCR4 requires the exocyst complex to be transported to the plasma membrane in PLC/PRF/5 cells. A: Western blotting analysis of PLC/PRF/5 cells treated with an EXOC4-targetting siRNA (siEXOC4) or with a control siRNA (siScrambled). β-actin is shown as a loading control. Left: a representative experiment; Right: mean±SD of the densitometric analysis of four independent experiments, expressed as relative to β-actin levels. (*p< 0.05, Student's T test) **B:** Flow cytometric analysis of sCXCR4 levels in PLC/PRF/5 cells transiently transfected with either a scrambled siRNA or the specific EXOC4 siRNA. Left: A representative plot. Right: Quantitative analysis, expressed as mean±SD of three independent experiments. (*p< 0.05, Student's T test).

To further confirm the existence of a functional link between CXCR4 cell surface localization and the exocyst complex, PLC/PRF/5 cells were co-trasfected with the CXCR4-EGFP plasmid and a plasmid encoding a different functional form of EXOC4, either a wild type or a dominant negative (S32A) form (Lyons et al., 2009). Cells co-transfected with the dominant negative form of EXOC4 (S32A) showed a much dispersed and cytoplasmic distribution of CXCR4-EGFP (**Figure 12**; lower panels; arrowheads) when compared to the distribution displayed by cells transfected with the wild type form of EXOC4 (**Figure 12**; upper panels).

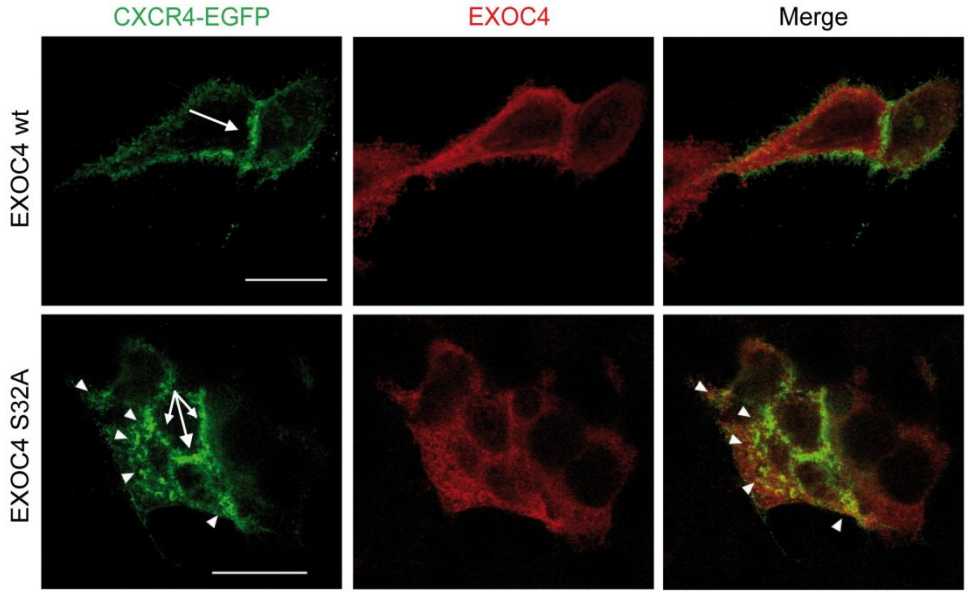

Figure 12. EXOC4 is required for the correct targeting of CXCR4 to the plasma membrane. Representative confocal images of PLC/PRF/5 cells co-transfected with CXCR4-EGFP and with a plasmid encoding the wild-type (upper panels) or dominant-negative (EXOC4^{S32A}) forms (lower panels) of rat EXOC4. In both panels, arrows show CXCR4-EGFP at the cell-cell junctions, and arrowheads indicate CXCR4-EGFP dispersed by the cytoplasm of pEXOC4^{S32A}-expressing cells. Shown are average projections of three confocal sections at a medium focal plane. Scale bars are 20 μm.

We also studied the subcellular distribution of EXOC4 and CXCR4-EGFP in Hep3B cells. CXCR4-EGFP and EXOC4 co-localized at discrete regions of the plasma membrane (**Figure 13A**; white arrows). Interestingly, several vesicles were found to contain CXCR4-EGFP and EXOC4, mainly at the tip of growing projections, suggesting a specific targeting of CXCR4-EGFP to the plasma membrane driven by the exocyst complex (**Figure 13A**; yellow arrows). Furthermore, and as already stated for PLC/PRF/5 cells, CXCR4-EGFP and EXOC4 were visualized at plasma membrane areas coinciding with cell-cell junctions, (**Figure 13B; arrows**), suggesting that CXCR4 needs the functionality of the exocyst complex to reach plasma membrane.

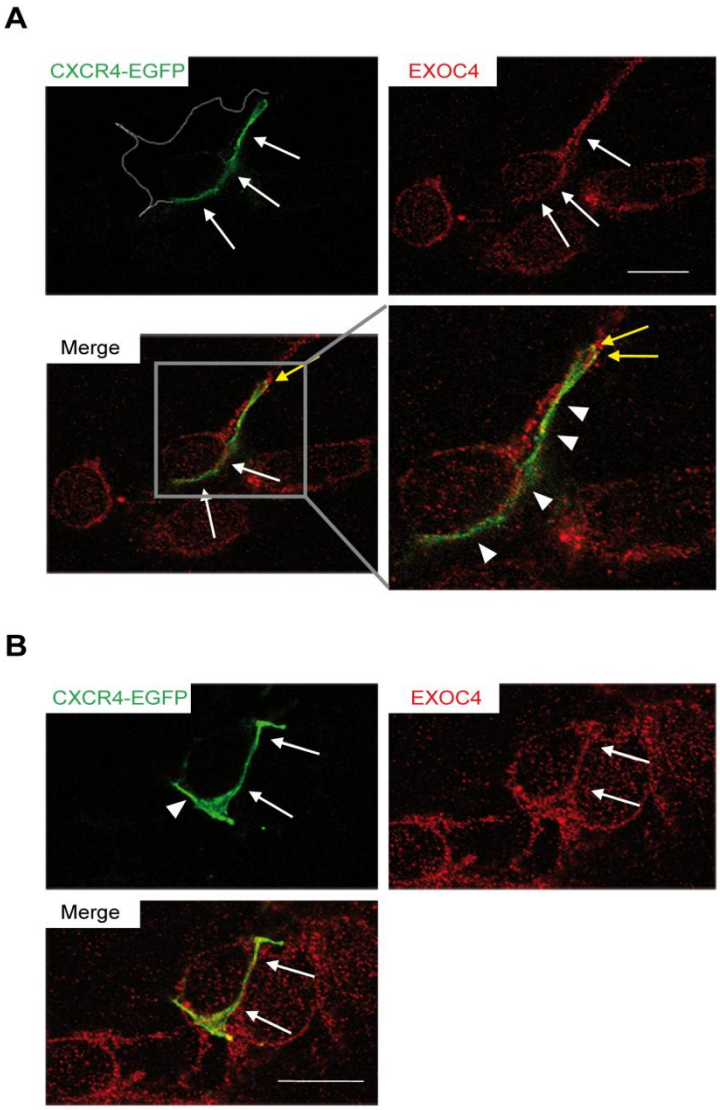

Figure 13. CXCR4-EGFP and EXOC4 co-localize at the plasma membrane in Hep3B cells. A: Representative confocal images of individualized Hep3B cells expressing the CXCR4-EGFP chimera (upper left panel), their staining with anti-EXOC4 (upper right panel), and the colocalization of both signals (yellow pixels at the lower left panel). The central cell showing CXCR4-EGFP and EXOC4 labels is magnified at the lower right panel. Arrows in the upper panels point to the presence of CXCR4-EGFP and EXOC4 at the membranes of Hep3B cells, as well as the arrowheads in the magnified panel. The yellow arrow in the magnified panel shows two vesicles, at the tip of a membrane projection, in which CXCR4-EGFP and EXOC4 can be detected together. The white line of the upper left panel draws the perimeter of the Hep3B cell. Shown are single confocal images at a medium focal plane. Scale bar is 20 µm. **B:** Representative confocal images of a group of Hep3B cells expressing the CXCR4-EGFP chimera (upper left panel), their staining with anti-EXOC4 (upper right panel), and the co-localization of both signals (yellow pixels at the lower panel). Arrowheads show sites of CXCR4-EGFP and EXOC4 co-localization at the cell-to cell junction, while the arrowhead at the upper left panel shows CXCR4-EGFP at the plasma membrane in the absence of cell-cell contact. Shown is the max. projection of three consecutive confocal images at a medium focal plane. Scale bar is 20 µm.

5. PLC/PRF/5 and Hep3B cells use different routes for CXCR4 internalization and recycling

5.1. The specific ligand SDF-1α induces CXCR4 internalization in PLC/PRF/5 and Hep3B cells

Membrane levels of chemokine receptors depend on the balance between their export and their internalization, after ligand binding or by tonic endocytosis. Thus, we next studied the mechanisms controlling CXCR4 internalization and their impact on the maintenance of receptor levels at the plasma membrane by stimulating PLC/PRF/5 and Hep3B cells with the specific CXCR4 ligand, SDF-1α. SDF-1α induced a similar internalization of CXCR4 in both PLC/PRF/5 and Hep3B cells with PLC/PRF/5 cells showing over a 40% decrease in sCXCR4 and Hep3B cells a 50% decrease in sCXCR4 after SDF-1α treatment (**Figure 14A** and **C**). Moreover, while the percentage of PLC/PRF/5 cells expressing sCXCR4 also diminished no changes were observed in Hep3B cells, which maintained the number of positive cells but reduced the level of sCXCR4 in cells expressing the highest levels of CXCR4.

5.2. PLC/PRF/5 use clathrin- or caveolin-mediated pathways for CXCR4 internalization while Hep3B cells use macropinocytosis

To investigate the contribution of different endocytic mechanisms in CXCR4 internalization, we studied two of the most important and better described pathways: clathrin-dependent and caveolin-mediated (clathrin-independent) endocytosis. To unravel the role of each endocytic mechanism in CXCR4 internalization, PLC/PRF/5 and Hep3B cells were treated with two endocytosis inhibitors: methyl-β-cyclodextrin (MβC), which inhibits caveolin-dependent internalization by disrupting the integrity of lipid rafts; and dynasore, which inhibits the activity of dynamins I and II and blocks both clathrin- and caveolin-dependent endocytosis.

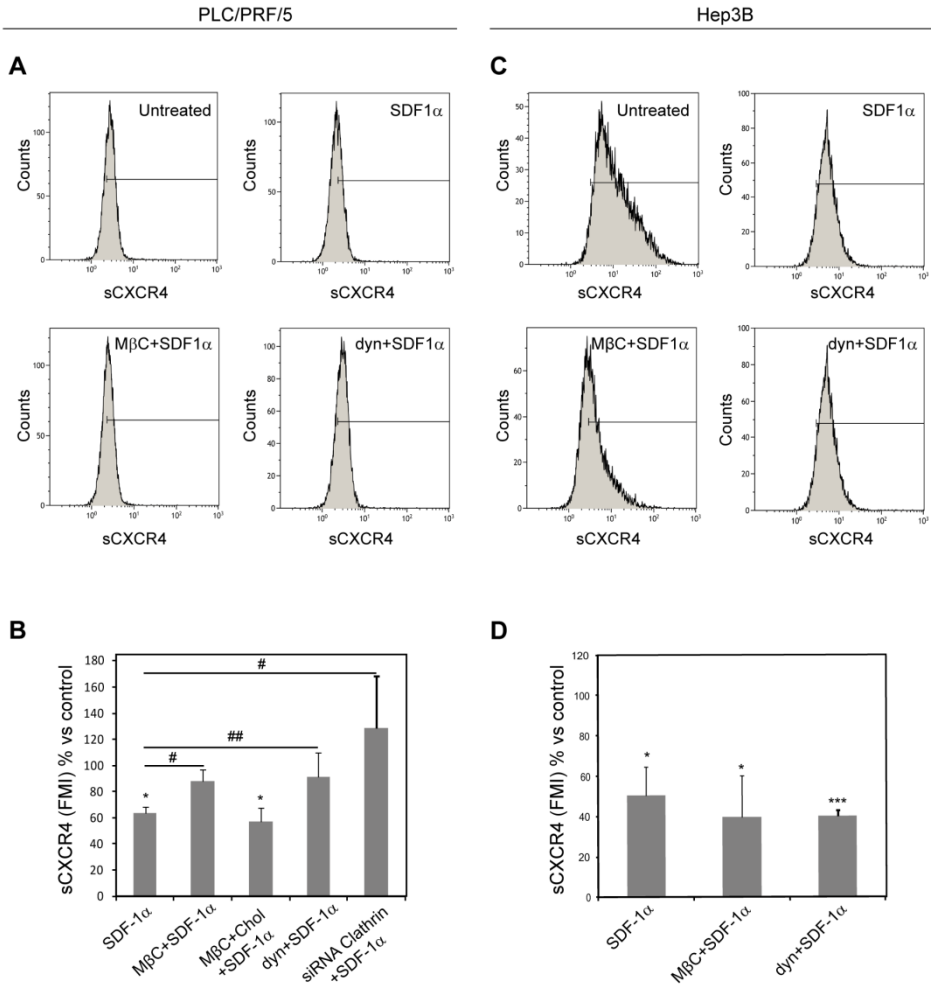

Figure 14. Endocytosis of CXCR4 in SDF-1α-treated PLC/PRF/5 and Hep3B cells. Effect of the endocytosis inhibitors MβC and dynasore. A and **C:** Flow cytometry plots showing sCXCR4 in PLC/PRF/5 (**A**, upper-left panel) and Hep3B (**C**, upper-left panel) cells, its internalization upon ligand binding (100 ng/mL SDF-1α treatment during 8 h, upper-right panels), as well as the effect caused by preincubation with MβC (2.5 μM, lower-left panels) and dynasore (dyn, at 80 μM, lower-right panels). A representative plot of three different experiments is shown. **B** and **D:** Quantitative analysis of the decrease in sCXCR4 after SDF-1α treatment in PLC/PRF/5 (**B**) and Hep3B cells (**D**), and how pre-treatment with MβC or dynasore interferes in this effect. Also shown are the recovery effect of cholesterol on SDF-1α-mediated endocytosis after MβC treatment (MβC+Chol+ SDF-1α), and the blockade of internalization after incubation with a clathrin-specific siRNA (siRNA Clathrin + SDF-1α), as complementary experiments for the two pathways studied. Results are mean±SD of three independent experiments. Statistical analysis: *p<0.05, ***p<0.001: values referred to each respective control (no SDF-1α treatment) and data analyzed by using the Student's t test; #p<0.05, ##p<0.01: values referred to the SDF-1α treated cells and data analyzed by Tukey's one-way Anova test.

PLC/PRF/5 and Hep3B cells were treated with dynasore or MβC for 30 min before adding SDF-1α, and sCXCR4 levels were analyzed by flow cytometry. In PLC/PRF/5 cells, both dynasore and MβC were shown to prevent the SDF-1α-induced internalization of CXCR4, which suggests that CXCR4 internalization proceeded via clathrin and/or caveolin-mediated endocytosis (**Figure 14A** and **B**). The specificity of MβC was proved by adding exogenous cholesterol to the cultured cells, which canceled the effect of the inhibitor (**Figure 14B**). The involvement of clathrin-dependent endocytosis was corroborated by siRNA-mediated targeting knock-down of its expression (**Figure 14B**). In contrast to the results observed in PLC/PRF/5, in Hep3B cells neither dynasore nor MβC were able to prevent the SDF-1α- induced internalization of CXCR4 (**Figure 14C** and **D**). We checked the efficiency of dynasore in inhibiting endocytosis in Hep3B cells by measuring the internalization of transferrin, a marker of clathrin-mediated endocytosis (Hanover et al., 1984). HCC cells were treated with dynasore for 30 min, prior to adding a transferrin-rhodamin conjugate to the culture medium, and cells were fixed after 5, 15 or 30 min of incubation at 37ºC. A clear perinuclear accumulation of transferrin-rhodamin conjugate was already visible in untreated PLC/PRF/5 cells after 15 min of incubation, in comparison with dynasore-treated cells which did not show this pattern (**Figure 15**; left panels). Similarly, untreated Hep3B cells showed a cytoplasmic localization of the transferrin-rhodamin conjugate, with some perinuclear accumulations, while in dynasore-treated cells this was barely visible (**Figure 15**; right panels). This result prompted us to investigate alternative paths for CXCR4 internalization in Hep3B cells.

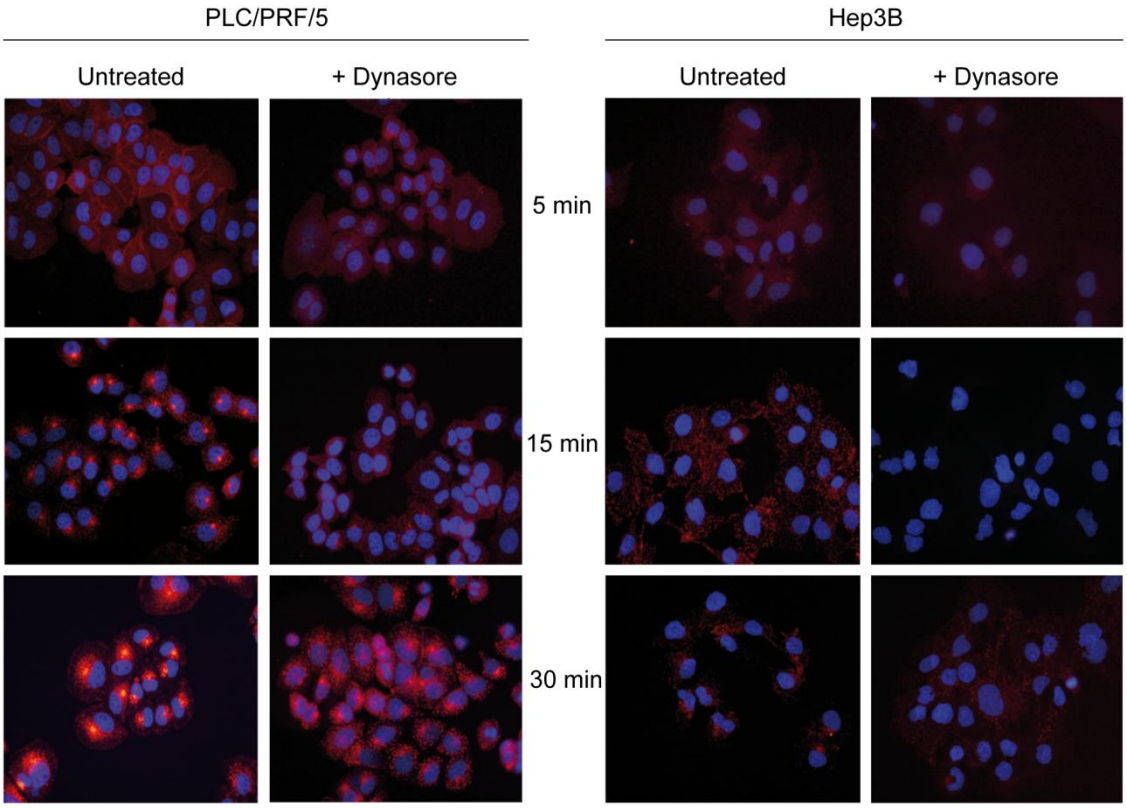

Figure 15. Dynasore inhibits the internalization of rhodamine-conjugated transferrin in PLC/PRF/5 and Hep3B cells. Cells were pre-treated with 80 µM dynasore for 30 min and were then incubated with 20 µg/ml of transferrin^{rhodamine} conjugate. Cells were left to internalize the label, and at the stated times were prepared for immunocytochemical analysis. Shown are representative microscopy pictures of the PLC/PRF/5 and Hep3B cells in which the internalized transferrin^{rhodamine} conjugate can be seen in red and the cell nuclei stained in blue (DAPI). While at 30 min most of the untreated PLC/PRF/5 or Hep3B cells showed the transferrin^{rhodamine} conjugate in perinuclear endosomal bodies, dynasore-treated cells showed the conjugate at cytoplasmic vesicles. All pictures were taken at a 40X magnification.

In order to obtain a deeper knowledge of CXCR4 internalization, we investigated alternative paths by which CXCR4 could be internalized in Hep3B cells. It has been recently reported that macropinocytosis may be implicated in CXCR4 internalization in several cell models (Tanaka et al., 2012), and that this is hindered by the specific inhibitor dimethylamiloride (DMA). We first treated Hep3B cells with increasing doses of DMA and checked Hep3B cell viability by crystal violet staining analysis to determine the working dose. This was established at 100 µM, since higher doses were toxic for the cells (cell viability under 50%) (**Figure 16A**). Thus, Hep3B cells were treated with 100 µM DMA for 30 min prior to adding 100 ng/mL SDF-1α for 8 hours. DMA treatment blocked

SDF-1α-mediated CXCR4 internalization in Hep3B cells, demonstrating that macropinocytosis played a significant role in the internalization of CXCR4 in these cells (**Figure 16B** and **C**).

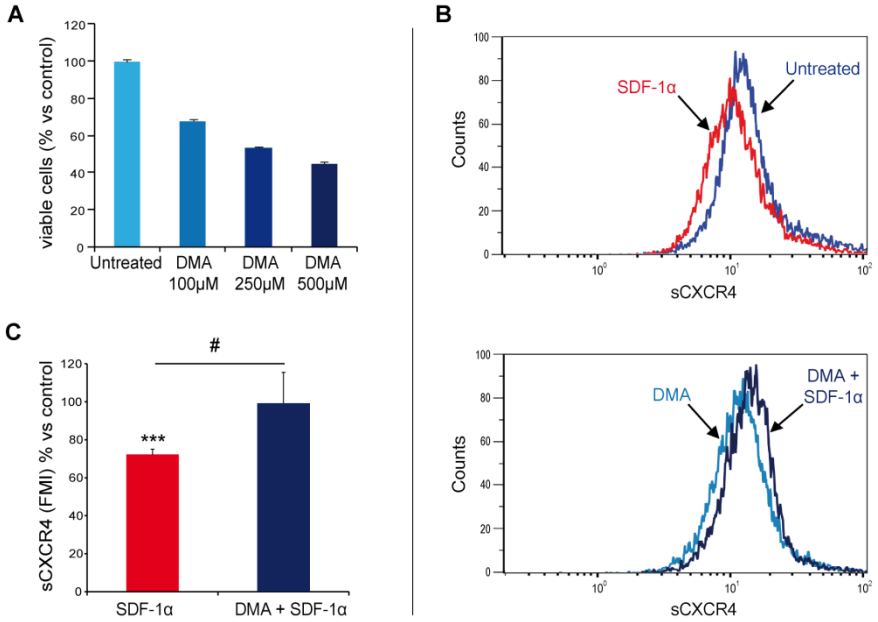

Figure 16. CXCR4 is internalized by macropinocytosis in SDF-1α-treated Hep3B cells. A: Cell viability analysis by crystal violet with increasing doses of DMA. **B:** Upper panel: Flow cytometric analysis of sCXCR4 in Hep3B cells and its internalization upon ligand binding (100 ng/mL SDF-1α treatment during 8 h). Lower panel: Prevention of SDF-1α-induced internalization of CXCR4 by preincubation of cells with 100 μM DMA. Representative plots of three independent experiments. **C:** Quantitative analysis as mean ± SD of the different experiments. Statistical analysis: ***p<0.001: value referred to control untreated cells (no significant differences were observed when treatment with DMA + SDF-1α was compared to DMA-treated or untreated cells); #p<0.05: values referred to the SDF-1α treated cells. In both cases, data were analyzed by using the Student's t test.

To prove the specificity of the macropinocytosis on the CXCR4 trafficking in SDF-1α-treated Hep3B cells, we analyzed the effect of DMA on the internalization of another cell surface receptor, the Epidermal Growth Factor Receptor (EGFR) known to be internalized through the clathrin-mediated pathway. The exposition of this receptor at the cell surface did not change by the treatment with DMA, neither in untreated nor in SDF-1α-treated cells (**Figure 17A** and **B**). DMA did not show any significant inhibitory effect on SDF-1α-mediated endocytosis in PLC/PRF/5 cells (data not shown). The above

results indicate that HCC cells activate different pathways for CXCR4 internalization. Thus, while in the epithelial-like PLC/PRF/5 cells CXCR4 is internalized through clathrin- and caveolin-mediated pathways, the mixed epithelial/mesenchymal-like Hep3B cells use macropinocytosis for CXCR4 endocytosis.

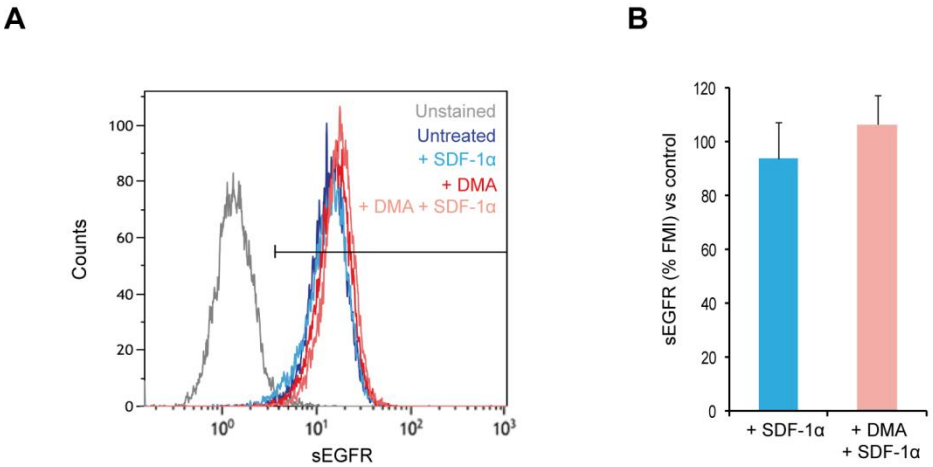

Figure 17. Macropinocytosis inhibition does not alter the intracellular distribution of other membrane receptors in Hep3B cells. Hep3B cells were treated with SDF-1α (100 ng/mL) in the presence or absence of DMA (macopinocytosis inhibitor) (100μM) during 8 h, and surface levels of EGFR (sEGFR) were analysed by flow cytometry. **A:** Representative plot showing cell count vs fluorescence intensity. **B:** Data, collected from 4 independent experiments, were expressed as sEGFR (% FMI) vs. corresponding control and are mean±SD (Untreated or treated with DMA, as indicated in the figure).

5.3. Role of the recycling pathways in CXCR4 trafficking in human HCC cells

Once internalized, membrane receptors could follow two different routes: 1) trafficking through late endosomes to lysosomes for degradation and definitive signal termination; or 2) recycling back to the plasma membrane, through the recycling endomose, to restart signaling.

The implication of the recycling pathway in CXCR4 trafficking after its internalization from the plasma membrane was tested by immunocytochemical assay. Confocal microscopy images demonstrated that in untreated PLC/PRF/5 and Hep3B cells the chimeric protein CXCR4-EGFP co-localized with Rab11, a marker of recycling endosomes (**Figure 18;** arrows at the panels displaying

"untreated" cells). In addition, co-localization of CXCR4-EGFP with Rab11 was not due to an autocrine secretion of the specific CXCR4 ligand SDF-1α, since cells treated with the SDF-1α antagonist AMD3100 displayed a similar staining pattern of distribution (**Figure 18;** arrows at the panels displaying "AMD3100-treated" cells). Equally, cells treated with SDF-1α maintained the same distribution of both proteins, indicating that the treatment with the ligand did not modify the intracellular trafficking path of CXCR4 (**Figure 18;** arrows at the panels displaying "SDF-1α -treated" cells). However, PLC/PRF/5 cells treated with SDF-1α showed a more dispersed cytoplasmic CXCR4 staining pattern with CXCR4-EGFP positive/Rab11 negative vesicles (**Figure 18**; white arrowheads at the panel displaying "SDF-1α -treated" PLC/PRF/5 cells) but still displaying CXCR4 at the cell-cell junctions (**Figure 18**; green arrowheads at the panel displaying "SDF-1α -treated" PLC/PRF/5 cells). Strikingly, some vesicles showing co-localization of CXCR4-EGFP and Rab11 were also found in AMD-treated Hep3B cells, an interesting finding taking into account, as we previously demonstrated, that these cells used macropinocytosis to internalize CXCR4 (**Figure 18;** arrows at the panels displaying "AMD3100-treated" cells). Thus, these data indicate that despite of using different endocytic mechanisms to internalize CXCR4, both PLC/PRF/5 and Hep3B cells may use common recycling hubs for receptor sorting.

We next studied the relationship among CXCR4-EGFP and Rab4, a monomeric GTPase associated with early endosomes and described as a regulator of the formation of recycling vesicles (Jones et al., 2006). In untreated PLC/PRF/5 cells we detected a limited co-localization of CXCR4-EGFP with Rab4-positive vesicles which significantly increased after SDF-1α treatment (**Figure 19**; upper panels). On the, contrary, Hep3B cells displayed much less co-localization of CXCR4-EGFP with Rab4 when compared to that found in PLC/PRF/5 cells (**Figure 19**; lower panels). This result suggests that after SDF-1α treatment, CXCR4 follow different trafficking routes in PLC/PRF/5 and in Hep3B cells, an expected result taking into account their different response to inhibitors of clathrin- and caveolin-dependent endocytic pathways.

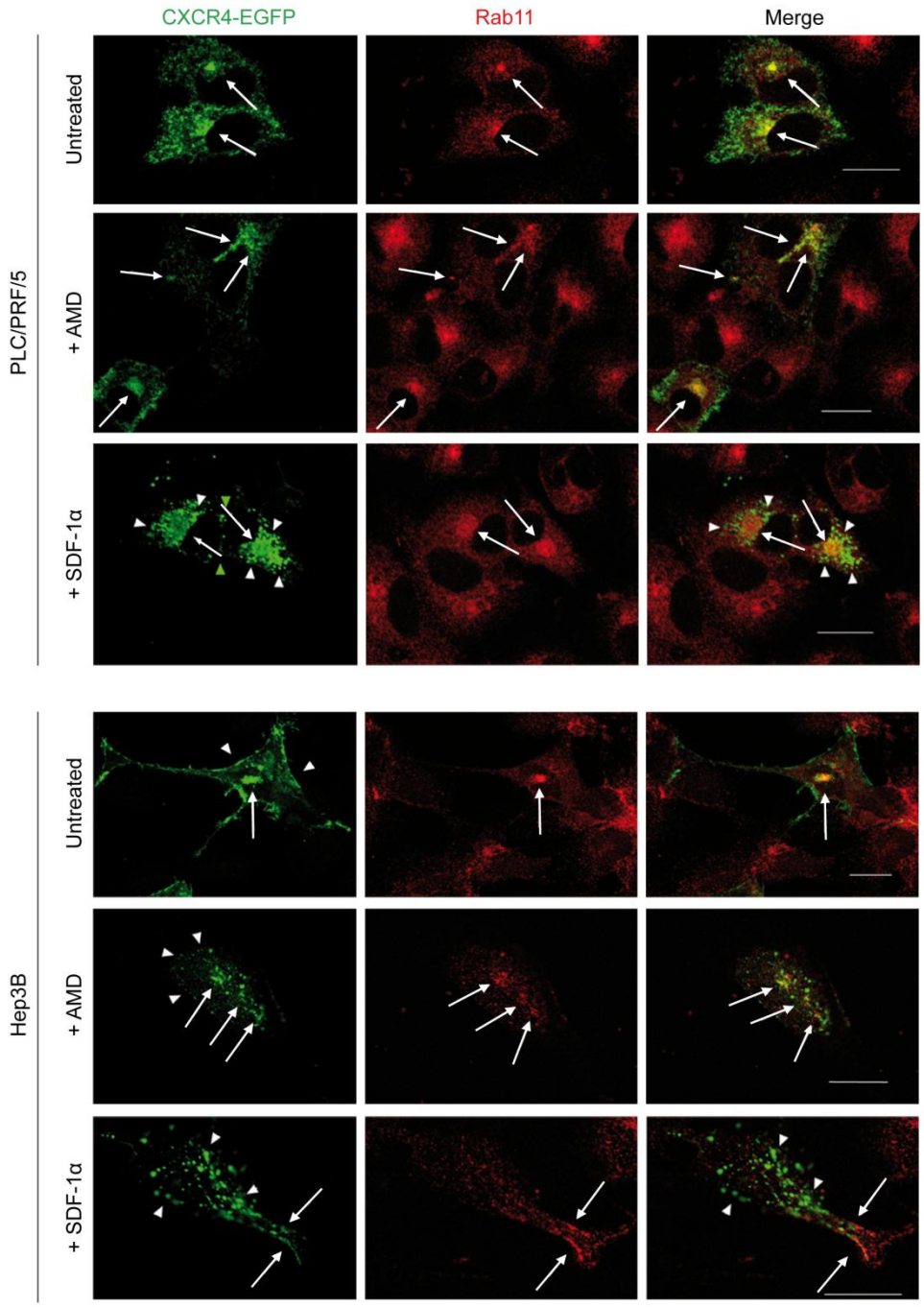

Figure 18. EGFP-CXCR4 accumulates in Rab11^{+} recycling endosomes in PLC/PRF/5 and Hep3B cells. Representative confocal images of PLC/PRF/5 and Hep3B cells expressing the CXCR4-EGFP chimera (left panel), their staining with anti-Rab11 (central panel), and the co-localization of both signals (yellow pixels at the right panel). Cells were untreated or treated with the SDF-1α antagonist AMD3100 (1 μg/mL) or SDF-1α (100 ng/mL) during 8 h. Arrows show colocalization of CXCR4-EGFP and Rab11. Arrowheads show CXCR4-EGFP positive/Rab11 negative vesicles and the green arrowheads the presence of EGFP-CXCR4 at cell-cell junctions. Shown is the average projection of three consecutive confocal sections at a medium focal plane. Scale bars are 20 μm.

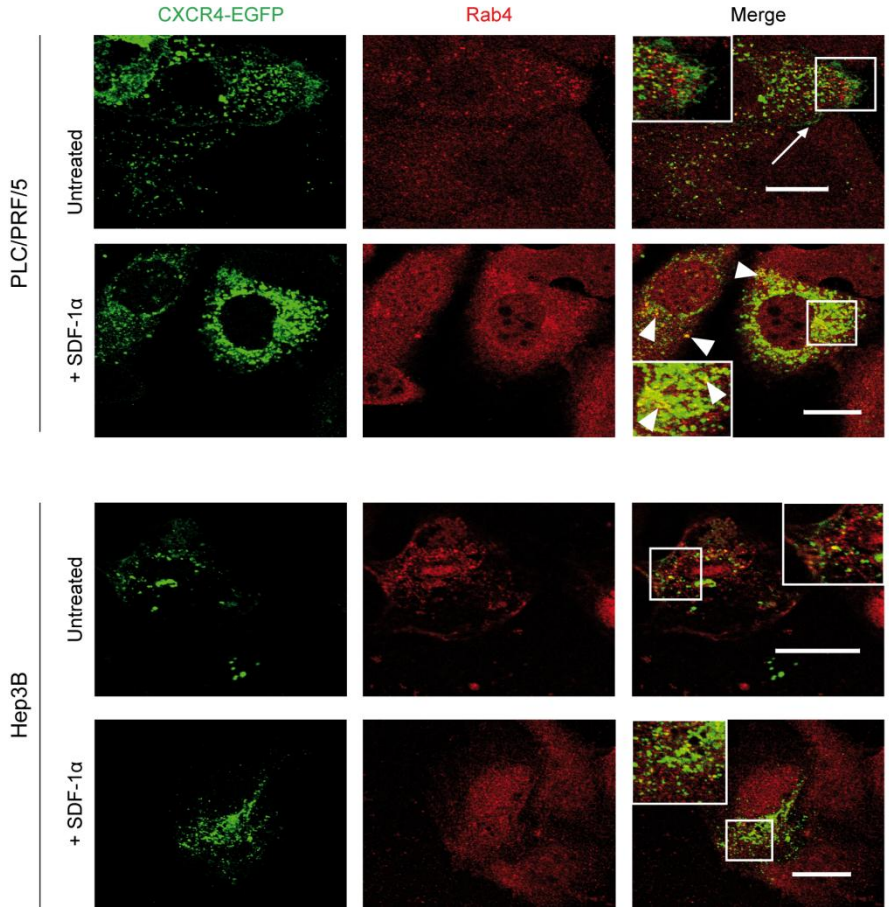

Figure 19. EGFP-CXCR4 is localized in Rab4$^+$ endosomes in PLC/PRF/5, but not in Hep3B cells. Representative confocal images of PLC/PRF/5 and Hep3B cells expressing the CXCR4-EGFP chimera (left panels), their staining with anti-Rab4 (central panels), and the co-localization of both signals (yellow pixels at the right panels) in untreated or treated cells with 100 ng/ml SDF-1α for 8 h. Arrowheads show colocalization of CXCR4-EGFP with Rab4. Arrow shows CXCR4 localized at the plasma membrane. Average projection of three to five confocal sections at a medium focal plane. Scale bars are 20 μm.

Rab11 is not restricted to recycling endosomes but it has been also described as a marker of the trans-Golgi network or of post-Golgi vesicles (Maxfield and McGraw, 2004). To better understand the role of Rab11 in the regulation of CXCR4 intracellular trafficking, we treated PLC/PRF/5 cells with brefeldin A, a well-known Golgi-disrupting agent which inhibits secretory protein transport. As shown in **Figure 20A,** upper left panel**,** in untreated PLC/PRF/5 cells, CXCR4-EGFP localized at cell-cell junctions and also at intracellular membrane compartments, showing a high degree of co-localization with Rab11 (**Figure 20A**, lower left panel), as observed in the plot of pixel intensity along the line

drawn at the insert area of merged panel (**Figure 20A**, lower right panel). Brefeldin A treatment disrupted the Golgi-like staining pattern of CXCR4-EGFP (**Figure 20B**, upper left panel) and the pericentriolar Rab11 staining (**Figure 20B**, upper right panel), and no co-localization of the main CXCR4-EGFP and Rab11 intracellular accumulations was found (**Figure 20B**, lower left panel). In addition, Brefeldin A attenuated the presence of CXCR4-EGFP at the plasma membrane, probably due to the blockade of secretory pathway of CXCR4 (**Figure 20A** and **B,** compare membrane CXCR4-EGFP in the untreated and BFA-treated panels).

The clear difference in the pixel intensity profiles of CXCR4 and Rab11 immuno-stainings suggests that BFA reduced the formation of $Rab11^{+}$/$CXCR4^{+}$ vesicles. Altogether, these results indicate that $Rab11^{+}$ endosomes also participate in the post-Golgi delivery of CXCR4–EGFP to the cell surface.

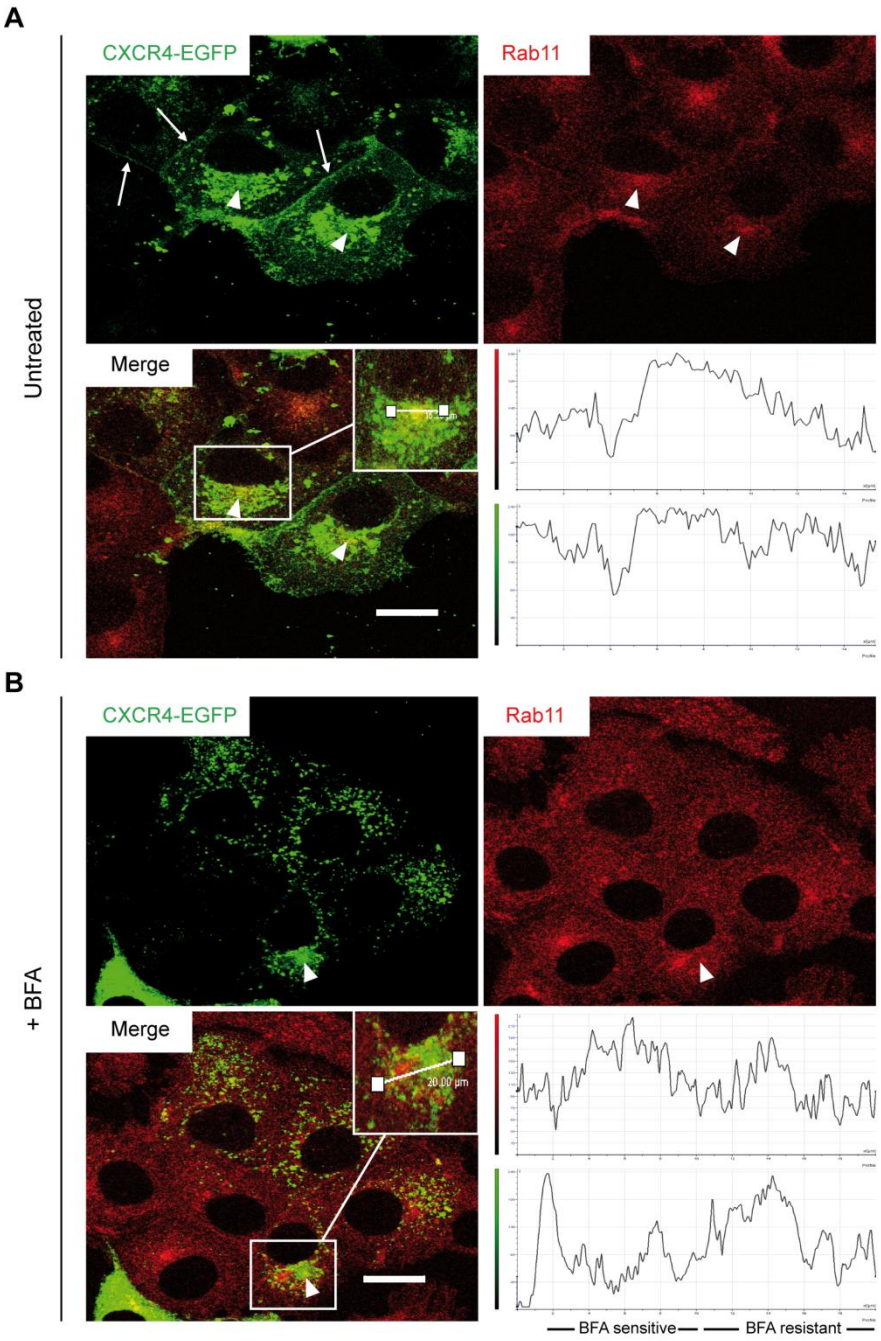

Figure 20. Brefeldin A treatment impairs exportation of CXCR4-EGFP to cell-cell junctions at the plasma membrane. A: Representative confocal images of untreated PLC/PRF/5 cells expressing the CXCR4-EGFP chimera (upper left panel), their staining with anti-Rab11 (upper right panel) and the co-localization of both signals (yellow pixels at the lower left panel). The profile of pixel intensity along the white line drawn in the insert (lower left) is presented in the lower right panel. Arrows indicate the presence of EGFP-CXCR4 at cell surface (cell-cell junctions), and arrowheads indicate $Rab11^{+}$ patches. **B:** As in A, but after treating cells with 10 µg/mL brefeldin A during 3 h. Both A and B show single confocal sections at a medium focal plane. The profiles of pixel intensity were performed on the max. projections of five consecutive confocal sections (see insert boxes) at a medium focal plane. Scale bars are 20 µm.

6. TGF-β, PAR3 and the maintenance of the epithelial phenotype in HCC cells

There are evidences of the involvement of TGF-β in the functional regulation of the PAR polarity complex (PAR3/PAR6/aPKC). TGF-β is signaling through a PAR6-dependent pathway, leading to the disruption of tight junctions and enhancing EMT (Ozdamar et al., 2005).

TGF-β has been shown to disrupt tight junctions and to enhance EMT by signaling through PAR6, one of the components of the PAR complex, as well as to down-regulate PAR3 expression in epithelial cells during the EMT process (Wang et al., 2008b). Considering the relevance of PAR3 for the mechanisms of epithelial cell polarity (see the *Introduction* section; *3.1. Apical-basal polarity complexes*), we underwent to study the involvement of PAR3 in the loss of cell polarization and acquisition of migratory potential by HCC cells after TGF-β treatment.

PARD3 mRNA expression was determined, by qPCR, in PLC/PRF/5 (epithelial-like), Hep3B (mixed epithelial/mesenchymal-like), and in the Snu449 and HLE (mesenchymal-like) HCC lines, but no clear correlation could be established between the epithelial/mesenchymal status of the cells and *PARD3*[1*] mRNA levels (**Figure 21**), with epithelial PLC/PRF/5 and Hep3B cells showing higher *PARD3* mRNA levels than HLE cells but lower than Snu449 cells, both with more mesenchymal features (**Figure 21A**). PAR3 protein levels, tested by western blot, essentially followed those of *PARD3* mRNA, with Snu449 cells expressing more PAR3 than the rest of cell lines tested (**Figure 21B**). We next studied PAR3 subcellular localization in these same HCC cells, and a clear difference was observed among epithelial and mesenchymal cells. As shown in **Figure 21C**, in clusters of PLC/PRF/5 cells PAR3 was detected at the plasma membrane of cells, at cell-cell junctions. In the case of Hep3B cells, which also form parenchymas with loose cell-cell junctions instead of tight clusters, PAR3 was located at cell-cell junctions as in the PLC/PRF/5 cells. On the contrary, mesenchymal-like cells Snu449 and HLE, which are more individualized and do

[*] *PARD3* refers to the gene encoding for PAR3 protein.

not form parenchymas, showed a predominantly cytoplasmic PAR3 localization (**Figure 21C**), although in HLE cells PAR3 could be also detected at the plasma membrane (**Figure 21C**, arrows).

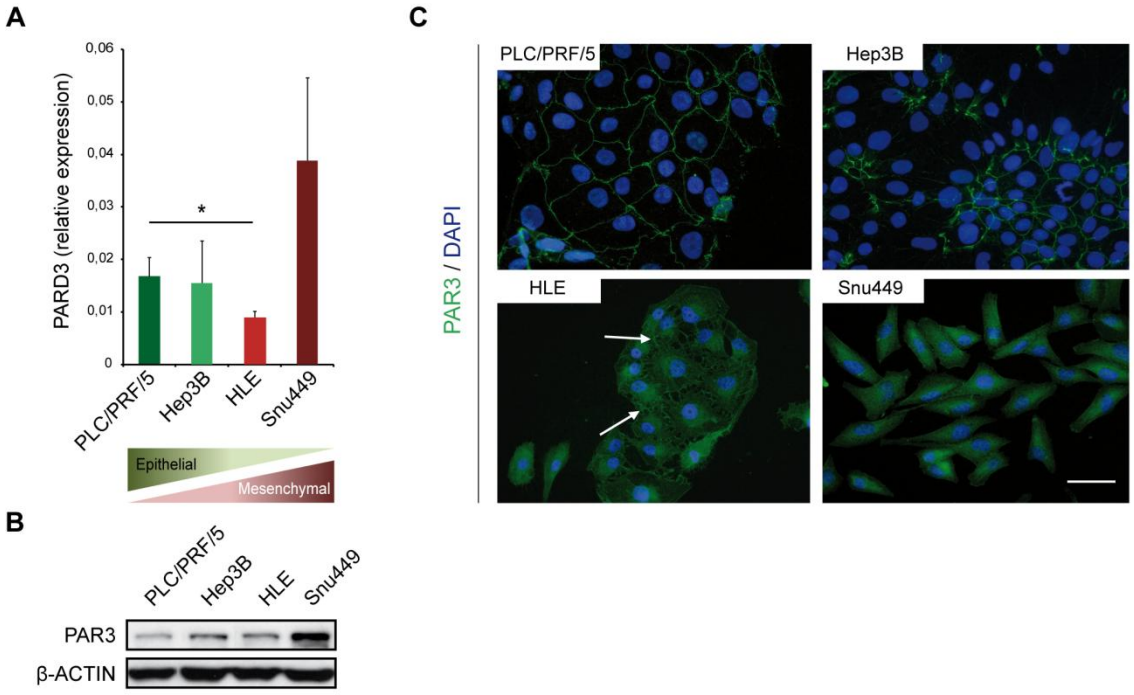

Figure 21. Expression and subcellular localization of PAR3 in different HCC cell lines. Localization of PAR3 depends on the epithelial/mesenchymal features of the cells. A: *PARD3* expression in the HCC cell lines stated, as determined by qPCR. Shown is the mean ± SD of three independent experiments. *p<0.05, Student's T test. **B:** Representative western blotting analysis of PAR3 in the stated HCC cell lines. β-ACTIN is shown as loading control. **C:** Representative immunofluorescence analysis of the stated HCC cell lines stained with an anti-PAR3 antibody (green) and DAPI (blue). Arrows show membrane-associated PAR3 in the HLE cells. Scale bar is 50 µm.

It is well known that the TGF-β pathway induces EMT in several cell models, including HCC cell lines, through the transcriptional activation of EMT-inducing transcription factors as SNAIL1 or ZEB1 (Franco et al., 2010; Thiery et al., 2009). Furthermore, and as described above, TGF-β is also a functional regulator of the PAR3/PAR6/aPKC polarity complex, what made us wonder on the role of the PAR complex, and more specifically of PAR3, in the TGF-β-induced EMT in HCC cells.

We first treated the different HCC cell lines with TGF-β and studied their morphological alterations as well as the changes in the subcellular distribution

of PAR3. As seen in **Figure 22**, PLC/PRF/5 cells did not show evident changes of morphology and maintained PAR3 at plasma membrane, at cell-cell junctions. Regarding Snu449 and HLE cells, which already show mesenchymal features in basal conditions, neither displayed changes in morphology or in the subcellular distribution of PAR3 after TGF-β treatment (**Figure 22**). On the contrary, TGF-β treatment of Hep3B cells, which respond to TGF-β by down-regulating E-CADHERIN levels and increasing N-CADHERIN ones (unpublished results), provoked clear changes in the PAR3 subcellular localization, which changed from a cortical, intercellular pattern to concentrate in the center of Hep3B parenchymas (**Figure 22,** arrows at the Hep3B panel).

Then, we wondered whether the change of PAR3 subcellular localization required the regulation of the PAR3 protein levels, and we tested by western blotting PAR3 levels in the PLC/PRF/5, Hep3B, HLE and Snu449 cell lines. Cells were treated with increasing doses of TGF-β (1 ng/mL, 2 ng/mL and 5 ng/mL), but no significant changes in PAR3 levels were detected for the PLC/PRF/5, Snu449 or HLE cells, a result somehow in agreement with their lack of response in terms of subcellular localization (**Figure 23A**). Nevertheless, Hep3B cells responded to the TGF-β by showing a gradual, clear down-regulation of PAR3 that reached a 40% reduction, from basal levels, at 2 ng/mL TGF-β (**Figure 23A**), the usual dose of TGF-β used to induce EMT in these HCC cells (**Figure 23B**).

We next studied the effect of cell density on the ability of TGF-β to change the subcellular distribution of PAR3 in Hep3B cells. Hep3B cells were seeded in glass coverslips following a drop assay protocol (see *Materials and Methods*) to obtain a cell culture with a radial gradient of cell density. Hep3B cells in the center of the drop-cultures showed a high cell density, with well defined cortical PAR3 at cell-cell junctions, while in peripheral areas cells were distributed in small parenchymas which also displayed cortical PAR3 localization at cell-cell junctions. In both cases, cortical F-actin was observed equally distributed at the cell perimeter (**Figure 24**; untreated panels). TGF-β treatment caused a change in PAR3 localization either in the high or low cell density areas, concentrating in the center of the parenchymas as described above (**Figure 24**, PAR3 panels). This change of PAR3 subcellular localization was concomitant with a

remodeling in the distribution of F-actin distribution from its cortical pattern to a concentrated one, similar to that of PAR3 (**Figure 24,** +TGF-β panels).

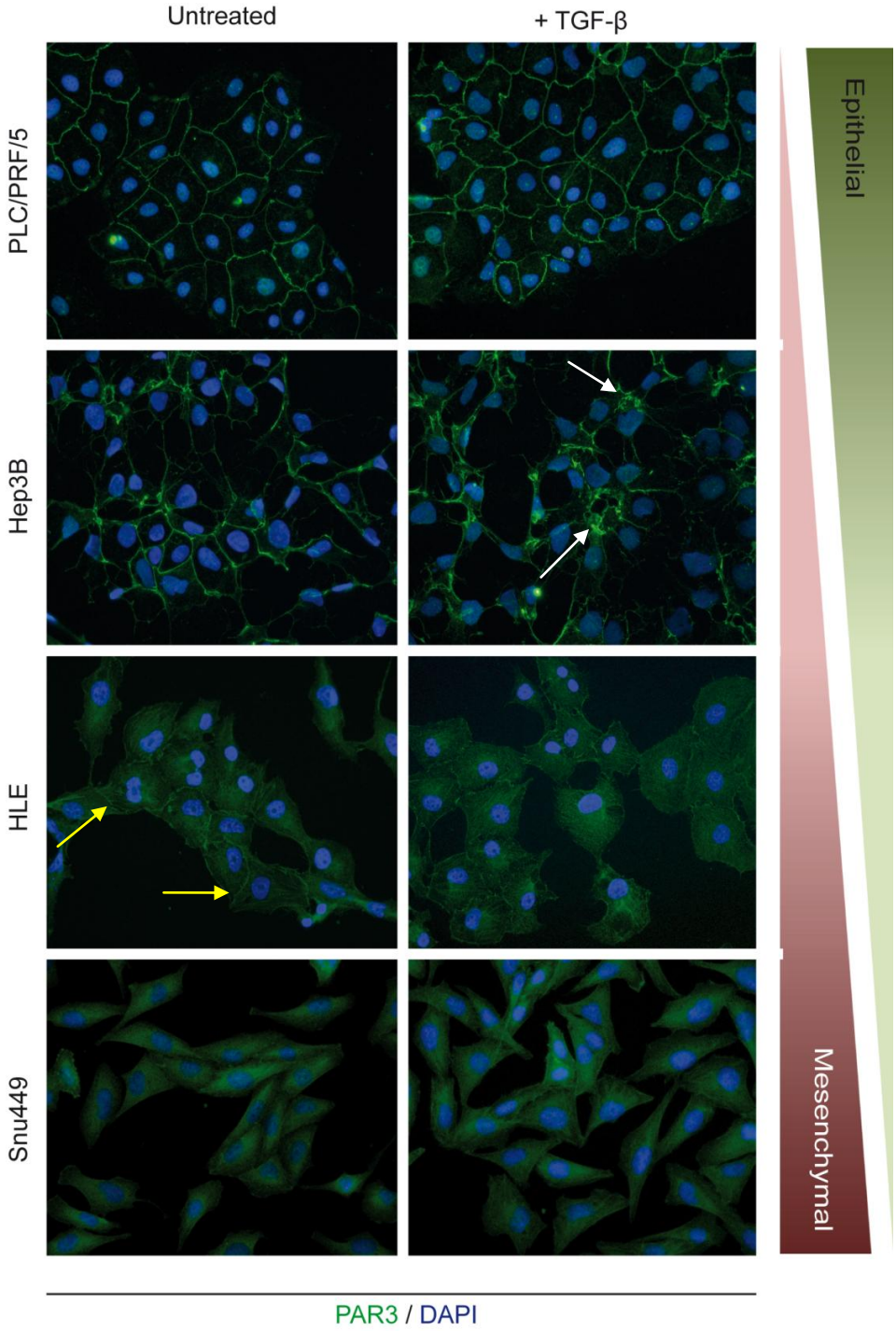

Figure 22. TGF-β changes PAR3 subcellular distribution in Hep3B cells, but not in PLC/PRF/5, Snu449 nor HLE cells. Representative fluorescence microscopy images of the stated HCC cell lines under basal conditions (untreated, left panels) or after 24h treatment with 2 ng/mL TGF-β (right panels), and stained with an anti-PAR3 antibody (green) and with DAPI (blue). White arrows indicate changes of PAR3 localization when compared to the untreated control. Yellow arrows point out to residual PAR3 localized at cell-cell junctions in HLE cells. Scale bar is 50 µm.

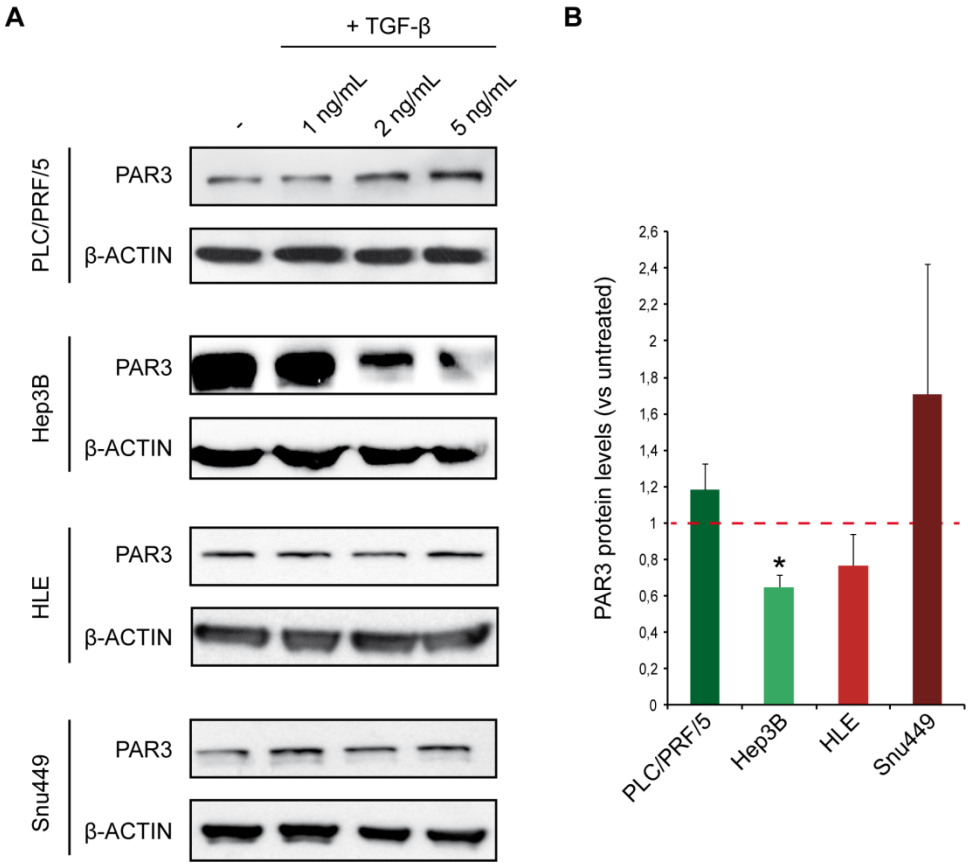

Figure 23. Effect of TGF-β treatment on PAR3 expression in different HCC cells. **A:** Western blotting analysis of PAR3 expression in PLC/PRF/5, Hep3B, HLE and Snu449 cells treated with 1, 2 and 5 ng/mL TGF-β. β-ACTIN is shown as loading control. A representative experiment is shown. **B:** Testing PAR3 expression in the stated HCC cells treated with 2 ng/mL TGF-β, with respect to untreated cells. Shown is the mean±SD of the densitometric analysis of three independent western blot experiments, expressed as relative to β-ACTIN levels. *p<0.05, Student's T test.

Since Snu449 cells produce high levels of autocrine TGF-β (Bertran et al., 2013) and they did not show membrane-associated PAR3, we next wondered whether TGF-β autocrine activation could be responsible for the lack of cortical PAR3 in these cells. Thus, Snu449 cells were treated for 72 h with LY364947, a TGF-β receptor I kinase inhibitor which blocks TGF-β signaling. **Figure 25A** shows that while untreated Snu449 cells were unable to form cell-cell junctions, the blockade of the TGF-β pathway partially shifted PAR3 from the cytoplasm to the newly formed cell junctions (**Figure 25A**). Interestingly, this re-localization of PAR3 to cell-cell junctions after LY364947 treatment coincided with an increase of PAR3 protein levels (**Figure 25B**) and with a reduction in the migratory ability of the LY364947-treated Snu449 cells (**Figure 25C**). Furthermore, those cells in

which the TGF-β pathway was blocked formed tight junctions, as observed by the presence of ZO-1 staining at cell-cell junctions, while untreated Snu449 cells, which do not display cell unions in basal conditions, did not (**Figure 26**). This result correlates with the previous demonstration that the blockade of TGF-β pathway in Snu449 cells also increased PAR3 at the cell-cell junctions.

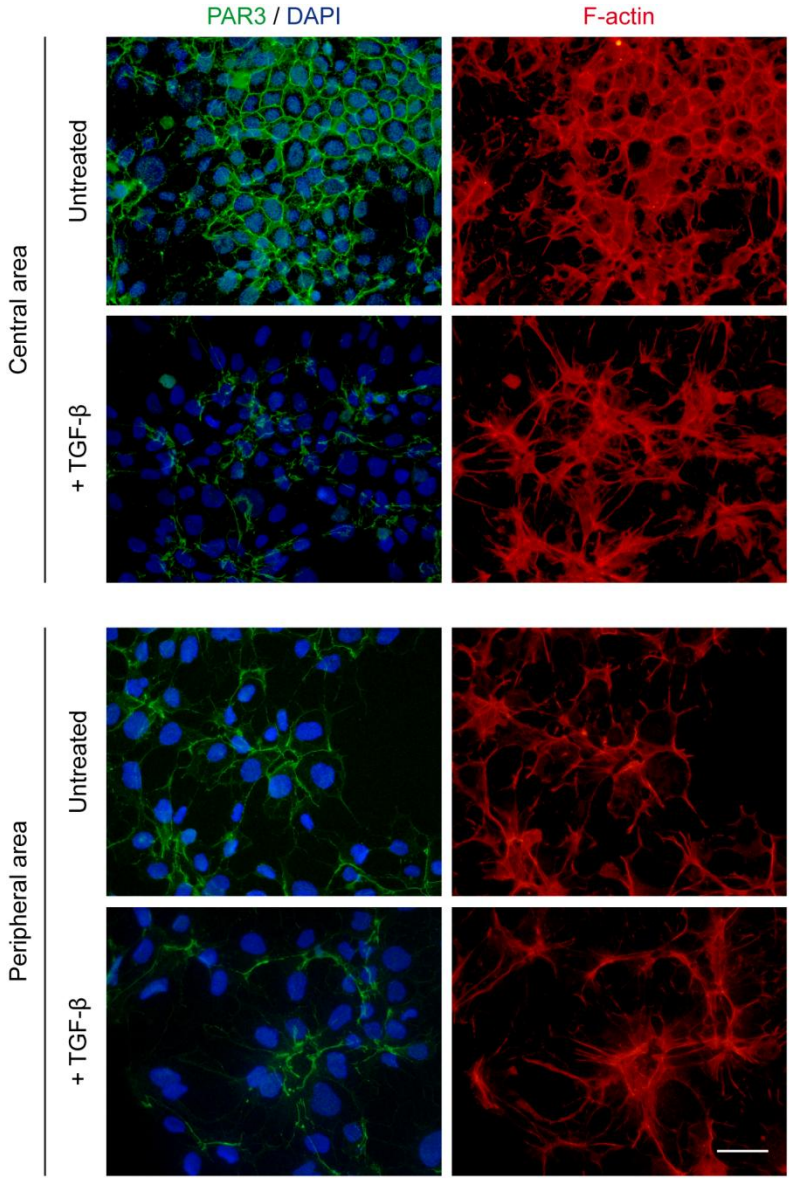

Figure 24. TGF-β-induced the mislocalization of PAR3 in Hep3B cells, independently of the cell density. Hep3B cells were seeded following a "drop assay" protocol, treated with 2 ng/mL TGF-β, and stained for PAR3 (green), phalloidin (red) or nuclei (DAPI). Shown are representative fluorescence microscopy images of treated cultures vs. untreated controls at the high cell density central area of the cultures (upper panels) as well as the low cell density periphery. Scale bar is 50 µm.

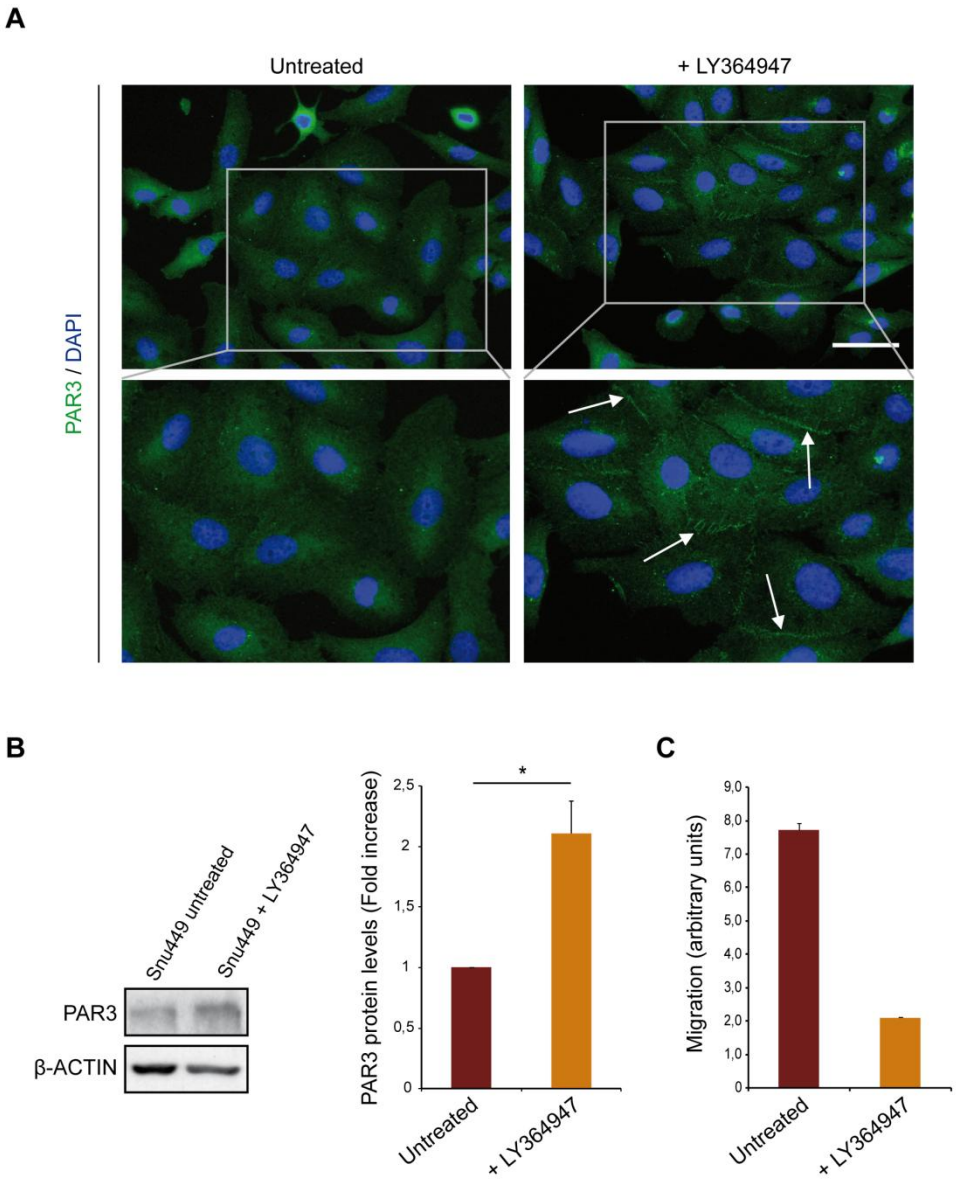

Figure 25. Blockade of the TGF-β pathway relocalizes PAR3 at newly formed cell-cell junctions in Snu449 cells. A: Immunofluorescence analysis of untreated control Snu449 cells or cells treated with 3μM LY364947 for 72h, and stained with anti-PAR3 and DAPI. Arrows in the bitmap amplification indicate the localization of PAR3 at the newly formed cell-cell junctions of LY364947-treated cells. Scale bar is 50 μm. **B:** Representative western blotting (left) and corresponding densitometric analysis of PAR3 levels in control and in LY364947-treated Snu449 cells (right). Result expressed as the mean±SD of the PAR3 levels from 3 independent experiments relative to β-ACTIN levels. *p<0.05, Student's T test. **C:** Real-time migration assay using the xCELLigence system on control (untreated) or LY 364947-treated Snu449 cells. Represented is the slope in the exponential phase of migration plot within the first 4 hours.

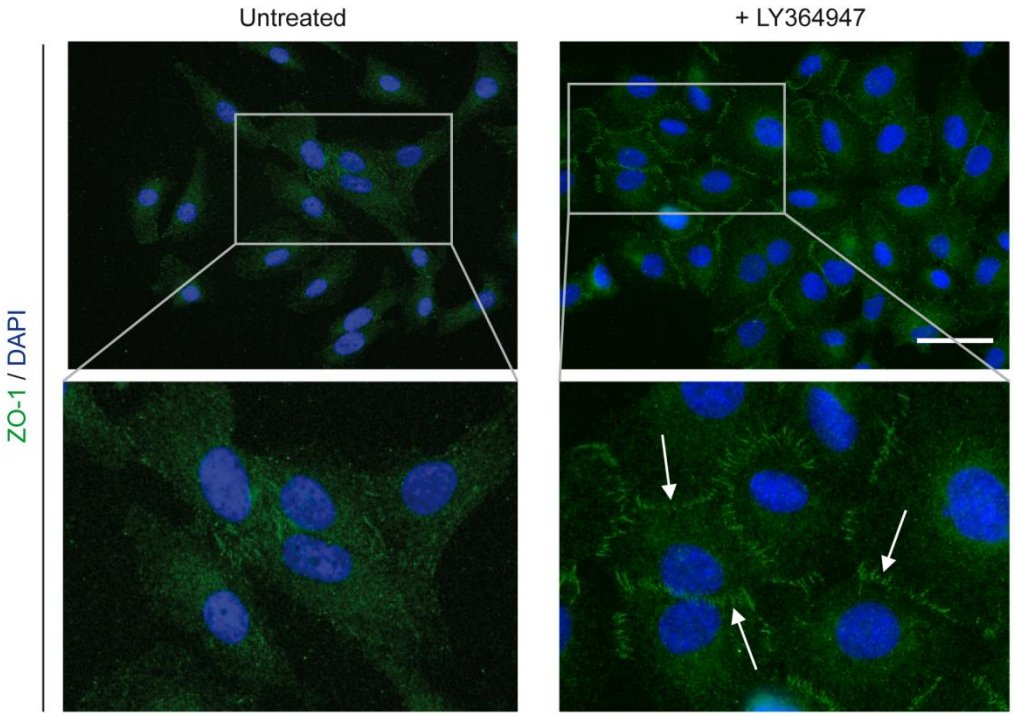

Figure 26. Blockade of the TGF-β pathway relocalizes ZO-1 at newly formed cell-cell junctions in Snu449 cells. Immunofluorescence analysis of untreated control Snu449 cells or cells treated with 3μM LY364947for 72h, and stained with anti-ZO-1 and DAPI. Arrows in the bitmap amplification indicate the localization of ZO-1 at the newly formed cell-cell junctions of LY364947-treated cells. Representative images are shown. Scale bar is 50 μm.

6.1. PAR3 by itself is capable to maintain the epithelial-like phenotype in HCC cells

The above results suggested a relevant role for PAR3 in the dynamics of cell-cell junctions, so that we decided to study more in deep the involvement of PAR3 in the maintenance of the epithelial phenotype in HCC cells. Thus, we silenced PAR3 expression in the epithelial-like PLC/PRF/5 cells, by using specific PAR3 siRNAs. We treated PLC/PRF/5 cells with two different PAR3 siRNAs (see *Material and Methods* section) and confirmed silencing by western blotting (**Figure 27**). As the silencing efficiency was similar for both siRNAs checked, we focus in the PAR3 siRNA#1 for the following experiments. As seen in **Figure 28A**, PAR3 protein and *PARD3* mRNA levels were significantly lower in the siRNA treated cells than in control cells transfected with a scrambled control siRNA (**Figure 28A**). Furthermore, PAR3-silenced PLC/PRF/5 cells showed a clear loss of PAR3 from the plasma membrane with the subsequent disaggregation of the cell clusters (**Figure 28B**, left panels), an effect that could not be reversed by treating silenced cells with TGF-β (**Figure 28B,** lower right panel).

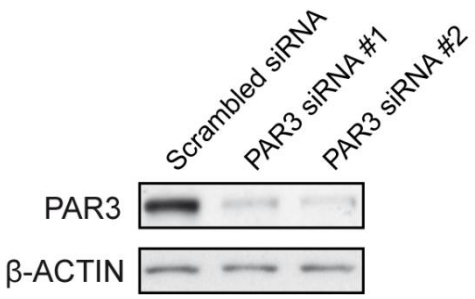

Figure 27. Transient PAR3 silencing in PLC/PRF/5 cells with specific siRNAs (I). Western blot analysis of PAR3 protein levels in scrambled or PAR3-silenced PLC/PRF/5 cells. β-ACTIN is shown as loading control.

Control and PAR3-silenced PLC/PRF/5 cells were then labeled with antibodies against different cell-cell junction markers and analyzed by fluorescence microscopy. **Figure 29** show representative images of control and PAR3-silenced cells stained for ZO-1 and showing a significant reduction in intercellular ZO-1 (**Figure 29,** compare upper right and lower right panels), and even some mislocalized, cytoplasmic ZO-1 (**Figure 29**, arrows at the lower panels) when compared to control cells.

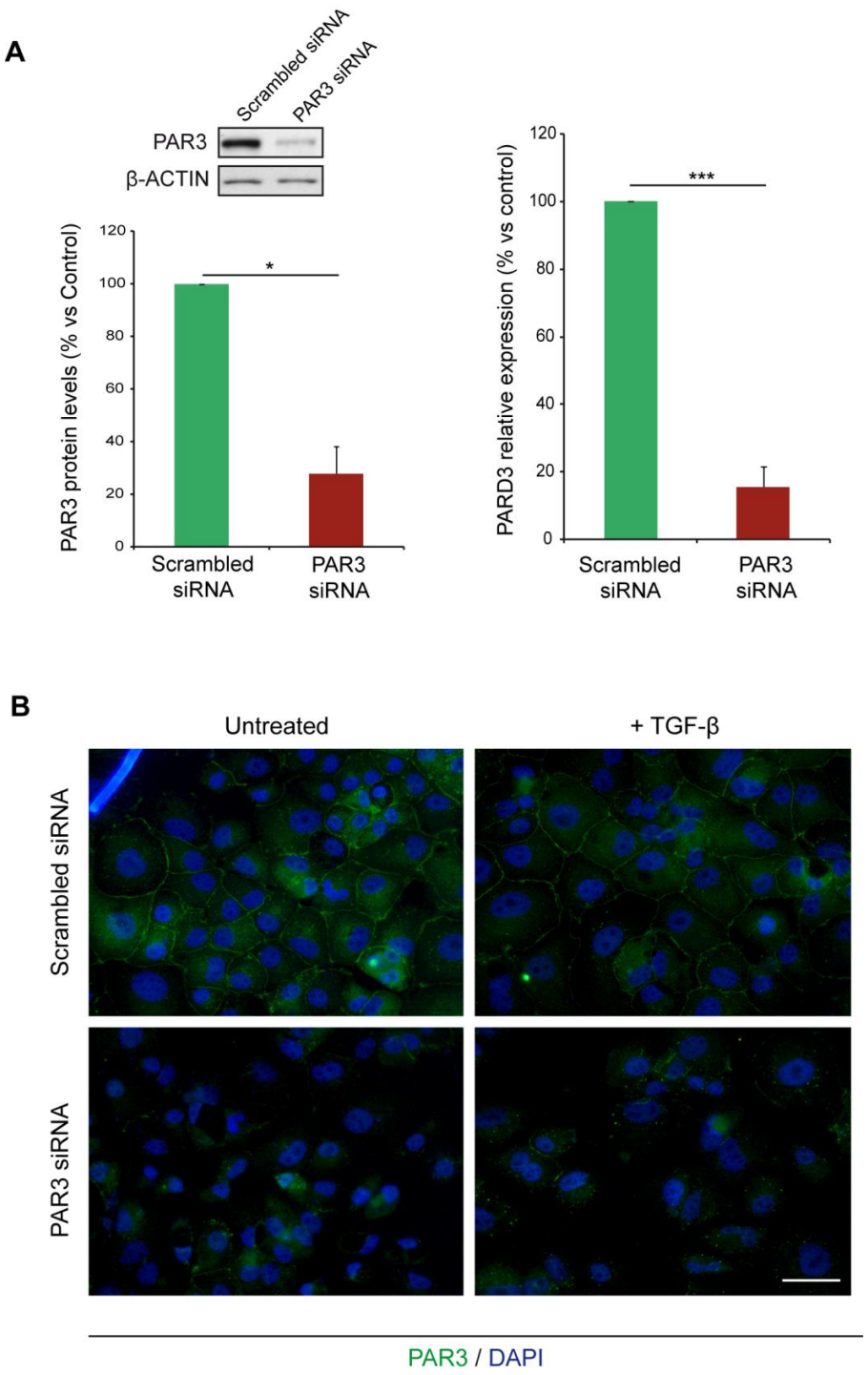

Figure 28. Transient PAR3 silencing in PLC/PRF/5 cells with specific siRNA (II). **A: Left:** Western blotting analysis of PAR3 protein levels in scrambled- or PAR3-silenced PLC/PRF/5 cells. β-ACTIN is shown as loading control. Quantification: mean ± SD of three independent experiments. **Right:** *PARD3* mRNA levels determined by qPCR. Mean ± SD of three representative experiments. *p<0.05 and ***p<0.001, Student's T test. **B:** Representative microscopy images of cells transiently transfected with the scrambled siRNA control (upper panels), or with the specific PAR3 siRNA (lower panels), and treated with 2 ng/mL TGF-β for 48 h. Cells were stained with an anti-PAR3 antibody (green), and nuclei were stained with DAPI (blue). Scale bar is 50 µm.

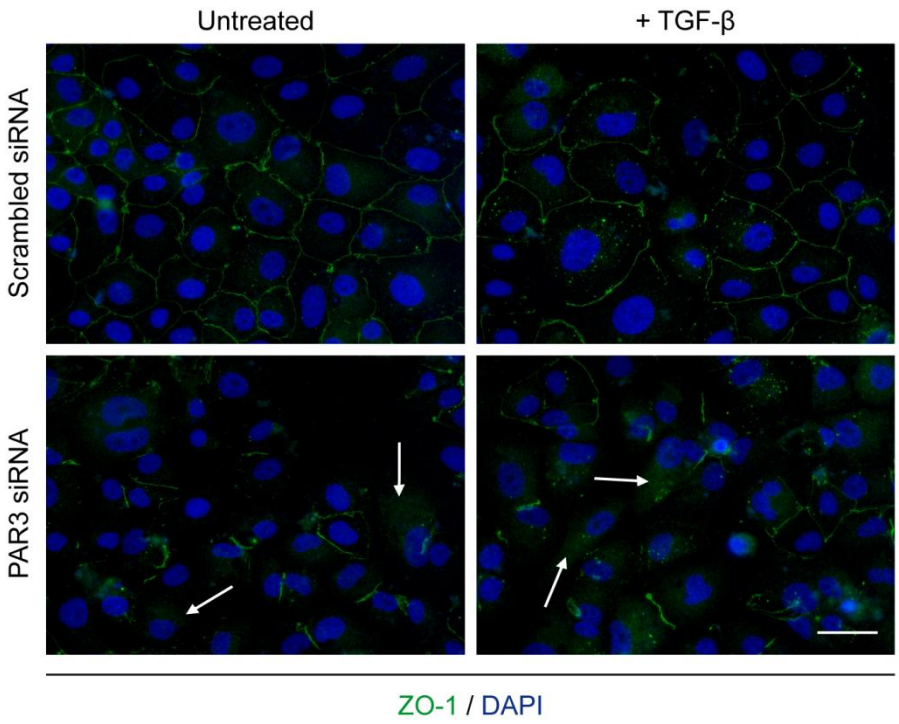

Figure 29. PAR3 silencing results in the disorganization of tight junctions in PLC/PRF/5 cells. Representative immunofluorescence images of cells transiently transfected with the scrambled siRNA control (upper panels), or with the specific PAR3 siRNA (lower panels), and treated with 2 ng/mL TGF-β for 48 h. Cells stained with an anti-ZO1 antibody (green), and nuclei with DAPI (blue). Scale bar is 50 µm.

Given the dramatic effect of PAR3-silencing on the stability of tight junctions, we next tested its effects on the adherens junctions of PLC/PRF/5 cells by studying E-CADHERIN/β-CATENIN dynamics. As for the tight junctions, adherens junctions were also disrupted in PAR3-silenced cells, as deduced from the reduction in E-CADHERIN (**Figure 30A**) and β-CATENIN (**Figure 30B**) stainings from the plasma membrane.

As seen in **Figure 30A** (left panels), loss of PAR3 in PLC/PRF/5 cells altered the structure of the adherens junctions and caused a reduction in intercellular E-CADHERIN, comparable to the effects caused by treating these cells with TGF-β (**Figure 30A**, right panels), as well as in the levels of β-CATENIN (**Figure 30B**, left panels). These facts prompted us to investigate more in deep the relationship among PAR3 and the adherens junction.

We firstly analyzed expression of *E-CADHERIN*, at the mRNA level, in PLC/PRF/5 cells silenced for PAR3. **Figure 31A** shows these significantly lower levels of *E-CADHERIN* mRNA, in comparison with cells treated with the scrambled, control siRNA. Interestingly, this effect did not correlate with an upregulation of EMT transcription fators, such as *SNA1* (which was even downregulated in PAR3-silenced cells, **Figure 31B**) or *ZEB1* (**Figure 31C**). We also analyzed the expression of other EMT transcriptions factors such as *SNAI2* and *TWIST1* but no expression of any of them was found in these cells (data not shown). On the other hand, no significant differences were found in the expression of the mesenchymal marker *VIMENTIN* in PAR3-silenced cells when untreated with respect to the control cells (**Figure 31D**). After TGF-β treatment, in both scrambled and PAR3-silenced cells an increase of *VIMENTIN* mRNA levels was observed, which was expected as TGF-β is a potent inductor of *VIMENTIN* expression (Thiery, 2002; Yang and Weinberg, 2008). Interestingly, PAR3 loss enhanced TGF-β-mediated increase of *VIMENTIN* expression (**Figure 31D**).

In the view of these results, we concluded that PAR3 plays an important role in the maintenance of the intercellular adhesion mechanisms that depended on ZO1 and E-CADHERIN.

The role of PAR3 on the subcellular distribution of CXCR4 was also analyzed in PAR3-silenced PLC/PRF/5 cells after treatment with TGF-β. While control cells displayed a homogeneous CXCR4 cytoplasmic distribution (**Figure 32A**, upper left panel), which upon TGF- β treatment underwent a reorganization which concentrated CXCR4 at one of the cell poles, PAR3-silenced cells displayed a strong asymmetrical distribution of CXCR4 which resembled the pattern induced by TGF-β treatment on the control cells even in the absence of this cytokine (**Figure 32A**, lower left panel). No additional effect on CXCR4 distibution was observed when silenced cells were treated with TGF-β (**Figure 32A** and **B**).

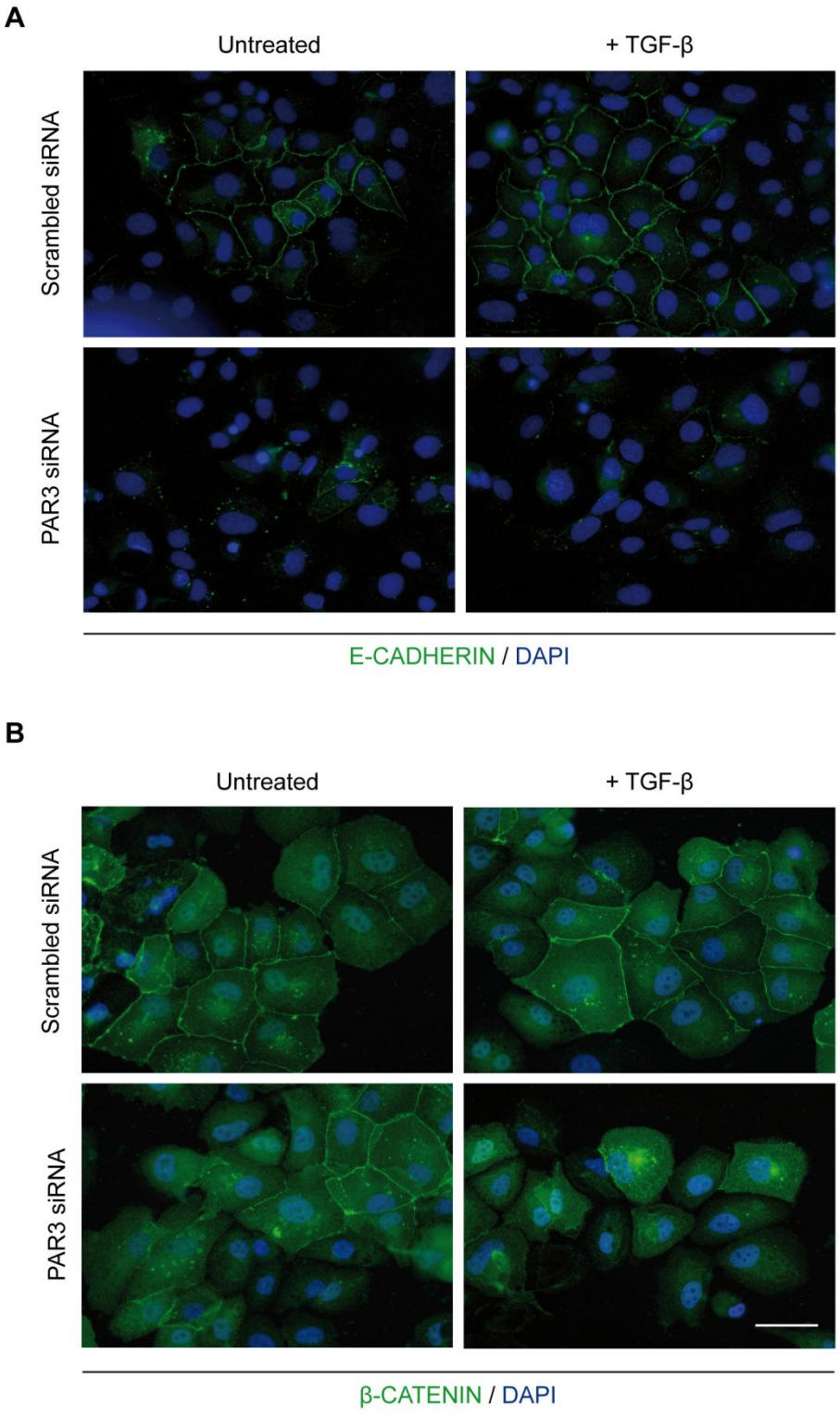

Figure 30. PAR3 is necessary for the maintenance of the adherens junctions in PLC/PRF/5 cells. Representative immunofluorescence images of cells transiently transfected with the scrambled siRNA control (upper panels), or with the specific PAR3 siRNA (lower panels), and treated with 2 ng/mL TGF-β for 48 h. Cells were stained with anti-E-CADHERIN (**A**) or anti-β-CATENIN (**B**) antibodies (green). Nuclei were stained with DAPI (blue). Scale bars are 50 µm.

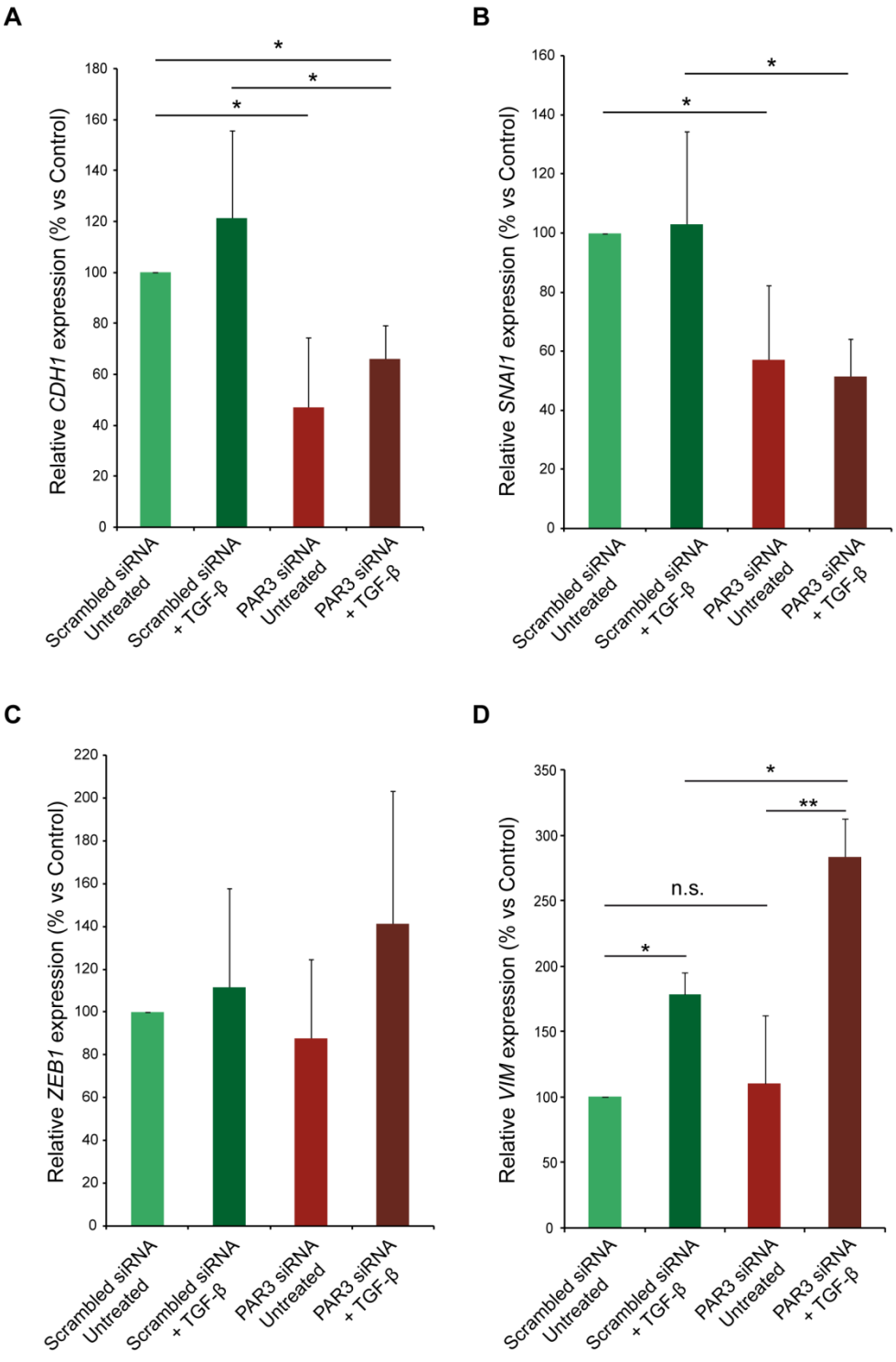

Figure 31. PAR3 silencing decreases *CDH1* levels, independently of changes in the expression of EMT transcription factors, but does not increase *VIM* levels. *CDH1* (**A**), *SNAI1* (**B**), *ZEB1* (**C**) and *VIM* (**D**) expression levels determined by qPCR in untreated or 48h TGF-β treated scrambled or PAR3-silenced PLC/PRF/5 cells. Mean ± SD (n=3). *p<0.05, **p<0.01, Student's T test.

Finally, we studied the relationship of PAR3 with cell motility. We used the xCELLigence system (see *Materials and Methods* section) to measure the migratory ability of PLC/PRF/5 cells transfected with PAR3 siRNA or with scrambled, control, siRNA. PAR3-silenced PLC/PRF/5 cells showed a significant increase in their migratory ability when compared to control cells transfected with the scrambled siRNA (**Figure 33**). TGF-β treatment increased the migratory ability of control PLC/PRF/5 cells, which was much higher than the increase observed in PAR3-silenced cells. TGF-β effects were closing similar in control than in PAR3-silenced cells (**Figure 33**). In resume, silencing of PAR3 facilitated the migratory potential of PLC/PRF/5 cells, likely by unstabilizing cell-cell junctions and contributing to the detachment of cells from their neighbors. In this sense, PAR3 could be considered as a molecular switch controlling the election of the collective/individual patterns of migration in PLC/PRF/5 cells.

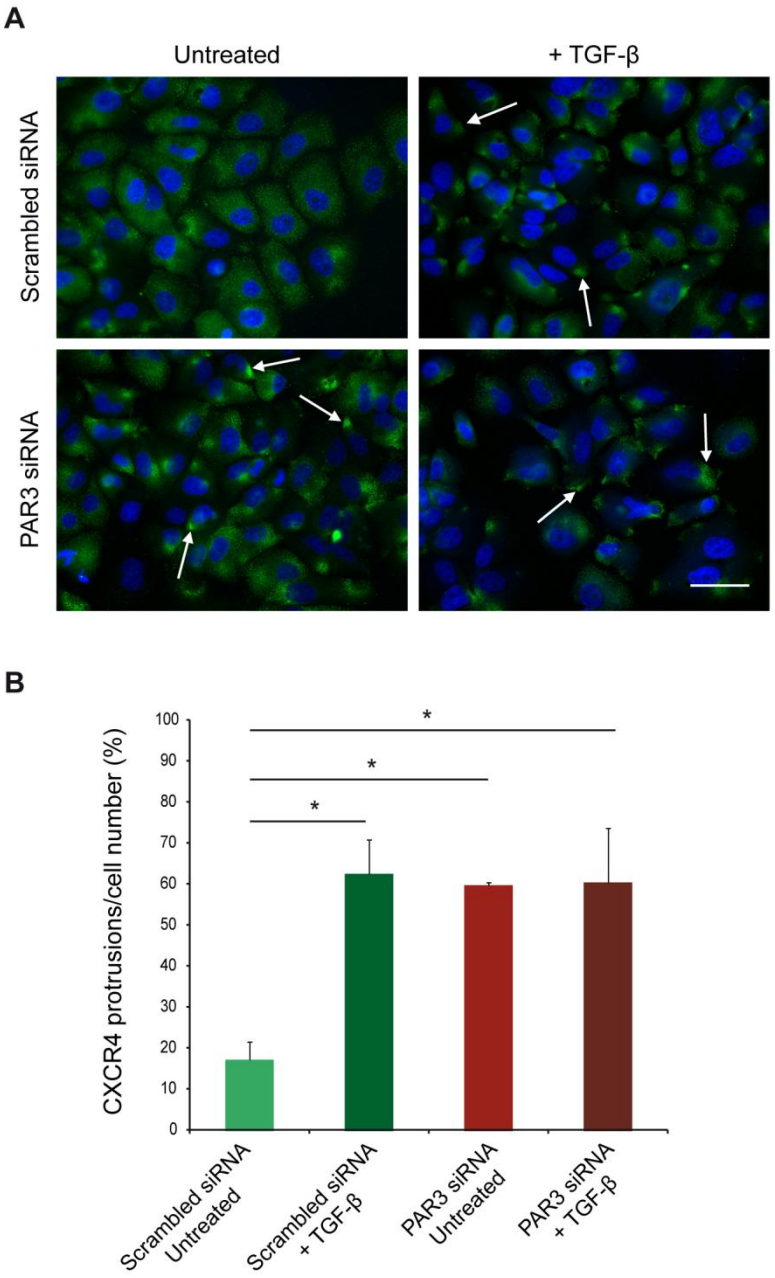

Figure 32. PAR3 silencing mimics the TGF-β-induced asymmetrical distribution of CXCR4. A: Representative immunofluorescence analysis of PLC/PRF/5 cells incubated with the PAR3 specific siRNA or with the scrambled siRNA as a control, left untreated or treated with TGF-β for 48 h and stained with an anti-CXCR4 antibody (green) and DAPI for nuclei (blue). Arrows indicate cell protrusions enriched in CXCR4. Scale bar is 50 µm. **B:** Quantification of the CXCR4 protrusions relative to the total cell number. 10 fields were counted for each experiment (n=3). *p<0.05, Student's T test.

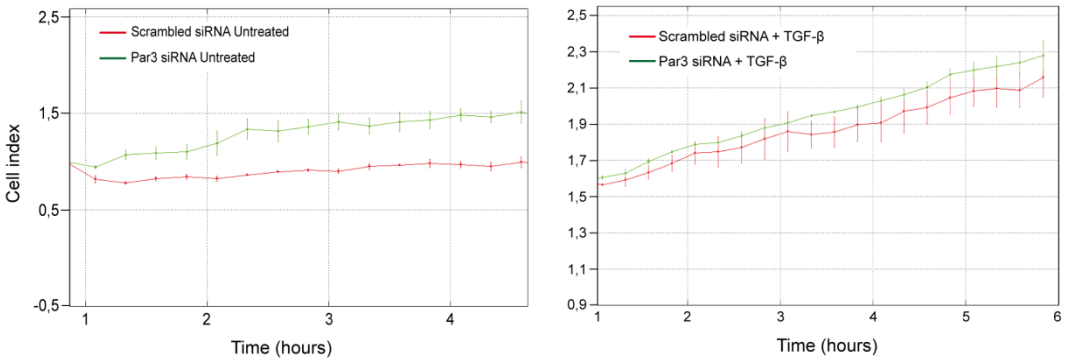

Figure 33. PAR3 silencing enhances cell motility of PLC/PRF/5 cells. Representative migration plots obtained by the xCELLigence system of PAR3-silenced PLC/PRF/5 cells, or of PLC/PRF/5 cells transfected with the scrambled, control, siRNA.

DISCUSSION

1. CXCR4 intracellular trafficking in HCC cells

The CXCR4/SDF-1α axis plays an important role in cancer progression and metastasis. We investigated the intracellular CXCR4 dynamics focusing on the mechanisms which regulate its export to the plasma membrane and its internalization in HCC cell lines. High levels of CXCR4 in intracellular compartments were found within this research. This has been already described in lymphocytes (Förster et al., 1998) and in some HCC cell lines, although no reference on the subcellular structures implicated was provided for these last ones (Kim et al., 2008).

The pathway followed for CXCR4 to reach the plasma membrane is mostly unknown. The mechanisms maintaining CXCR4 in the cell surface are complex and are subjected to multiple regulatory signals, which can be classified in three points: export, cell surface restriction and internalization and traffic through endosomal compartments. Here, working with the HCC cell lines PLC/PRF/5 and Hep3B, we demonstrate that CXCR4 shows a perinuclear distribution, compatible with the Golgi apparatus, and that it co-localizes within AP1-positive vesicles, indicating that CXCR4 uses the Golgi/AP1 axis to reach the cell surface. Although in both PLC/PRF/5 and Hep3B cells high levels of intracellular CXCR4 were found, a clear difference in cell surface levels between them was also found. Remarkably, most Hep3B cells were positive for sCXCR4 but presenting very heterogeneous cell surface levels when compared to PLC/PRF/5 cells. Previous reports of our group demonstrated a higher expression of *CXCR4* in Hep3B cells than in PLC/PRF/5, correlating with increased autocrine activation by TGF-β (Bertran et al., 2013). In this work we further demonstrate that the localization of CXCR4 at the cell surface of Hep3B cells is clearly dependent on TGF-β signaling, as stable silencing of TβRI resulted in a significant decrease of sCXCR4, in contrast to the PLC/PRF/5 cells.

HCC cells express CXCR4 in an asymmetrically distributed, polarized way (Bertran et al., 2009) that requires the establishment of a front-rear polarization axis, placing some receptors at the leading edge of migration to act as guides of cell motility in a process requiring a reorientation of the membrane traffic

pathways (Etienne-Manneville, 2008; Nelson, 2009). Here, we demonstrate that trafficking of CXCR4 to the plasma membrane depends on the functionality of the exocyst complex, which is an evolutionarily conserved complex responsible for the tethering of the exocytic vesicles to the lateral membrane of epithelial cells (Grindstaff et al., 1998). Subcellular localization of the exocyst complex depends on the membrane polarization of cells and it has been described to be associated to Golgi apparatus in cells with non polarized membranes (Yeaman et al., 2001) or at the cell-cell junctions when they are formed (Grindstaff et al., 1998). Consequently, specific export of CXCR4 to the lateral membrane through the exocyst complex comprises a new aproximation in the study of the acquisition of the front-rear polarity in cell migration guidance and the mechanisms regulating the change of CXCR4 localization from lateral plasma membrane to the migration front.

Previous reports have found that the fraction of CXCR4 present at the cell surface of T lymphocytes is internalized through a slow, tonic, process to intracellular compartments through the clathrin-dependent pathway (Signoret et al., 1997), while SDF-1α incubation induces a rapid CXCR4 endocytosis (Haribabu et al., 1997; Signoret et al., 1997). Our results indicate that PLC/PRF/5 cells, which show an epithelial-like phenotype, internalize CXCR4 following dynamin-dependent pathways, mainly by clathrin-mediated endocytosis but also participating the caveolin-dependent one. Strikingly, we found that Hep3B cells, which display a mixed epithelial/mesenchymal-like phenotype, use macropinocytosis, a dynamin-independent pathway which plays an important role in stimulating nutrient uptake in cancer cells (Zwartkruis and Burgering, 2013), in establishing chemotactic responses in highly motile cells as neutrophyls (Carpentier et al., 1991) and in modulating cell locomotion through modification of endocytic membrane traffic (Amyere et al., 2002; Bretscher and Aguado-Velasco, 1998). Thus, we demonstrate a differential internalization between PLC/PRF/5 and Hep3B cells, distinguishing different endocytosis pathways depending on the HCC cell line and their epithelial/mesenchymal features.

Finally, following internalized CXCR4 through different endosomal compartments, we observed in PLC/PRF/5 cells the presence of CXCR4-EGFP in $Rab11^+$ and $Rab4^+$ membrane compartments, whereas in Hep3B cells CXCR4 mainly co-localized with Rab11. This latter might indicate that macropinocytic-associated vesicles are used not only for the entrance of CXCR4, but sorting endosomes to its recycling to the plasma membrane too. A similar result has been recently described for the internal redistribution of integrins during the PDGF-induced migration of fibroblasts (Gu et al., 2011) and suggests that this could be a common mechanism of receptor sorting used by motile cells. However, here we also show that brefeldin A decreased the presence of $Rab11^+$ vesicles and attenuated membrane location of CXCR4-EGFP in PLC/PRF/5 cells. Furthermore, a subpopulation or $Rab11^+$ endosomes were mostly depleted of CXCR4-EGFP, which could correspond to the trans-Golgi-associated secretory transport, whereas other population of intracellular vesicles maintained CXCR4, which could reflect recycling endosomes. These results suggest a post-Golgi transport of CXCR4-EGFP through the $Rab11^+$ endosomes. In support of this interpretation, other plasma membrane proteins, such as E-CADHERIN, exit the Golgi complex in pleomorphic tubulovesicular carriers, which, instead of moving directly to the cell surface, usually fuse first with an intermediate compartment, subsequently identified as a Rab11-positive recycling endosome (Lock and Stow, 2005).

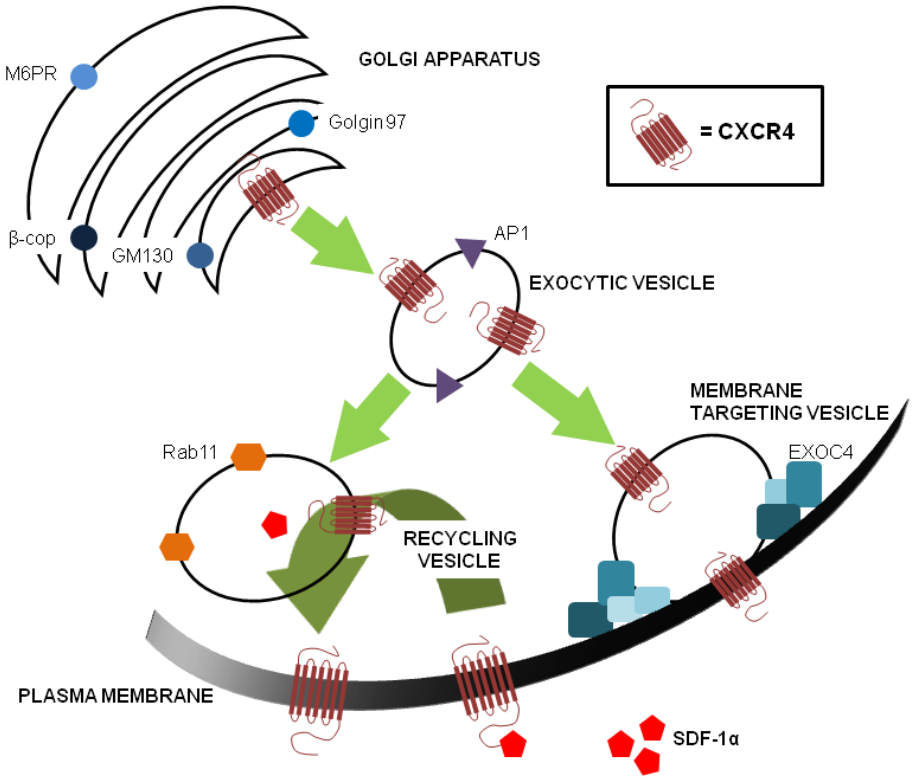

Figure D.1. Schematic view of the CXCR4 intracellular trafficking.

2. Role of TGF-β in the regulation of the localization and expression of PAR3 in HCC cells

Currently, an increasing number of publications highlight the crucial role that cell polarity plays in tissue development and homeostasis. Moreover, the loss of this cell polarity facilitates the cancer initiation and progression (Ellenbroek et al., 2012). The PAR protein complex (PAR3/PAR6/aPKC) participates in migration processes coordinating the polarized cell movement (Gérard et al., 2007), interacting with other signaling pathways such as Ras pathway (Wang et al., 2010) and some GTPases (Etienne-Manneville and Hall, 2002) and modulating oncogenic and tumor supressor pathways, for instance inducing cell proliferation and activating mitogenic pathways by overexpression of PAR6β (Nolan et al., 2008). *PAR3* expression has also been described as a modulator of the signaling pathways related to the acquisition of an invasive phenotype in breast tumor cells (McCaffrey et al., 2012).

It has been reported that some extracellular stimuli regulate some components of PAR complex. In this sense, TGF-β phosphorylates PAR6, consequently promoting the loss of the tight junctions and becoming a key point for EMT induction (Bose and Wrana, 2006). Although it has been reported that incubation of normal rat kidney epithelial NRK52E cells with TGF-β induces EMT and a decrease in Par3 levels (Wang et al., 2008b), very little is known about the role of TGF-β in the regulation of PAR3 in human cells, neither the molecular mechanisms, nor the context dependency.

Our work shows that PAR3 is localized at cell-cell junctions of epithelial-like cells, while a predominant cytoplasmic localization is observed in the mesenchymal-like ones. Mesenchymal HCC cells, such as Snu449 and HLE, display a more migratory and invasive phenotype, when compared to the epithelial ones (Bertran et al., 2013). It is interesting to point out that Dagher et al have recently described that a cytoplasmic PAR3 profile appears to be implicated in worse clinical and pathological cancer features in clear cell renal cell carcinomas (Dagher et al., 2014).

We also demonstrate that TGF-β down-regulates PAR3 in Hep3B cells, which are susceptible to switch to a mesenchymal phenotype after TGF-β treatment. In none of the other epithelial or mesenchymal-like HCC cells tested differences in PAR3 protein levels were found, fitting with the inability of PLC/PRF/5 cells to undergo EMT after TGF-β treatment or with the basal mesenchymal phenotype exhibited by Snu449 and HLE cells, concordant with high autocrine TGF-β production. Down-regulation of PAR3 in Hep3B cells was concomitant with its mislocalization, reducing its presence at the cell-cell junctions, thus establishing a correlation between the mesenchymal cell grade and subcellular localization and protein levels of PAR3. Furthermore, a partial recovery of cell-cell junctions in Snu449 cells after treatment with LY364947 (inhibitor of the TβRI) was observed, suggesting that TGF-β has a role in the subcellular localization of PAR3.

EMT is a process that provides cell plasticity during development and cancer metastasis. EMT is associated with enhanced cell migration and invasion and a disruption of apical-basal polarity and loss of *E-CADHERIN* expression (Thiery et al., 2009). Classically, it is known that some signaling pathways such as TGF-β and oncogenic Ras induce EMT by enhancing the expression of EMT transcription factors, for example *SNAI1* and *ZEB1*, that finally repress *E-CADHERIN* gene promoter (Sleeman and Thiery, 2011; Thiery et al., 2009). Otherwise, EMT can be induced by affecting the levels and function of PAR3 and PAR6 proteins, but the precise mechanisms regulating PAR proteins remain obscure (Wang et al., 2010, 2014). Here we found out that the loss of PAR3 in PLC/PRF/5 cells implies a disruption of tight junctions, but also a disruption of adherens junctions, correlating with *E-CADHERIN* down-regulation at the mRNA level. However, neither *SNAI1* nor *ZEB1*, both transcription factors involved in the regulation of EMT-related genes, were up-regulated after PAR3-silencing, indicating that the loss of PAR3 may regulate *E-CADHERIN* expression without changes in the mRNA levels of classical EMT transcription factors. Interestingly, *VIMENTIN* expression does not appear to be directly regulated by PAR3, but TGF-β-mediated up-regulation was significantly enhanced when PAR3 was silenced. To sum up, PAR3 is involved in the regulation of the epithelial/mesenchymal phenotype in Hep3B cells through a

non-classical pathway, without changes in the expression of the well-known EMT transcription factors. Further work will be necessary to better understand this process.

Currently, no data has been published about the implication of PAR complex in HCC cells ability to migrate. However, loss of PAR3 has been previously described to promote metastasis in cell models of breast cancer (Xue et al., 2013) and in lung squamous cell carcinomas (Bonastre et al., 2015). Here we demonstrate that the loss of PAR3 facilitates migration of epithelial PLC/PRF/5 cells, although the increased level is lower than that observed after treatment of cells with TGF-β. It is important to mention that PAR3 is able to disrupt cell-cell junctions and decrease expression of *E-CADHERIN*, but it is unable to induce mesenchymal features, contrary to TGF-β-treated cells which actually increased *VIMENTIN* mRNA levels, but maintain *E-CADHERIN* expression. Taken together, it is suggested that additional mechanisms needed for a fully efficient migration that are triggered by TGF-β are not regulated by PAR3. The acquisition of mesenchymal features, even though cell-cell adhesions are maintained, results more efficient in inducing the migration of PLC/PRF/5 cells than only loosing cell-cell adhesions without the acquisition of mesenchymal features.

Despite the fact that CXCR4 is described as a protein localized in the leading edge of the migratory cells (Delongchamps et al., 2015), no reports have been yet published about the mechanisms controlling the CXCR4 polarization in HCC cells. In the opposite way, some publications have indicated a role for CXCR4 in modulation of cell polarity through other pathways, implicating for instance the activation of Rac1 and Rac2 (Shen et al., 2012). In PLC/PRF/5 cells CXCR4 displays a mainly non-polarized cytoplasmic localization, even though some cells presented a polarized pattern (Bertran et al., 2013). Here we found a role for PAR3 in the regulation of CXCR4 localization, since PAR3-silenced PLC/PRF/5 cells showed a high, significant, increase of cells showing a subcellular asymmetrically distributed CXCR4, mimicking the effect of TGF-β for this issue and proving a not additive effect of PAR3 silencing and TGF-β stimulation. Hence, PAR3 loss provoked a polarization of CXCR4 independently of TGF-β.

In conclusion, we highlight in this work the existence of a cross-talk linking the intracellular trafficking of CXCR4, the cell polarity PAR3 protein and the TGF-β pathway. However, further studies would shed light to the functional relationship between the CXCR4/SDF-1α axis and the cell polarity proteins unraveling the concrete mechanisms regulating invasion and other cell features relevant for the understanding of tumoral processes.

CONCLUSIONS

1. CXCR4 is expressed at the cell surface of human HCC cells, but significant higher levels are found at intracellular compartments. Autocrine overactivation of the TGF-β pathway mediates CXCR4 expression and surface localization.

2. CXCR4 reaches plasma membrane through the Golgi-AP1-exocyst axis and requires the functionality of the exocyst complex for the tethering of the exocytic vesicle to the plasma membrane.

3. CXCR4 is internalized through different endocytic pathways depending on the epithelial or mesenchymal profile of the HCC cells. While epithelial PLC/PRF/5 cells internalize CXCR4 through dynamin-dependent pathways, Hep3B cells, which display some mesenchymal characteristics, use macropinocytosis.

4. SDF-1α induces the internalization of CXCR4 from the plasma membrane to recycling endosomes in PLC/PRF/5 and Hep3B cells. A common $Rab11^+$ recycling pathway is used by both cell lines, while a $Rab4^+$ recycling pathway is only used by PLC/PRF/5 cells.

5. TGF-β regulates the subcellular localization of PAR3 in HCC cells depending on the epithelial/mesenchymal cell features displayed. Blockade of TGF-β pathway in mesenchymal HCC cells promotes the cell surface localization of PAR3, coinciding with formation of cell-cell junctions.

6. PAR3 is a key player in the maintenance of the epithelial-like phenotype of HCC cells through the preservation of both tight and adherens junctions, a process that does not depend on changes in the expression of classical EMT transcription factors.

7. Plasma membrane localized PAR3 prevents the cytoplasmic asymmetrical distribution of CXCR4 within epithelial PLC/PRF/5 cells, inhibiting cell migration.

REFERENCES

Adler, P.N. (2002). *Planar signaling and morphogenesis in Drosophila*. Dev. Cell *2*, 525–535.

Akhurst, R.J., and Hata, A. (2012). *Targeting the TGFβ signalling pathway in disease*. Nat. Rev. Drug Discov. *11*, 790–811.

Alsayed, Y., Ngo, H., Runnels, J., Leleu, X., Singha, U.K., Pitsillides, C.M., Spencer, J.A., Kimlinger, T., Ghobrial, J.M., Jia, X., et al. (2007). *Mechanisms of regulation of CXCR4/SDF-1 (CXCL12)-dependent migration and homing in multiple myeloma*. Blood *109*, 2708–2717.

Amyere, M., Mettlen, M., Van Der Smissen, P., Platek, A., Payrastre, B., Veithen, A., and Courtoy, P.J. (2002). *Origin, originality, functions, subversions and molecular signalling of macropinocytosis*. Int. J. Med. Microbiol. IJMM *291*, 487–494.

Anderson, D.C., Gill, J.S., Cinalli, R.M., and Nance, J. (2008). *Polarization of the C. elegans embryo by RhoGAP-mediated exclusion of PAR-6 from cell contacts*. Science *320*, 1771–1774.

Aranda, V., Haire, T., Nolan, M.E., Calarco, J.P., Rosenberg, A.Z., Fawcett, J.P., Pawson, T., and Muthuswamy, S.K. (2006). *Par6-aPKC uncouples ErbB2 induced disruption of polarized epithelial organization from proliferation control*. Nat. Cell Biol. *8*, 1235–1245.

Aranda, V., Nolan, M.E., and Muthuswamy, S.K. (2008a). *Par complex in cancer: a regulator of normal cell polarity joins the dark side*. Oncogene *27*, 6878–6887.

Aranda, V., Nolan, M.E., and Muthuswamy, S.K. (2008b). *Par complex in cancer: a regulator of normal cell polarity joins the dark side*. Oncogene *27*, 6878–6887.

Aravalli, R.N., Steer, C.J., and Cressman, E.N.K. (2008). *Molecular mechanisms of hepatocellular carcinoma*. Hepatol. Baltim. Md *48*, 2047–2063.

Arora, S., Bhardwaj, A., Singh, S., Srivastava, S.K., McClellan, S., Nirodi, C.S., Piazza, G.A., Grizzle, W.E., Owen, L.B., and Singh, A.P. (2013). *An undesired effect of chemotherapy: gemcitabine promotes pancreatic cancer cell invasiveness through reactive oxygen species-dependent, nuclear factor κB- and hypoxia-inducible factor 1α-mediated up-regulation of CXCR4*. J. Biol. Chem. *288*, 21197–21207.

Baggiolini, M. (1998). *Chemokines and leukocyte traffic*. Nature *392*, 565–568.

Balabanian, K., Lagane, B., Infantino, S., Chow, K.Y.C., Harriague, J., Moepps, B., Arenzana-Seisdedos, F., Thelen, M., and Bachelerie, F. (2005). *The chemokine SDF-1/CXCL12 binds to and signals through the orphan receptor RDC1 in T lymphocytes*. J. Biol. Chem. *280*, 35760–35766.

Barrallo-Gimeno, A., and Nieto, M.A. (2005). *The Snail genes as inducers of cell movement and survival: implications in development and cancer*. Dev. Camb. Engl. *132*, 3151–3161.

Bartolomé, R.A., Gálvez, B.G., Longo, N., Baleux, F., Van Muijen, G.N.P., Sánchez-Mateos, P., Arroyo, A.G., and Teixidó, J. (2004). *Stromal cell-derived factor-1alpha promotes melanoma cell invasion across basement membranes involving*

stimulation of membrane-type 1 matrix metalloproteinase and Rho GTPase activities. Cancer Res. *64*, 2534–2543.

Bertran, E., Caja, L., Navarro, E., Sancho, P., Mainez, J., Murillo, M.M., Vinyals, A., Fabra, A., and Fabregat, I. (2009). *Role of CXCR4/SDF-1 alpha in the migratory phenotype of hepatoma cells that have undergone epithelial-mesenchymal transition in response to the transforming growth factor-beta*. Cell. Signal. *21*, 1595–1606.

Bertran, E., Crosas-Molist, E., Sancho, P., Caja, L., Lopez-Luque, J., Navarro, E., Egea, G., Lastra, R., Serrano, T., Ramos, E., et al. (2013). *Overactivation of the TGF-β pathway confers a mesenchymal-like phenotype and CXCR4-dependent migratory properties to liver tumor cells*. Hepatol. Baltim. Md *58*, 2032–2044.

Bieberich, E. (2014). *Synthesis, Processing, and Function of N-glycans in N-glycoproteins*. Adv. Neurobiol. *9*, 47–70.

Boeckeler, K., Rosse, C., Howell, M., and Parker, P.J. (2010). *Manipulating signal delivery - plasma-membrane ERK activation in aPKC-dependent migration*. J. Cell Sci. *123*, 2725–2732.

Bonastre, E., Verdura, S., Zondervan, I., Facchinetti, F., Lantuejoul, S., Chiara, M.D., Rodrigo, J.P., Carretero, J., Condom, E., Vidal, A., et al. (2015). *PARD3 Inactivation in Lung Squamous Cell Carcinomas Impairs STAT3 and Promotes Malignant Invasion*. Cancer Res. *75*, 1287–1297.

Bonifacino, J.S., and Rojas, R. (2006). *Retrograde transport from endosomes to the trans-Golgi network*. Nat. Rev. Mol. Cell Biol. *7*, 568–579.

Bose, R., and Wrana, J.L. (2006). *Regulation of Par6 by extracellular signals*. Curr. Opin. Cell Biol. *18*, 206–212.

Branda, M., and Wands, J.R. (2006). *Signal transduction cascades and hepatitis B and C related hepatocellular carcinoma*. Hepatol. Baltim. Md *43*, 891–902.

Braun, L., Mead, J.E., Panzica, M., Mikumo, R., Bell, G.I., and Fausto, N. (1988). *Transforming growth factor beta mRNA increases during liver regeneration: a possible paracrine mechanism of growth regulation*. Proc. Natl. Acad. Sci. U. S. A. *85*, 1539–1543.

Bretscher, M.S., and Aguado-Velasco, C. (1998). *Membrane traffic during cell locomotion*. Curr. Opin. Cell Biol. *10*, 537–541.

Bruix, J., Gores, G.J., and Mazzaferro, V. (2014). *Hepatocellular carcinoma: clinical frontiers and perspectives*. Gut *63*, 844–855.

Bryant, D.M., Datta, A., Rodríguez-Fraticelli, A.E., Peränen, J., Martín-Belmonte, F., and Mostov, K.E. (2010). *A molecular network for de novo generation of the apical surface and lumen*. Nat. Cell Biol. *12*, 1035–1045.

Burger, J.A., and Peled, A. (2009). *CXCR4 antagonists: targeting the microenvironment in leukemia and other cancers*. Leukemia *23*, 43–52.

Caja, L., Ortiz, C., Bertran, E., Murillo, M.M., Miró-Obradors, M.J., Palacios, E., and Fabregat, I. (2007). *Differential intracellular signalling induced by TGF-beta in rat*

adult hepatocytes and hepatoma cells: implications in liver carcinogenesis. Cell. Signal. *19*, 683–694.

Caja, L., Sancho, P., Bertran, E., Iglesias-Serret, D., Gil, J., and Fabregat, I. (2009). *Overactivation of the MEK/ERK pathway in liver tumor cells confers resistance to TGF-{beta}-induced cell death through impairing up-regulation of the NADPH oxidase NOX4*. Cancer Res. *69*, 7595–7602.

Caja, L., Sancho, P., Bertran, E., Ortiz, C., Campbell, J.S., Fausto, N., and Fabregat, I. (2011a). *The tyrphostin AG1478 inhibits proliferation and induces death of liver tumor cells through EGF receptor-dependent and independent mechanisms*. Biochem. Pharmacol. *82*, 1583–1592.

Caja, L., Sancho, P., Bertran, E., and Fabregat, I. (2011b). *Dissecting the effect of targeting the epidermal growth factor receptor on TGF-β-induced-apoptosis in human hepatocellular carcinoma cells*. J. Hepatol. *55*, 351–358.

Campbell, J.J., and Butcher, E.C. (2000). *Chemokines in tissue-specific and microenvironment-specific lymphocyte homing*. Curr. Opin. Immunol. *12*, 336–341.

Carpentier, J.L., Lew, D.P., Paccaud, J.P., Gil, R., Iacopetta, B., Kazatchkine, M., Stendahl, O., and Pozzan, T. (1991). *Internalization pathway of C3b receptors in human neutrophils and its transmodulation by chemoattractant receptors stimulation*. Cell Regul. *2*, 41–55.

Carr, B.I., Hayashi, I., Branum, E.L., and Moses, H.L. (1986). *Inhibition of DNA synthesis in rat hepatocytes by platelet-derived type beta transforming growth factor*. Cancer Res. *46*, 2330–2334.

Castello, G., Scala, S., Palmieri, G., Curley, S.A., and Izzo, F. (2010). *HCV-related hepatocellular carcinoma: From chronic inflammation to cancer*. Clin. Immunol. Orlando Fla *134*, 237–250.

Del Castillo, G., Murillo, M.M., Alvarez-Barrientos, A., Bertran, E., Fernández, M., Sánchez, A., and Fabregat, I. (2006). *Autocrine production of TGF-beta confers resistance to apoptosis after an epithelial-mesenchymal transition process in hepatocytes: Role of EGF receptor ligands*. Exp. Cell Res. *312*, 2860–2871.

Castriconi, R., Dondero, A., Bellora, F., Moretta, L., Castellano, A., Locatelli, F., Corrias, M.V., Moretta, A., and Bottino, C. (2013). *Neuroblastoma-derived TGF-β1 modulates the chemokine receptor repertoire of human resting NK cells*. J. Immunol. Baltim. Md 1950 *190*, 5321–5328.

Cau, J., and Hall, A. (2005). *Cdc42 controls the polarity of the actin and microtubule cytoskeletons through two distinct signal transduction pathways*. J. Cell Sci. *118*, 2579–2587.

Charette, N., Holland, P., Frazer, J., Allen, H., and Dupré, D.J. (2011). *Dependence on different Rab GTPases for the trafficking of CXCR4 and CCR5 homo or heterodimers between the endoplasmic reticulum and plasma membrane in Jurkat cells*. Cell. Signal. *23*, 1738–1749.

Chen, X., and Macara, I.G. (2006). *Par-3 mediates the inhibition of LIM kinase 2 to regulate cofilin phosphorylation and tight junction assembly*. J. Cell Biol. *172*, 671–678.

Chetram, M.A., Don-Salu-Hewage, A.S., and Hinton, C.V. (2011). *ROS enhances CXCR4-mediated functions through inactivation of PTEN in prostate cancer cells*. Biochem. Biophys. Res. Commun. *410*, 195–200.

Chu, H., Zhou, H., Liu, Y., Liu, X., Hu, Y., and Zhang, J. (2007). *Functional expression of CXC chemokine recepter-4 mediates the secretion of matrix metalloproteinases from mouse hepatocarcinoma cell lines with different lymphatic metastasis ability*. Int. J. Biochem. Cell Biol. *39*, 197–205.

Cicchini, C., Filippini, D., Coen, S., Marchetti, A., Cavallari, C., Laudadio, I., Spagnoli, F.M., Alonzi, T., and Tripodi, M. (2006). *Snail controls differentiation of hepatocytes by repressing HNF4alpha expression*. J. Cell. Physiol. *209*, 230–238.

Cohen, E.E.W., Lingen, M.W., Zhu, B., Zhu, H., Straza, M.W., Pierce, C., Martin, L.E., and Rosner, M.R. (2006). *Protein kinase C zeta mediates epidermal growth factor-induced growth of head and neck tumor cells by regulating mitogen-activated protein kinase*. Cancer Res. *66*, 6296–6303.

Cojoc, M., Peitzsch, C., Trautmann, F., Polishchuk, L., Telegeev, G.D., and Dubrovska, A. (2013). *Emerging targets in cancer management: role of the CXCL12/CXCR4 axis*. OncoTargets Ther. *6*, 1347–1361.

Coulouarn, C., Factor, V.M., and Thorgeirsson, S.S. (2008). *Transforming growth factor-beta gene expression signature in mouse hepatocytes predicts clinical outcome in human cancer*. Hepatol. Baltim. Md *47*, 2059–2067.

Coyle, B., Freathy, C., Gant, T.W., Roberts, R.A., and Cain, K. (2003). *Characterization of the transforming growth factor-beta 1-induced apoptotic transcriptome in FaO hepatoma cells*. J. Biol. Chem. *278*, 5920–5928.

Delongchamps, N.B., Beuvon, F., Mathieu, J.R.R., Delmas, S., Metzger, I., Prats, H., and Cabon, F. (2015). *CXCR4 is highly expressed at the tumor front but not in the center of prostate cancers*. World J. Urol. *33*, 281–287.

Ding, X., Wang, K., Wang, H., Zhang, G., Liu, Y., Yang, Q., Chen, W., and Hu, S. (2012). *High expression of CCL20 is associated with poor prognosis in patients with hepatocellular carcinoma after curative resection*. J. Gastrointest. Surg. Off. J. Soc. Surg. Aliment. Tract *16*, 828–836.

Domanska, U.M., Kruizinga, R.C., Nagengast, W.B., Timmer-Bosscha, H., Huls, G., de Vries, E.G.E., and Walenkamp, A.M.E. (2013). *A review on CXCR4/CXCL12 axis in oncology: no place to hide*. Eur. J. Cancer Oxf. Engl. 1990 *49*, 219–230.

Drabsch, Y., and Dijke, P. ten (2012). *TGF-β signalling and its role in cancer progression and metastasis*. Cancer Metastasis Rev. *31*, 553–568.

Dragani, T.A. (2010). *Risk of HCC: genetic heterogeneity and complex genetics*. J. Hepatol. *52*, 252–257.

Drewes, G., Ebneth, A., Preuss, U., Mandelkow, E.M., and Mandelkow, E. (1997). *MARK, a novel family of protein kinases that phosphorylate microtubule-associated proteins and trigger microtubule disruption*. Cell *89*, 297–308.

Drysdale, B.E., Zacharchuk, C.M., and Shin, H.S. (1983). *Mechanism of macrophage-mediated cytotoxicity: production of a soluble cytotoxic factor*. J. Immunol. Baltim. Md 1950 *131*, 2362–2367.

Edlund, S., Landström, M., Heldin, C.-H., and Aspenström, P. (2004). *Smad7 is required for TGF-beta-induced activation of the small GTPase Cdc42*. J. Cell Sci. *117*, 1835–1847.

Ellenbroek, S.I.J., Iden, S., and Collard, J.G. (2012). *Cell polarity proteins and cancer*. Semin. Cancer Biol. *22*, 208–215.

Espinosa, L., and Navarro, E. (1998). *Human serine/threonine protein kinase EMK1: genomic structure and cDNA cloning of isoforms produced by alternative splicing*. Cytogenet. Cell Genet. *81*, 278–282.

Etienne-Manneville, S. (2008). *Polarity proteins in migration and invasion*. Oncogene *27*, 6970–6980.

Etienne-Manneville, S. (2013). *Microtubules in cell migration*. Annu. Rev. Cell Dev. Biol. *29*, 471–499.

Etienne-Manneville, S., and Hall, A. (2002). *Rho GTPases in cell biology*. Nature *420*, 629–635.

Etienne-Manneville, S., Manneville, J.-B., Nicholls, S., Ferenczi, M.A., and Hall, A. (2005). *Cdc42 and Par6-PKCzeta regulate the spatially localized association of Dlg1 and APC to control cell polarization*. J. Cell Biol. *170*, 895–901.

European Association For The Study Of The Liver, and European Organisation For Research And Treatment Of Cancer (2012). *EASL-EORTC clinical practice guidelines: management of hepatocellular carcinoma*. J. Hepatol. *56*, 908–943.

Fabregat, I., Fernando, J., Mainez, J., and Sancho, P. (2014). *TGF-beta signaling in cancer treatment*. Curr. Pharm. Des. *20*, 2934–2947.

Farooqui, R., Zhu, S., and Fenteany, G. (2006). *Glycogen synthase kinase-3 acts upstream of ADP-ribosylation factor 6 and Rac1 to regulate epithelial cell migration*. Exp. Cell Res. *312*, 1514–1525.

Farquhar, M.G., and Palade, G.E. (1998). *The Golgi apparatus: 100 years of progress and controversy*. Trends Cell Biol. *8*, 2–10.

Fausto, N., and Campbell, J.S. (2003). *The role of hepatocytes and oval cells in liver regeneration and repopulation*. Mech. Dev. *120*, 117–130.

Feng, Y., Broder, C.C., Kennedy, P.E., and Berger, E.A. (1996). *HIV-1 entry cofactor: functional cDNA cloning of a seven-transmembrane, G protein-coupled receptor*. Science *272*, 872–877.

Förster, R., Kremmer, E., Schubel, A., Breitfeld, D., Kleinschmidt, A., Nerl, C., Bernhardt, G., and Lipp, M. (1998). *Intracellular and surface expression of the*

HIV-1 coreceptor CXCR4/fusin on various leukocyte subsets: rapid internalization and recycling upon activation. J. Immunol. Baltim. Md 1950 *160*, 1522–1531.

Franco, D.L., Mainez, J., Vega, S., Sancho, P., Murillo, M.M., de Frutos, C.A., Del Castillo, G., López-Blau, C., Fabregat, I., and Nieto, M.A. (2010). *Snail1 suppresses TGF-beta-induced apoptosis and is sufficient to trigger EMT in hepatocytes*. J. Cell Sci. *123*, 3467–3477.

Franitza, S., Kollet, O., Brill, A., Vaday, G.G., Petit, I., Lapidot, T., Alon, R., and Lider, O. (2002). *TGF-beta1 enhances SDF-1alpha-induced chemotaxis and homing of naive T cells by up-regulating CXCR4 expression and downstream cytoskeletal effector molecules*. Eur. J. Immunol. *32*, 193–202.

Franklin, C.C., Rosenfeld-Franklin, M.E., White, C., Kavanagh, T.J., and Fausto, N. (2003). *TGFbeta1-induced suppression of glutathione antioxidant defenses in hepatocytes: caspase-dependent post-translational and caspase-independent transcriptional regulatory mechanisms*. FASEB J. Off. Publ. Fed. Am. Soc. Exp. Biol. *17*, 1535–1537.

Fujii, H., Itoh, Y., Yamaguchi, K., Yamauchi, N., Harano, Y., Nakajima, T., Minami, M., and Okanoue, T. (2004). *Chemokine CCL20 enhances the growth of HuH7 cells via phosphorylation of p44/42 MAPK in vitro*. Biochem. Biophys. Res. Commun. *322*, 1052–1058.

Gagescu, R., Gruenberg, J., and Smythe, E. (2000). *Membrane dynamics in endocytosis: structure--function relationship*. Traffic Cph. Den. *1*, 84–88.

George, G.P.C., Pisaneschi, F., Nguyen, Q.-D., and Aboagye, E.O. (2014). *Positron emission tomographic imaging of CXCR4 in cancer: challenges and promises*. Mol. Imaging *13*, 1–19.

Gérard, A., Mertens, A.E.E., van der Kammen, R.A., and Collard, J.G. (2007). *The Par polarity complex regulates Rap1- and chemokine-induced T cell polarization*. J. Cell Biol. *176*, 863–875.

Ghanem, I., Riveiro, M.E., Paradis, V., Faivre, S., de Parga, P.M.V., and Raymond, E. (2014). *Insights on the CXCL12-CXCR4 axis in hepatocellular carcinoma carcinogenesis*. Am. J. Transl. Res. *6*, 340–352.

Gomes, E.R., Jani, S., and Gundersen, G.G. (2005). *Nuclear movement regulated by Cdc42, MRCK, myosin, and actin flow establishes MTOC polarization in migrating cells*. Cell *121*, 451–463.

Goodrich, L.V., and Strutt, D. (2011). *Principles of planar polarity in animal development*. Dev. Camb. Engl. *138*, 1877–1892.

Grindstaff, K.K., Yeaman, C., Anandasabapathy, N., Hsu, S.C., Rodriguez-Boulan, E., Scheller, R.H., and Nelson, W.J. (1998). *Sec6/8 complex is recruited to cell-cell contacts and specifies transport vesicle delivery to the basal-lateral membrane in epithelial cells*. Cell *93*, 731–740.

Gu, Z., Noss, E.H., Hsu, V.W., and Brenner, M.B. (2011). *Integrins traffic rapidly via circular dorsal ruffles and macropinocytosis during stimulated cell migration*. J. Cell Biol. *193*, 61–70.

Halaoui, R., and McCaffrey, L. (2015). *Rewiring cell polarity signaling in cancer*. Oncogene *34*, 939–950.

Hanover, J.A., Willingham, M.C., and Pastan, I. (1984). *Kinetics of transit of transferrin and epidermal growth factor through clathrin-coated membranes*. Cell *39*, 283–293.

Harding, J.J., and Abou-Alfa, G.K. (2013). *Systemic therapy for hepatocellular carcinoma*. Chin. Clin. Oncol. *2*, 37.

Haribabu, B., Richardson, R.M., Fisher, I., Sozzani, S., Peiper, S.C., Horuk, R., Ali, H., and Snyderman, R. (1997). *Regulation of human chemokine receptors CXCR4. Role of phosphorylation in desensitization and internalization*. J. Biol. Chem. *272*, 28726–28731.

Hassan, S., Buchanan, M., Jahan, K., Aguilar-Mahecha, A., Gaboury, L., Muller, W.J., Alsawafi, Y., Mourskaia, A.A., Siegel, P.M., Salvucci, O., et al. (2011). *CXCR4 peptide antagonist inhibits primary breast tumor growth, metastasis and enhances the efficacy of anti-VEGF treatment or docetaxel in a transgenic mouse model*. Int. J. Cancer J. Int. Cancer *129*, 225–232.

Heider, M.R., and Munson, M. (2012). *Exorcising the exocyst complex*. Traffic Cph. Den. *13*, 898–907.

Heldin, C.-H., Landström, M., and Moustakas, A. (2009). *Mechanism of TGF-beta signaling to growth arrest, apoptosis, and epithelial-mesenchymal transition*. Curr. Opin. Cell Biol. *21*, 166–176.

Heldin, C.-H., Vanlandewijck, M., and Moustakas, A. (2012). *Regulation of EMT by TGFβ in cancer*. FEBS Lett. *586*, 1959–1970.

Herrera, B., Murillo, M.M., Alvarez-Barrientos, A., Beltrán, J., Fernández, M., and Fabregat, I. (2004). *Source of early reactive oxygen species in the apoptosis induced by transforming growth factor-beta in fetal rat hepatocytes*. Free Radic. Biol. Med. *36*, 16–26.

Hertzog, M., and Chavrier, P. (2011). *Cell polarity during motile processes: keeping on track with the exocyst complex*. Biochem. J. *433*, 403–409.

Hinshaw, J.E. (2000). *Dynamin and its role in membrane fission*. Annu. Rev. Cell Dev. Biol. *16*, 483–519.

Hirano, Y., Yoshinaga, S., Takeya, R., Suzuki, N.N., Horiuchi, M., Kohjima, M., Sumimoto, H., and Inagaki, F. (2005). *Structure of a cell polarity regulator, a complex between atypical PKC and Par6 PB1 domains*. J. Biol. Chem. *280*, 9653–9661.

Hirose, T., Izumi, Y., Nagashima, Y., Tamai-Nagai, Y., Kurihara, H., Sakai, T., Suzuki, Y., Yamanaka, T., Suzuki, A., Mizuno, K., et al. (2002). *Involvement of ASIP/PAR-3 in the promotion of epithelial tight junction formation*. J. Cell Sci. *115*, 2485–2495.

Hollier, B.G., Evans, K., and Mani, S.A. (2009). *The epithelial-to-mesenchymal transition and cancer stem cells: a coalition against cancer therapies*. J. Mammary Gland Biol. Neoplasia *14*, 29–43.

Huang, F., and Geng, X.-P. (2010). *Chemokines and hepatocellular carcinoma*. World J. Gastroenterol. WJG *16*, 1832–1836.

Hugo, H., Ackland, M.L., Blick, T., Lawrence, M.G., Clements, J.A., Williams, E.D., and Thompson, E.W. (2007). *Epithelial--mesenchymal and mesenchymal--epithelial transitions in carcinoma progression*. J. Cell. Physiol. *213*, 374–383.

Humbert, P.O., Dow, L.E., and Russell, S.M. (2006). *The Scribble and Par complexes in polarity and migration: friends or foes?* Trends Cell Biol. *16*, 622–630.

Huse, M., Lillemeier, B.F., Kuhns, M.S., Chen, D.S., and Davis, M.M. (2006). *T cells use two directionally distinct pathways for cytokine secretion*. Nat. Immunol. *7*, 247–255.

Hutterer, A., Betschinger, J., Petronczki, M., and Knoblich, J.A. (2004). *Sequential roles of Cdc42, Par-6, aPKC, and Lgl in the establishment of epithelial polarity during Drosophila embryogenesis*. Dev. Cell *6*, 845–854.

Iden, S., and Collard, J.G. (2008). *Crosstalk between small GTPases and polarity proteins in cell polarization*. Nat. Rev. Mol. Cell Biol. *9*, 846–859.

Imamichi, Y., and Menke, A. (2007). *Signaling pathways involved in collagen-induced disruption of the E-cadherin complex during epithelial-mesenchymal transition*. Cells Tissues Organs *185*, 180–190.

Ivanov, A.I. (2008). *Exocytosis and endocytosis*. Methods Mol. Biol. Clifton NJ *440*, v – vi.

Izumi, Y., Hirose, T., Tamai, Y., Hirai, S., Nagashima, Y., Fujimoto, T., Tabuse, Y., Kemphues, K.J., and Ohno, S. (1998). *An atypical PKC directly associates and colocalizes at the epithelial tight junction with ASIP, a mammalian homologue of Caenorhabditis elegans polarity protein PAR-3*. J. Cell Biol. *143*, 95–106.

Joberty, G., Petersen, C., Gao, L., and Macara, I.G. (2000). *The cell-polarity protein Par6 links Par3 and atypical protein kinase C to Cdc42*. Nat. Cell Biol. *2*, 531–539.

Jones, M.C., Caswell, P.T., and Norman, J.C. (2006). *Endocytic recycling pathways: emerging regulators of cell migration*. Curr. Opin. Cell Biol. *18*, 549–557.

Kallay, L.M., McNickle, A., Brennwald, P.J., Hubbard, A.L., and Braiterman, L.T. (2006). *Scribble associates with two polarity proteins, Lgl2 and Vangl2, via distinct molecular domains*. J. Cell. Biochem. *99*, 647–664.

Kametaka, S., and Waguri, S. (2012). *Visualization of TGN-endosome trafficking in mammalian and Drosophila cells*. Methods Enzymol. *504*, 255–271.

Kang, W., and Shin, E.-C. (2011). *Clinical implications of chemokines in acute and chronic hepatitis C virus infection*. Yonsei Med. J. *52*, 871–878.

Kemphues, K.J., Priess, J.R., Morton, D.G., and Cheng, N.S. (1988). *Identification of genes required for cytoplasmic localization in early C. elegans embryos*. Cell *52*, 311–320.

Khursheed, M., and Bashyam, M.D. (2014). *Apico-basal polarity complex and cancer*. J. Biosci. *39*, 145–155.

Kim, S.-W., Kim, H.-Y., Song, I.-C., Jin, S.-A., Lee, H.-J., Yun, H.-J., Kim, S., and Jo, D.-Y. (2008). *Cytoplasmic trapping of CXCR4 in hepatocellular carcinoma cell lines*. Cancer Res. Treat. Off. J. Korean Cancer Assoc. *40*, 53–61.

Krohn, A., Song, Y.-H., Muehlberg, F., Droll, L., Beckmann, C., and Alt, E. (2009). *CXCR4 receptor positive spheroid forming cells are responsible for tumor invasion in vitro*. Cancer Lett. *280*, 65–71.

Kuehn, E.W., Walz, G., and Benzing, T. (2007). *Von hippel-lindau: a tumor suppressor links microtubules to ciliogenesis and cancer development*. Cancer Res. *67*, 4537–4540.

Kukreja, P., Abdel-Mageed, A.B., Mondal, D., Liu, K., and Agrawal, K.C. (2005). *Up-regulation of CXCR4 expression in PC-3 cells by stromal-derived factor-1alpha (CXCL12) increases endothelial adhesion and transendothelial migration: role of MEK/ERK signaling pathway-dependent NF-kappaB activation*. Cancer Res. *65*, 9891–9898.

Kuribayashi, K., Nakamura, K., Tanaka, M., Sato, T., Kato, J., Sasaki, K., Takimoto, R., Kogawa, K., Terui, T., Takayama, T., et al. (2007). *Essential role of protein kinase C zeta in transducing a motility signal induced by superoxide and a chemotactic peptide, fMLP*. J. Cell Biol. *176*, 1049–1060.

Ladinsky, M.S., Mastronarde, D.N., McIntosh, J.R., Howell, K.E., and Staehelin, L.A. (1999). *Golgi structure in three dimensions: functional insights from the normal rat kidney cell*. J. Cell Biol. *144*, 1135–1149.

Laemmli, U.K. (1970). *Cleavage of structural proteins during the assembly of the head of bacteriophage T4*. Nature *227*, 680–685.

Lamouille, S., Xu, J., and Derynck, R. (2014). *Molecular mechanisms of epithelial-mesenchymal transition*. Nat. Rev. Mol. Cell Biol. *15*, 178–196.

Larrubia, J.R., Benito-Martínez, S., Calvino, M., Sanz-de-Villalobos, E., and Parra-Cid, T. (2008). *Role of chemokines and their receptors in viral persistence and liver damage during chronic hepatitis C virus infection*. World J. Gastroenterol. WJG *14*, 7149–7159.

Lee, M., and Vasioukhin, V. (2008). *Cell polarity and cancer--cell and tissue polarity as a non-canonical tumor suppressor*. J. Cell Sci. *121*, 1141–1150.

Lee, J.M., Dedhar, S., Kalluri, R., and Thompson, E.W. (2006). *The epithelial-mesenchymal transition: new insights in signaling, development, and disease*. J. Cell Biol. *172*, 973–981.

Levoye, A., Balabanian, K., Baleux, F., Bachelerie, F., and Lagane, B. (2009). *CXCR7 heterodimerizes with CXCR4 and regulates CXCL12-mediated G protein signaling*. Blood *113*, 6085–6093.

Liang, Z., Brooks, J., Willard, M., Liang, K., Yoon, Y., Kang, S., and Shim, H. (2007). *CXCR4/CXCL12 axis promotes VEGF-mediated tumor angiogenesis through Akt signaling pathway*. Biochem. Biophys. Res. Commun. *359*, 716–722.

Lieu, Z.Z., Lock, J.G., Hammond, L.A., La Gruta, N.L., Stow, J.L., and Gleeson, P.A. (2008). *A trans-Golgi network golgin is required for the regulated secretion of TNF in activated macrophages in vivo*. Proc. Natl. Acad. Sci. U. S. A. *105*, 3351–3356.

Lim, J.P., and Gleeson, P.A. (2011). *Macropinocytosis: an endocytic pathway for internalising large gulps*. Immunol. Cell Biol. *89*, 836–843.

Liu, J., and Guo, W. (2012). *The exocyst complex in exocytosis and cell migration*. Protoplasma *249*, 587–597.

Liu, H., Pan, Z., Li, A., Fu, S., Lei, Y., Sun, H., Wu, M., and Zhou, W. (2008). *Roles of chemokine receptor 4 (CXCR4) and chemokine ligand 12 (CXCL12) in metastasis of hepatocellular carcinoma cells*. Cell. Mol. Immunol. *5*, 373–378.

Liu, J., Yue, P., Artym, V.V., Mueller, S.C., and Guo, W. (2009). *The role of the exocyst in matrix metalloproteinase secretion and actin dynamics during tumor cell invadopodia formation*. Mol. Biol. Cell *20*, 3763–3771.

Liu, J., Liao, S., Huang, Y., Samuel, R., Shi, T., Naxerova, K., Huang, P., Kamoun, W., Jain, R.K., Fukumura, D., et al. (2011). *PDGF-D improves drug delivery and efficacy via vascular normalization, but promotes lymphatic metastasis by activating CXCR4 in breast cancer*. Clin. Cancer Res. Off. J. Am. Assoc. Cancer Res. *17*, 3638–3648.

Llovet, J.M., and Bruix, J. (2008). *Molecular targeted therapies in hepatocellular carcinoma*. Hepatol. Baltim. Md *48*, 1312–1327.

Lock, J.G., and Stow, J.L. (2005). *Rab11 in recycling endosomes regulates the sorting and basolateral transport of E-cadherin*. Mol. Biol. Cell *16*, 1744–1755.

Lock, J.G., Hammond, L.A., Houghton, F., Gleeson, P.A., and Stow, J.L. (2005). *E-cadherin transport from the trans-Golgi network in tubulovesicular carriers is selectively regulated by golgin-97*. Traffic Cph. Den. *6*, 1142–1156.

Low, S.H., Chapin, S.J., Weimbs, T., Kömüves, L.G., Bennett, M.K., and Mostov, K.E. (1996). *Differential localization of syntaxin isoforms in polarized Madin-Darby canine kidney cells*. Mol. Biol. Cell *7*, 2007–2018.

Lynch CJ (2014). *Web Resources: G.I. Normal Biology and Diseases - GI723*, accessed 30 July 2015 https://wikispaces.psu.edu/pages/viewpage.action?pageId=201229851. Pennstate University.

Lyons, P.D., Peck, G.R., Kettenbach, A.N., Gerber, S.A., Roudaia, L., and Lienhard, G.E. (2009). *Insulin stimulates the phosphorylation of the exocyst protein Sec8 in adipocytes*. Biosci. Rep. *29*, 229–235.

Ma, Q., Jones, D., Borghesani, P.R., Segal, R.A., Nagasawa, T., Kishimoto, T., Bronson, R.T., and Springer, T.A. (1998). *Impaired B-lymphopoiesis, myelopoiesis, and derailed cerebellar neuron migration in CXCR4- and SDF-1-deficient mice*. Proc. Natl. Acad. Sci. U. S. A. *95*, 9448–9453.

Malarkey, D.E., Johnson, K., Ryan, L., Boorman, G., and Maronpot, R.R. (2005). *New insights into functional aspects of liver morphology*. Toxicol. Pathol. *33*, 27–34.

Mañes, S., Mira, E., Gómez-Moutón, C., Lacalle, R.A., Keller, P., Labrador, J.P., and Martínez-A, C. (1999). *Membrane raft microdomains mediate front-rear polarity in migrating cells*. EMBO J. *18*, 6211–6220.

Martin-Belmonte, F., and Mostov, K. (2007). *Phosphoinositides control epithelial development*. Cell Cycle Georget. Tex *6*, 1957–1961.

Massagué, J. (2008). *TGFbeta in Cancer*. Cell *134*, 215–230.

Massimi, P., Narayan, N., Thomas, M., Gammoh, N., Strand, S., Strand, D., and Banks, L. (2008). *Regulation of the hDlg/hScrib/Hugl-1 tumour suppressor complex*. Exp. Cell Res. *314*, 3306–3317.

Maxfield, F.R., and McGraw, T.E. (2004). *Endocytic recycling*. Nat. Rev. Mol. Cell Biol. *5*, 121–132.

McCaffrey, L.M., Montalbano, J., Mihai, C., and Macara, I.G. (2012). *Loss of the Par3 polarity protein promotes breast tumorigenesis and metastasis*. Cancer Cell *22*, 601–614.

McMahon, H.T., and Boucrot, E. (2011). *Molecular mechanism and physiological functions of clathrin-mediated endocytosis*. Nat. Rev. Mol. Cell Biol. *12*, 517–533.

Mead, J.E., and Fausto, N. (1989). *Transforming growth factor alpha may be a physiological regulator of liver regeneration by means of an autocrine mechanism*. Proc. Natl. Acad. Sci. U. S. A. *86*, 1558–1562.

Médina, E., Williams, J., Klipfell, E., Zarnescu, D., Thomas, G., and Le Bivic, A. (2002). *Crumbs interacts with moesin and beta(Heavy)-spectrin in the apical membrane skeleton of Drosophila*. J. Cell Biol. *158*, 941–951.

Mellman, I., and Nelson, W.J. (2008). *Coordinated protein sorting, targeting and distribution in polarized cells*. Nat. Rev. Mol. Cell Biol. *9*, 833–845.

Mertens, A.E.E., Rygiel, T.P., Olivo, C., van der Kammen, R., and Collard, J.G. (2005). *The Rac activator Tiam1 controls tight junction biogenesis in keratinocytes through binding to and activation of the Par polarity complex*. J. Cell Biol. *170*, 1029–1037.

Mitra, P., Shibuta, K., Mathai, J., Shimoda, K., Banner, B.F., Mori, M., and Barnard, G.F. (1999). *CXCR4 mRNA expression in colon, esophageal and gastric cancers and hepatitis C infected liver*. Int. J. Oncol. *14*, 917–925.

Mitra, P., De, A., Ethier, M.F., Mimori, K., Kodys, K., Shibuta, K., Mori, M., Madison, J.M., Miller-Graziano, C., and Barnard, G.F. (2001). *Loss of chemokine SDF-1alpha-mediated CXCR4 signalling and receptor internalization in human hepatoma cell line HepG2*. Cell. Signal. *13*, 311–319.

Miyoshi, A., Kitajima, Y., Kido, S., Shimonishi, T., Matsuyama, S., Kitahara, K., and Miyazaki, K. (2005). *Snail accelerates cancer invasion by upregulating MMP expression and is associated with poor prognosis of hepatocellular carcinoma*. Br. J. Cancer *92*, 252–258.

Montcouquiol, M., Sans, N., Huss, D., Kach, J., Dickman, J.D., Forge, A., Rachel, R.A., Copeland, N.G., Jenkins, N.A., Bogani, D., et al. (2006). *Asymmetric localization*

of Vangl2 and Fz3 indicate novel mechanisms for planar cell polarity in mammals. J. Neurosci. Off. J. Soc. Neurosci. *26*, 5265–5275.

Moreno-Bueno, G., Portillo, F., and Cano, A. (2008). *Transcriptional regulation of cell polarity in EMT and cancer*. Oncogene *27*, 6958–6969.

Moreno-Càceres, J., Caja, L., Mainez, J., Mayoral, R., Martín-Sanz, P., Moreno-Vicente, R., Del Pozo, M.Á., Dooley, S., Egea, G., and Fabregat, I. (2014). *Caveolin-1 is required for TGF-β-induced transactivation of the EGF receptor pathway in hepatocytes through the activation of the metalloprotease TACE/ADAM17*. Cell Death Dis. *5*, e1326.

Morrison, C.D., Parvani, J.G., and Schiemann, W.P. (2013). *The relevance of the TGF-β Paradox to EMT-MET programs*. Cancer Lett. *341*, 30–40.

Moscat, J., Rennert, P., and Diaz-Meco, M.T. (2006). *PKCzeta at the crossroad of NF-kappaB and Jak1/Stat6 signaling pathways*. Cell Death Differ. *13*, 702–711.

Moustakas, A., and Heldin, C.-H. (2007). *Signaling networks guiding epithelial-mesenchymal transitions during embryogenesis and cancer progression*. Cancer Sci. *98*, 1512–1520.

Mu, X., Chen, Y., Wang, S., Huang, X., Pan, H., and Li, M. (2009). *Overexpression of VCC-1 gene in human hepatocellular carcinoma cells promotes cell proliferation and invasion*. Acta Biochim. Biophys. Sin. *41*, 631–637.

Müller, A., Homey, B., Soto, H., Ge, N., Catron, D., Buchanan, M.E., McClanahan, T., Murphy, E., Yuan, W., Wagner, S.N., et al. (2001). *Involvement of chemokine receptors in breast cancer metastasis*. Nature *410*, 50–56.

Murillo, M.M., del Castillo, G., Sánchez, A., Fernández, M., and Fabregat, I. (2005). *Involvement of EGF receptor and c-Src in the survival signals induced by TGF-beta1 in hepatocytes*. Oncogene *24*, 4580–4587.

Murillo, M.M., Carmona-Cuenca, I., Del Castillo, G., Ortiz, C., Roncero, C., Sánchez, A., Fernández, M., and Fabregat, I. (2007). *Activation of NADPH oxidase by transforming growth factor-beta in hepatocytes mediates up-regulation of epidermal growth factor receptor ligands through a nuclear factor-kappaB-dependent mechanism*. Biochem. J. *405*, 251–259.

Muthuswamy, S.K., and Xue, B. (2012). *Cell polarity as a regulator of cancer cell behavior plasticity*. Annu. Rev. Cell Dev. Biol. *28*, 599–625.

Nagai-Tamai, Y., Mizuno, K., Hirose, T., Suzuki, A., and Ohno, S. (2002). *Regulated protein-protein interaction between aPKC and PAR-3 plays an essential role in the polarization of epithelial cells*. Genes Cells Devoted Mol. Cell. Mech. *7*, 1161–1171.

Nagasawa, T. (2014). *CXC chemokine ligand 12 (CXCL12) and its receptor CXCR4*. J. Mol. Med. Berl. Ger. *92*, 433–439.

Nakamura, N., Rabouille, C., Watson, R., Nilsson, T., Hui, N., Slusarewicz, P., Kreis, T.E., and Warren, G. (1995). *Characterization of a cis-Golgi matrix protein, GM130*. J. Cell Biol. *131*, 1715–1726.

Nakayama, M., Goto, T.M., Sugimoto, M., Nishimura, T., Shinagawa, T., Ohno, S., Amano, M., and Kaibuchi, K. (2008). *Rho-kinase phosphorylates PAR-3 and disrupts PAR complex formation*. Dev. Cell *14*, 205–215.

Neel, N.F., Schutyser, E., Sai, J., Fan, G.-H., and Richmond, A. (2005). *Chemokine receptor internalization and intracellular trafficking*. Cytokine Growth Factor Rev. *16*, 637–658.

Nelson, W.J. (2009). *Remodeling epithelial cell organization: transitions between front-rear and apical-basal polarity*. Cold Spring Harb. Perspect. Biol. *1*, a000513.

Newell, P., Toffanin, S., Villanueva, A., Chiang, D.Y., Minguez, B., Cabellos, L., Savic, R., Hoshida, Y., Lim, K.H., Melgar-Lesmes, P., et al. (2009). *Ras pathway activation in hepatocellular carcinoma and anti-tumoral effect of combined sorafenib and rapamycin in vivo*. J. Hepatol. *51*, 725–733.

Nguyen, D.H., and Taub, D. (2002). *CXCR4 function requires membrane cholesterol: implications for HIV infection*. J. Immunol. Baltim. Md 1950 *168*, 4121–4126.

Niessen, C.M., and Gottardi, C.J. (2008). *Molecular components of the adherens junction*. Biochim. Biophys. Acta *1778*, 562–571.

Nolan, M.E., Aranda, V., Lee, S., Lakshmi, B., Basu, S., Allred, D.C., and Muthuswamy, S.K. (2008). *The polarity protein Par6 induces cell proliferation and is overexpressed in breast cancer*. Cancer Res. *68*, 8201–8209.

Odemis, V., Lipfert, J., Kraft, R., Hajek, P., Abraham, G., Hattermann, K., Mentlein, R., and Engele, J. (2012). *The presumed atypical chemokine receptor CXCR7 signals through G(i/o) proteins in primary rodent astrocytes and human glioma cells*. Glia *60*, 372–381.

Orimo, A., Gupta, P.B., Sgroi, D.C., Arenzana-Seisdedos, F., Delaunay, T., Naeem, R., Carey, V.J., Richardson, A.L., and Weinberg, R.A. (2005). *Stromal fibroblasts present in invasive human breast carcinomas promote tumor growth and angiogenesis through elevated SDF-1/CXCL12 secretion*. Cell *121*, 335–348.

Orsini, M.J., Parent, J.L., Mundell, S.J., Marchese, A., and Benovic, J.L. (1999). *Trafficking of the HIV coreceptor CXCR4. Role of arrestins and identification of residues in the c-terminal tail that mediate receptor internalization*. J. Biol. Chem. *274*, 31076–31086.

Ozdamar, B., Bose, R., Barrios-Rodiles, M., Wang, H.-R., Zhang, Y., and Wrana, J.L. (2005). *Regulation of the polarity protein Par6 by TGFbeta receptors controls epithelial cell plasticity*. Science *307*, 1603–1609.

Padua, D., and Massagué, J. (2009). *Roles of TGFbeta in metastasis*. Cell Res. *19*, 89–102.

Pardali, K., and Moustakas, A. (2007). *Actions of TGF-beta as tumor suppressor and pro-metastatic factor in human cancer*. Biochim. Biophys. Acta *1775*, 21–62.

Park, S.S., Eom, Y.-W., Kim, E.H., Lee, J.H., Min, D.S., Kim, S., Kim, S.-J., and Choi, K.S. (2004). *Involvement of c-Src kinase in the regulation of TGF-beta1-induced apoptosis*. Oncogene *23*, 6272–6281.

Pelekanos, R.A., Ting, M.J., Sardesai, V.S., Ryan, J.M., Lim, Y.-C., Chan, J.K.Y., and Fisk, N.M. (2014). *Intracellular trafficking and endocytosis of CXCR4 in fetal mesenchymal stem/stromal cells*. BMC Cell Biol. *15*, 15.

Peng, Y.-H., Yang, W.-K., Lin, W.-H., Lai, T.-T., and Chien, C.-T. (2009). *Nak regulates Dlg basal localization in Drosophila salivary gland cells*. Biochem. Biophys. Res. Commun. *382*, 108–113.

Pfeffer, S.R. (2001). *Rab GTPases: specifying and deciphering organelle identity and function*. Trends Cell Biol. *11*, 487–491.

Phillips, R.J., Burdick, M.D., Lutz, M., Belperio, J.A., Keane, M.P., and Strieter, R.M. (2003). *The stromal derived factor-1/CXCL12-CXC chemokine receptor 4 biological axis in non-small cell lung cancer metastases*. Am. J. Respir. Crit. Care Med. *167*, 1676–1686.

Reynders, E., Foulquier, F., Annaert, W., and Matthijs, G. (2011). *How Golgi glycosylation meets and needs trafficking: the case of the COG complex*. Glycobiology *21*, 853–863.

Roberts, L.R. (2005). *Chemokines as attractive targets in liver carcinogenesis*. Am. J. Gastroenterol. *100*, 499–501.

Robinson, M.S. (2004). *Adaptable adaptors for coated vesicles*. Trends Cell Biol. *14*, 167–174.

Roeth, J.F., Sawyer, J.K., Wilner, D.A., and Peifer, M. (2009). *Rab11 helps maintain apical crumbs and adherens junctions in the Drosophila embryonic ectoderm*. PloS One *4*, e7634.

Ross, S., and Hill, C.S. (2008). *How the Smads regulate transcription*. Int. J. Biochem. Cell Biol. *40*, 383–408.

Rosse, C., Formstecher, E., Boeckeler, K., Zhao, Y., Kremerskothen, J., White, M.D., Camonis, J.H., and Parker, P.J. (2009). *An aPKC-exocyst complex controls paxillin phosphorylation and migration through localised JNK1 activation*. PLoS Biol. *7*, e1000235.

Rossmanith, W., and Schulte-Hermann, R. (2001). *Biology of transforming growth factor beta in hepatocarcinogenesis*. Microsc. Res. Tech. *52*, 430–436.

Sánchez, A., Alvarez, A.M., Benito, M., and Fabregat, I. (1996). *Apoptosis induced by transforming growth factor-beta in fetal hepatocyte primary cultures: involvement of reactive oxygen intermediates*. J. Biol. Chem. *271*, 7416–7422.

Sánchez, A., Alvarez, A.M., Benito, M., and Fabregat, I. (1997). *Cycloheximide prevents apoptosis, reactive oxygen species production, and glutathione depletion induced by transforming growth factor beta in fetal rat hepatocytes in primary culture*. Hepatol. Baltim. Md *26*, 935–943.

Sánchez, A., Pagan, R., Alvarez, A.M., Roncero, C., Vilaró, S., Benito, M., and Fabregat, I. (1998). *Transforming growth factor-beta (TGF-beta) and EGF promote cord-like structures that indicate terminal differentiation of fetal hepatocytes in primary culture*. Exp. Cell Res. *242*, 27–37.

Sánchez, A., Alvarez, A.M., López Pedrosa, J.M., Roncero, C., Benito, M., and Fabregat, I. (1999). *Apoptotic response to TGF-beta in fetal hepatocytes depends upon their state of differentiation*. Exp. Cell Res. *252*, 281–291.

Sancho, P., Bertran, E., Caja, L., Carmona-Cuenca, I., Murillo, M.M., and Fabregat, I. (2009). *The inhibition of the epidermal growth factor (EGF) pathway enhances TGF-beta-induced apoptosis in rat hepatoma cells through inducing oxidative stress coincident with a change in the expression pattern of the NADPH oxidases (NOX) isoforms*. Biochim. Biophys. Acta *1793*, 253–263.

Schmierer, B., and Hill, C.S. (2007). *TGFbeta-SMAD signal transduction: molecular specificity and functional flexibility*. Nat. Rev. Mol. Cell Biol. *8*, 970–982.

Shen, L., Gao, Y., Qian, J., Sun, A., and Ge, J. (2011). *A novel mechanism for endothelial progenitor cells homing: The SDF-1/CXCR4-Rac pathway may regulate endothelial progenitor cells homing through cellular polarization*. Med. Hypotheses *76*, 256–258.

Shen, L., Gao, Y., Qian, J., Wu, Y., Zhou, M., Sun, A., Zou, Y., and Ge, J. (2012). *The role of SDF-1α/Rac pathway in the regulation of endothelial progenitor cell polarity; homing and expression of Rac1, Rac2 during endothelial repair*. Mol. Cell. Biochem. *365*, 1–7.

Shin, K., Wang, Q., and Margolis, B. (2007). *PATJ regulates directional migration of mammalian epithelial cells*. EMBO Rep. *8*, 158–164.

Shuman Moss, L.A., Jensen-Taubman, S., and Stetler-Stevenson, W.G. (2012). *Matrix metalloproteinases: changing roles in tumor progression and metastasis*. Am. J. Pathol. *181*, 1895–1899.

Signoret, N., Oldridge, J., Pelchen-Matthews, A., Klasse, P.J., Tran, T., Brass, L.F., Rosenkilde, M.M., Schwartz, T.W., Holmes, W., Dallas, W., et al. (1997). *Phorbol esters and SDF-1 induce rapid endocytosis and down modulation of the chemokine receptor CXCR4*. J. Cell Biol. *139*, 651–664.

Si-Tayeb, K., Lemaigre, F.P., and Duncan, S.A. (2010). *Organogenesis and development of the liver*. Dev. Cell *18*, 175–189.

Sleeman, J.P., and Thiery, J.P. (2011). *SnapShot: The epithelial-mesenchymal transition*. Cell *145*, 162.e1.

Slusarewicz, P., Nilsson, T., Hui, N., Watson, R., and Warren, G. (1994). *Isolation of a matrix that binds medial Golgi enzymes*. J. Cell Biol. *124*, 405–413.

Soliman, H.H., Nagy, H., Kotb, N., and Alm El-Din, M.A. (2012). *The role of chemokine CC ligand 20 in patients with liver cirrhosis and hepatocellular carcinoma*. Int. J. Biol. Markers *27*, e125–e131.

Song, K., Wang, H., Krebs, T.L., and Danielpour, D. (2006). *Novel roles of Akt and mTOR in suppressing TGF-beta/ALK5-mediated Smad3 activation*. EMBO J. *25*, 58–69.

Sönnichsen, B., De Renzis, S., Nielsen, E., Rietdorf, J., and Zerial, M. (2000). *Distinct membrane domains on endosomes in the recycling pathway visualized by multicolor imaging of Rab4, Rab5, and Rab11*. J. Cell Biol. *149*, 901–914.

Sotillos, S., Díaz-Meco, M.T., Caminero, E., Moscat, J., and Campuzano, S. (2004). *DaPKC-dependent phosphorylation of Crumbs is required for epithelial cell polarity in Drosophila*. J. Cell Biol. *166*, 549–557.

De Souza, A.T., Hankins, G.R., Washington, M.K., Orton, T.C., and Jirtle, R.L. (1995). *M6P/IGF2R gene is mutated in human hepatocellular carcinomas with loss of heterozygosity*. Nat. Genet. *11*, 447–449.

Spear, B.T., Jin, L., Ramasamy, S., and Dobierzewska, A. (2006). *Transcriptional control in the mammalian liver: liver development, perinatal repression, and zonal gene regulation*. Cell. Mol. Life Sci. CMLS *63*, 2922–2938.

Stenmark, H. (2009). *Rab GTPases as coordinators of vesicle traffic*. Nat. Rev. Mol. Cell Biol. *10*, 513–525.

Stow, J.L., Low, P.C., Offenhäuser, C., and Sangermani, D. (2009). *Cytokine secretion in macrophages and other cells: pathways and mediators*. Immunobiology *214*, 601–612.

Sugimachi, K., Tanaka, S., Kameyama, T., Taguchi, K., Aishima, S., Shimada, M., Sugimachi, K., and Tsuneyoshi, M. (2003). *Transcriptional repressor snail and progression of human hepatocellular carcinoma*. Clin. Cancer Res. Off. J. Am. Assoc. Cancer Res. *9*, 2657–2664.

Sun, R., Gao, P., Chen, L., Ma, D., Wang, J., Oppenheim, J.J., and Zhang, N. (2005). *Protein kinase C zeta is required for epidermal growth factor-induced chemotaxis of human breast cancer cells*. Cancer Res. *65*, 1433–1441.

Taguchi, T. (2013). *Emerging roles of recycling endosomes*. J. Biochem. (Tokyo) *153*, 505–510.

Tanaka, G., Nakase, I., Fukuda, Y., Masuda, R., Oishi, S., Shimura, K., Kawaguchi, Y., Takatani-Nakase, T., Langel, U., Gräslund, A., et al. (2012). *CXCR4 stimulates macropinocytosis: implications for cellular uptake of arginine-rich cell-penetrating peptides and HIV*. Chem. Biol. *19*, 1437–1446.

Tang, D., and Wang, Y. (2013). *Cell cycle regulation of Golgi membrane dynamics*. Trends Cell Biol. *23*, 296–304.

Teicher, B.A., and Fricker, S.P. (2010). *CXCL12 (SDF-1)/CXCR4 pathway in cancer*. Clin. Cancer Res. Off. J. Am. Assoc. Cancer Res. *16*, 2927–2931.

Thiery, J.P. (2002). *Epithelial-mesenchymal transitions in tumour progression*. Nat. Rev. Cancer *2*, 442–454.

Thiery, J.P. (2003). *Epithelial-mesenchymal transitions in development and pathologies*. Curr. Opin. Cell Biol. *15*, 740–746.

Thiery, J.P., and Sleeman, J.P. (2006). *Complex networks orchestrate epithelial-mesenchymal transitions*. Nat. Rev. Mol. Cell Biol. *7*, 131–142.

Thiery, J.P., Acloque, H., Huang, R.Y.J., and Nieto, M.A. (2009). *Epithelial-mesenchymal transitions in development and disease*. Cell *139*, 871–890.

Tsuchiya, A., Imai, M., Kamimura, H., Takamura, M., Yamagiwa, S., Sugiyama, T., Nomoto, M., Heike, T., Nagasawa, T., Nakahata, T., et al. (2012). *Increased susceptibility to severe chronic liver damage in CXCR4 conditional knock-out mice*. Dig. Dis. Sci. *57*, 2892–2900.

Tsukita, S., Furuse, M., and Itoh, M. (2001). *Multifunctional strands in tight junctions*. Nat. Rev. Mol. Cell Biol. *2*, 285–293.

Tsukita, S., Yamazaki, Y., Katsuno, T., Tamura, A., and Tsukita, S. (2008). *Tight junction-based epithelial microenvironment and cell proliferation*. Oncogene *27*, 6930–6938.

Uchida, H., Iwashita, Y., Sasaki, A., Shibata, K., Matsumoto, T., Ohta, M., and Kitano, S. (2006). *Chemokine receptor CCR6 as a prognostic factor after hepatic resection for hepatocellular carcinoma*. J. Gastroenterol. Hepatol. *21*, 161–168.

Valdés, F., Alvarez, A.M., Locascio, A., Vega, S., Herrera, B., Fernández, M., Benito, M., Nieto, M.A., and Fabregat, I. (2002). *The epithelial mesenchymal transition confers resistance to the apoptotic effects of transforming growth factor Beta in fetal rat hepatocytes*. Mol. Cancer Res. MCR *1*, 68–78.

Valdés, F., Murillo, M.M., Valverde, A.M., Herrera, B., Sánchez, A., Benito, M., Fernández, M., and Fabregat, I. (2004). *Transforming growth factor-beta activates both pro-apoptotic and survival signals in fetal rat hepatocytes*. Exp. Cell Res. *292*, 209–218.

Vandercappellen, J., Van Damme, J., and Struyf, S. (2008). *The role of CXC chemokines and their receptors in cancer*. Cancer Lett. *267*, 226–244.

Venkatesan, S., Rose, J.J., Lodge, R., Murphy, P.M., and Foley, J.F. (2003). *Distinct mechanisms of agonist-induced endocytosis for human chemokine receptors CCR5 and CXCR4*. Mol. Biol. Cell *14*, 3305–3324.

Villanueva, A., Newell, P., Chiang, D.Y., Friedman, S.L., and Llovet, J.M. (2007). *Genomics and signaling pathways in hepatocellular carcinoma*. Semin. Liver Dis. *27*, 55–76.

Wald, O., Pappo, O., Safadi, R., Dagan-Berger, M., Beider, K., Wald, H., Franitza, S., Weiss, I., Avniel, S., Boaz, P., et al. (2004). *Involvement of the CXCL12/CXCR4 pathway in the advanced liver disease that is associated with hepatitis C virus or hepatitis B virus*. Eur. J. Immunol. *34*, 1164–1174.

Wallace, M.C., and Friedman, S.L. (2014). *Hepatic fibrosis and the microenvironment: fertile soil for hepatocellular carcinoma development*. Gene Expr. *16*, 77–84.

Walston, T.D., and Hardin, J. (2006). *Wnt-dependent spindle polarization in the early C. elegans embryo*. Semin. Cell Dev. Biol. *17*, 204–213.

Wang, J.-B., Wu, W.J., and Cerione, R.A. (2005). *Cdc42 and Ras cooperate to mediate cellular transformation by intersectin-L*. J. Biol. Chem. *280*, 22883–22891.

Wang, S.E., Xiang, B., Guix, M., Olivares, M.G., Parker, J., Chung, C.H., Pandiella, A., and Arteaga, C.L. (2008a). *Transforming growth factor beta engages TACE and ErbB3 to activate phosphatidylinositol-3 kinase/Akt in ErbB2-overexpressing*

breast cancer and desensitizes cells to trastuzumab. Mol. Cell. Biol. *28*, 5605–5620.

Wang, X., Nie, J., Zhou, Q., Liu, W., Zhu, F., Chen, W., Mao, H., Luo, N., Dong, X., and Yu, X. (2008b). *Downregulation of Par-3 expression and disruption of Par complex integrity by TGF-beta during the process of epithelial to mesenchymal transition in rat proximal epithelial cells*. Biochim. Biophys. Acta *1782*, 51–59.

Wang, Y., Ngo, V.N., Marani, M., Yang, Y., Wright, G., Staudt, L.M., and Downward, J. (2010). *Critical role for transcriptional repressor Snail2 in transformation by oncogenic RAS in colorectal carcinoma cells*. Oncogene *29*, 4658–4670.

Wang, Y., Bu, F., Royer, C., Serres, S., Larkin, J.R., Soto, M.S., Sibson, N.R., Salter, V., Fritzsche, F., Turnquist, C., et al. (2014). *ASPP2 controls epithelial plasticity and inhibits metastasis through β-catenin-dependent regulation of ZEB1*. Nat. Cell Biol. *16*, 1092–1104.

Warner, D.R., Pisano, M.M., Roberts, E.A., and Greene, R.M. (2003). *Identification of three novel Smad binding proteins involved in cell polarity*. FEBS Lett. *539*, 167–173.

Weisz, O.A., and Rodriguez-Boulan, E. (2009). *Apical trafficking in epithelial cells: signals, clusters and motors*. J. Cell Sci. *122*, 4253–4266.

Weyrich, P., Kapp, K., Niederfellner, G., Melzer, M., Lehmann, R., Häring, H.-U., and Lammers, R. (2004). *Partitioning-defective protein 6 regulates insulin-dependent glycogen synthesis via atypical protein kinase C*. Mol. Endocrinol. Baltim. Md *18*, 1287–1300.

Weyrich, P., Neuscheler, D., Melzer, M., Hennige, A.M., Häring, H.-U., and Lammers, R. (2007). *The Par6alpha/aPKC complex regulates Akt1 activity by phosphorylating Thr34 in the PH-domain*. Mol. Cell. Endocrinol. *268*, 30–36.

Wheelock, M.J., and Johnson, K.R. (2003). *Cadherins as modulators of cellular phenotype*. Annu. Rev. Cell Dev. Biol. *19*, 207–235.

Wilkes, M.C., Mitchell, H., Penheiter, S.G., Doré, J.J., Suzuki, K., Edens, M., Sharma, D.K., Pagano, R.E., and Leof, E.B. (2005). *Transforming growth factor-beta activation of phosphatidylinositol 3-kinase is independent of Smad2 and Smad3 and regulates fibroblast responses via p21-activated kinase-2*. Cancer Res. *65*, 10431–10440.

Williams, D.A., Zheng, Y., and Cancelas, J.A. (2008). *Rho GTPases and regulation of hematopoietic stem cell localization*. Methods Enzymol. *439*, 365–393.

Wirtz-Peitz, F., and Knoblich, J.A. (2006). *Lethal giant larvae take on a life of their own*. Trends Cell Biol. *16*, 234–241.

Wu, H., Rossi, G., and Brennwald, P. (2008). *The ghost in the machine: small GTPases as spatial regulators of exocytosis*. Trends Cell Biol. *18*, 397–404.

Wu, J., Wu, X., Liang, W., Chen, C., Zheng, L., and An, H. (2014). *Clinicopathological and prognostic significance of chemokine receptor CXCR4 overexpression in patients with esophageal cancer: a meta-analysis*. Tumour Biol. J. Int. Soc. Oncodevelopmental Biol. Med. *35*, 3709–3715.

Xiang, Y., and Wang, Y. (2011). *New components of the Golgi matrix*. Cell Tissue Res. *344*, 365–379.

Xiang, Z.-L., Zeng, Z.-C., Tang, Z.-Y., Fan, J., Zhuang, P.-Y., Liang, Y., Tan, Y.-S., and He, J. (2009). *Chemokine receptor CXCR4 expression in hepatocellular carcinoma patients increases the risk of bone metastases and poor survival*. BMC Cancer *9*, 176.

Xiao, X., Kinter, A., Broder, C.C., and Dimitrov, D.S. (2000). *Interactions of CCR5 and CXCR4 with CD4 and gp120 in human blood monocyte-derived dendritic cells*. Exp. Mol. Pathol. *68*, 133–138.

Xue, B., Krishnamurthy, K., Allred, D.C., and Muthuswamy, S.K. (2013). *Loss of Par3 promotes breast cancer metastasis by compromising cell-cell cohesion*. Nat. Cell Biol. *15*, 189–200.

Yamamoto, A., Kasamatsu, A., Ishige, S., Koike, K., Saito, K., Kouzu, Y., Koike, H., Sakamoto, Y., Ogawara, K., Shiiba, M., et al. (2013). *Exocyst complex component Sec8: a presumed component in the progression of human oral squamous-cell carcinoma by secretion of matrix metalloproteinases*. J. Cancer Res. Clin. Oncol. *139*, 533–542.

Yamanaka, T., and Ohno, S. (2008). *Role of Lgl/Dlg/Scribble in the regulation of epithelial junction, polarity and growth*. Front. Biosci. J. Virtual Libr. *13*, 6693–6707.

Yang, J., and Weinberg, R.A. (2008). *Epithelial-mesenchymal transition: at the crossroads of development and tumor metastasis*. Dev. Cell *14*, 818–829.

Yarden, Y., and Sliwkowski, M.X. (2001). *Untangling the ErbB signalling network*. Nat. Rev. Mol. Cell Biol. *2*, 127–137.

Yeaman, C., Grindstaff, K.K., Wright, J.R., and Nelson, W.J. (2001). *Sec6/8 complexes on trans-Golgi network and plasma membrane regulate late stages of exocytosis in mammalian cells*. J. Cell Biol. *155*, 593–604.

Yu, J., Zhang, L., Chen, A., Xiang, G., Wang, Y., Wu, J., Mitchelson, K., Cheng, J., and Zhou, Y. (2008). *Identification of the gene transcription and apoptosis mediated by TGF-beta-Smad2/3-Smad4 signaling*. J. Cell. Physiol. *215*, 422–433.

Zeelenberg, I.S., Ruuls-Van Stalle, L., and Roos, E. (2003). *The chemokine receptor CXCR4 is required for outgrowth of colon carcinoma micrometastases*. Cancer Res. *63*, 3833–3839.

Zegers, M.M., and Hoekstra, D. (1998). *Mechanisms and functional features of polarized membrane traffic in epithelial and hepatic cells*. Biochem. J. *336 (Pt 2)*, 257–269.

Zender, L., Villanueva, A., Tovar, V., Sia, D., Chiang, D.Y., and Llovet, J.M. (2010). *Cancer gene discovery in hepatocellular carcinoma*. J. Hepatol. *52*, 921–929.

Zhang, Y.E. (2009). *Non-Smad pathways in TGF-beta signaling*. Cell Res. *19*, 128–139.

Zhang, H., and Macara, I.G. (2006). *The polarity protein PAR-3 and TIAM1 cooperate in dendritic spine morphogenesis*. Nat. Cell Biol. *8*, 227–237.

Zhang, R., Pan, X., Huang, Z., Weber, G.F., and Zhang, G. (2011). *Osteopontin enhances the expression and activity of MMP-2 via the SDF-1/CXCR4 axis in hepatocellular carcinoma cell lines*. PloS One *6*, e23831.

Zhao, B.-C., Wang, Z.-J., Mao, W.-Z., Ma, H.-C., Han, J.-G., Zhao, B., and Xu, H.-M. (2011). *CXCR4/SDF-1 axis is involved in lymph node metastasis of gastric carcinoma*. World J. Gastroenterol. WJG *17*, 2389–2396.

Zheng, D.Q., Woodard, A.S., Fornaro, M., Tallini, G., and Languino, L.R. (1999). *Prostatic carcinoma cell migration via alpha(v)beta3 integrin is modulated by a focal adhesion kinase pathway*. Cancer Res. *59*, 1655–1664.

Zhou, H., and Tai, H.-H. (1999). *Characterization of Recombinant Human CXCR4 in Insect Cells: Role of Extracellular Domains and N-Glycosylation in Ligand Binding*. Arch. Biochem. Biophys. *369*, 267–276.

Zhou, Z., Lu, X., Zhu, P., Zhu, W., Mu, X., Qu, R., and Li, M. (2012). *VCC-1 over-expression inhibits cisplatin-induced apoptosis in HepG2 cells*. Biochem. Biophys. Res. Commun. *420*, 336–342.

Zhu, Q., Han, X., Peng, J., Qin, H., and Wang, Y. (2012). *The role of CXC chemokines and their receptors in the progression and treatment of tumors*. J. Mol. Histol. *43*, 699–713.

Zlotnik, A., and Yoshie, O. (2000). *Chemokines: a new classification system and their role in immunity*. Immunity *12*, 121–127.

Zwartkruis, F.J.T., and Burgering, B.M.T. (2013). *Ras and macropinocytosis: trick and treat*. Cell Res. *23*, 982–983.

ANNEXES

I WAS JUST GUESSING
AT NUMB3R5 AND FIGURES
PULLING YOUR PUZZLES APART.
QUESTIONS OF SCIENCE,
SCIENCE AND PROGRESS,
DO NOT SPEAK AS LOUD AS MY HEART.

TELL ME YOU LOVE ME,
COME BACK AND HAUNT ME
AND I RUSH TO THE START.
RUNNING IN CIRCLES,
CHASING OUR TAILS
COMING BACK AS WE ARE.

NOBODY SAID IT WAS EASY,
IT IS SUCH A SHAME FOR US TO PART.
NOBODY SAID IT WAS EASY,
NO ONE EVER SAID IT WOULD BE
THIS HARD.
OH! TAKE ME BACK TO THE START.